Contribution à l'étude par TDM du retentissement sur le coeur gauche de la pathologie pulmonaire.

Lucie Cassagnes

Université Blaise Pascal Université d'Auvergne

Année 2016 N° d'ordre

ECOLE DOCTORALE
DES SCIENCES DE LA VIE ET DE LA SANTE
N° d'ordre :

Thèse

Présentée à l'Université d'Auvergne

pour l'obtention du grade de DOCTEUR
(Décret du 5 juillet 1984)

Spécialité
Radiologie et Imagerie médicale

Soutenue le 16 Décembre 2016

Lucie CASSAGNES

CONTRIBUTION A L'ÉTUDE PAR TDM DU RETENTISSEMENT SUR LE COEUR GAUCHE DE LA PATHOLOGIE PULMONAIRE

Membres : Pr Martine REMY-JARDIN
Pr Marc FILAIRE
Pr Jean-Marc GARCIER

Rapporteurs : Pr Hélène VERNHET-KOVACSIK
Pr Jean-Michel BARTOLI

ISIT, UMR CNRS 6284 - université d'Auvergne Clermont1

REMERCIEMENTS

Au Professeur **Martine REMY-JARDIN**, qui a accepté de co-diriger ce travail de thèse et m'a accueillie dans son service, me permettant de bénéficier de son enseignement en imagerie cardio-thoracique. Que ce travail soit le témoignage de mon profond respect.

Aux Professeurs **Hélène VERNHET-KOVACSIK** et **Jean-Michel BARTOLI**, qui m'ont fait l'honneur d 'être rapporteurs de ce travail, merci de votre confiance. Soyez assurés de mon profond respect.

Aux Professeurs **Marc FILAIRE** et **Jean-Marc GARCIER**, qui ont accepté de participer à ce jury. Merci de votre jugement que je sais juste et pertinent.

Au Professeur **Louis BOYER**, qui m'a fait confiance dès mon premier semestre d'internat et m'a soutenue jusqu'à aujourd'hui. Votre implication aussi bien dans l'organisation hospitalière que dans la prise en charge des patients est pour moi un exemple.

Au Professeur **Jacques REMY**, qui a su me faire bénéficier de ses connaissances encyclopédiques en imagerie cardio-thoracique.

SOMMAIRE

INTRODUCTION **4**

CONSIDERATIONS TECHNIQUES TDM **6**

PERFORMANCES DES MACHINES 6

PROTOCOLES D'EXPLORATION 8

DONNEES ACQUISES = SYNTHESE **11**

TRAVAUX PERSONNELS ORIGINAUX **13**

LE COEUR GAUCHE DANS LA PATHOLOGIE INTERSTITIELLE CHRONIQUE 13

Prévalence de la pathologie coronaire asymptomatique dans la fibrose pulmonaire idiopathique. *13*

LE COEUR GAUCHE DANS LA PATHOLOGIE OBSTRUCTIVE CHRONIQUE : 25

Left atrial volume in chronic obstructive pulmonary disease. *25*

LE COEUR GAUCHE DANS LA PATHOLOGIE THROMBO-EMBOLIQUE 35

Acute Pulmonary Embolism: evaluating middle-term mortality with multidetector computed tomography: a retrospective cohort study *35*

Étude de la corrélation par imagerie spectrale entre le volume de défaut de perfusion pulmonaire/ volume pulmonaire total et le rapport VD/VG, le score de Qanadli et le score de Genève dans l'embolie pulmonaire aigue. *53*

LE COEUR GAUCHE ET LA PATHOLOGIE NEOPLASIQUE PULMONAIRE 81

Left atrial resection for T4 lung cancer without cardiopulmonary bypass: technical aspects and outcomes *81*

Analyse de critères tomodensitométriques d'envahissement cardiaque dans la pathologie néoplasique pulmonaire, comparaison à l'anatomopathologie. *90*

CONCLUSION GENERALE **107**

RÉFERENCES BIBLIOGRAPHIQUES **108**

Introduction

L'interaction cœur-poumon est devenue aujourd'hui une étape clé de l'analyse tomodensitométrique thoracique.

L'implication du cœur droit concerne aussi bien la pathologie embolique que les pathologies interstitielles, avec l'évaluation indirecte de l'hypertension pulmonaire qui peut être la conséquence de ces différentes atteintes pulmonaires.

La dysfonction cardiaque gauche est aussi à l'origine de nombreuses modifications connues au sein du parenchyme pulmonaire, pouvant entraîner des modifications vasculaires, bronchiques, un œdème interstitiel, un œdème alvéolaire ou des effusions pleurales.

Nous nous sommes attachés dans cette thèse à participer à l'évaluation du retentissement sur le cœur gauche de certaines pathologies pulmonaires fréquentes, qu'il s'agisse :

- de la pathologie interstitielle chronique (fibrose pulmonaire)
- de la bronchopathie chronique obstructive
- des néoplasies pulmonaires
- de la pathologie thrombo-embolique pulmonaire

Le scanner constitue la technique de référence pour l'exploration du parenchyme pulmonaire, alors que parallèlement il est utilisé en pratique quotidienne pour imager cœur et coronaires.

La sophistication des scanners multi détecteurs autorise, avec une résolution temporelle et spatiale augmentées, une évaluation simultanée du massif cardiaque, du parenchyme et la vascularisation pulmonaire. Quand cet examen est indiqué pour explorer une pathologie pulmonaire, l'examen du cœur droit est devenu en TDM systématique ; mais l'analyse des cavités gauches est souvent moins exploitée quand elle n'est pas orientée. Or l'intoxication tabagique est un facteur de risque principal à la fois pour la pathologie néoplasique pulmonaire et la pathologie coronarienne, et il paraît donc légitime d'évaluer systématiquement sur un même examen cœur droit et cœur gauche.

Un retentissement sur le cœur gauche de la pathologie pulmonaire est en effet possible : par envahissement médiastinal et ses conséquences cardiaques dans la pathologie néoplasique, par retentissement hémodynamique dans la pathologie

thromboembolique, et par atteinte inflammatoire chronique dans la pathologie interstitielle chronique.

Considérations techniques TDM

Performances des machines

Le développement technique des machines de tomodensitométrie permet aujourd'hui l'exploration cardiaque, coronaire et du parenchyme pulmonaire lors d'une même acquisition.

L'amélioration conjointe de la résolution spatiale et de la résolution temporelle avec le développement des machines multi détecteurs et bitubes, avec des vitesses de rotation augmentées, permet non seulement de réduire considérablement les artefacts dus aux mouvements cardiaques, affectant le massif cardiaque et les structures adjacentes, mais également de réaliser des acquisitions cardiaques synchronisées à l'ECG de bonne qualité avec un surplus de dose modéré (1).

Une méta-analyse a comparé les doses d'irradiation de scanners cardiaques avec synchronisation prospective et rétrospective, retrouvant évidemment une dose d'irradiation bien moindre pour les acquisitions prospectives (3,5 mSv vs 12,3 mSv), mais cette technique nécessite un rythme cardiaque stable compris entre 65 et 75 c/min (2).

Le développement des machines avec une résolution temporelle très augmentée permet de réaliser des acquisitions prospectives pour des rythmes cardiaques de plus en plus élevés (3).

La dose délivrée pour la réalisation des scanners cardiaques est corrélée à la vitesse de déplacement de la table, donc à la valeur du pitch utilisé. Plusieurs techniques ont été développées pour réduire l'irradiation lors de la réalisation de ces examens (4):

- Modulation de dose liée à l'ECG : cette technique permet de diminuer les constantes (mAs) d'acquisition en dehors de la diastole (qui est la phase la plus utilisée pour l'interprétation).
- Diminution du voltage lors de l'acquisition : cette technique permettant évidemment de diminuer de manière importante la dose délivrée au patient, mais également d'augmenter le contraste et de diminuer l'effet Compton.
- Acquisition avec synchronisation prospective à l'ECG (technique Step and Shoot) : l'acquisition ne se fait alors qu'à un moment déterminé du cycle cardiaque, généralement en diastole, mais nécessite un rythme stable et généralement en dessous de 65 bpm.

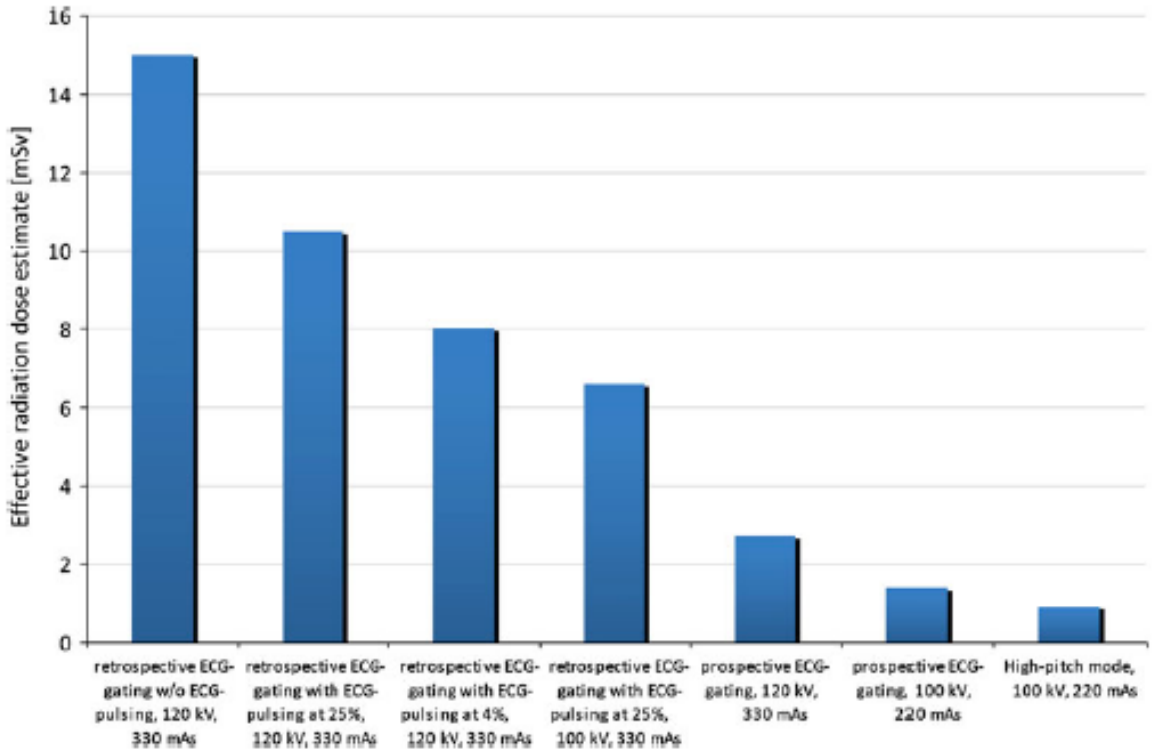
Effective radiation dose estimate [mSv]
16
14
12
10
8
6
4
2
0
retrospective ECG-gating w/o ECG-pulsing, 120 kV, 330 mAs
retrospective ECG-gating with ECG-pulsing at 25%, 120 kV, 330 mAs
retrospective ECG-gating with ECG-pulsing at 4%, 120 kV, 330 mAs
retrospective ECG-gating with ECG-pulsing at 25%, 100 kV, 330 mAs
prospective ECG-gating, 120 kV, 330 mAs
prospective ECG-gating, 100 kV, 220 mAs
High-pitch mode, 100 kV, 220 mAs

Protocoles d'exploration

Le cœur et les poumons peuvent être explorés avec divers protocoles d'acquisition :

- sans ou avec gating cardiaque
- sans ou avec injection de produit de contraste iodé

Une acquisition sans gating cardiaque permettra d'approcher une éventuelle pathologie péricardique, valvulaire ou myocardique, mais dans l'optique d'un simple dépistage d'une pathologie cardiaque. Les nouvelles modalités d'acquisition permettent également une évaluation des segments coronaires proximaux, même sans synchronisation cardiaque. Un bilan avec gating cardiaque sera nécessaire afin de réaliser un bilan plus complet, et notamment l'évaluation de la totalité de l'arbre coronaire et de la fonction ventriculaire.

Les nouvelles machines nous permettent des acquisitions rétrospectives avec synchronisation à l'ECG, fournissant une acquisition incluant l'ensemble du cycle cardiaque et rendant donc possible l'évaluation de la fonction ventriculaire par post-traitement dédié.

Par défaut, la reconstruction à 75% de l'espace R-R est privilégiée car elle permet une analyse des coronaires (phase de télé diastole). Mais la coronaire droite, la plus sujette aux artéfacts de mouvements cardiaque, notamment dans son segment 2, sera au mieux analysée à 40 % de l'espace R-R (6). L'utilisation de bêtabloquants trouve là tout son intérêt, permettant d'assurer un rythme cardiaque ralenti et stable, et réduisant de fait les écueils de la technique d'acquisition.

Des post-traitement dédiés ont été développés chez les constructeurs pour pallier à ces artefacts de mouvements liés à un rythme cardiaque trop élevé : on citera par exemple le post traitement Snap Shot Freeze développé par General Electric, qui permet une évaluation statistique du mouvement coronaire par étude des phases adjacentes à la phase 75% et création d'une « néo-série » dénuée d'artefacts de mouvements cardiaques. Une étude menée dans notre centre sur plus de 60 patients retrouvait ainsi une augmentation de 40 % de l'interprétabilité des segments coronaires chez des patients non béta-bloqués (7).

Les acquisitions prospectives seront chaque fois que possible privilégiées du fait de leur plus faible irradiation, mais restent réalisables chez des patients avec un rythme cardiaque <55 bpm. Elles présentent l'inconvénient de ne donner des informations

que sur une seule partie du cycle cardiaque, ne permettant pas d'approcher la fonction ventriculaire.

En cas d'arythmie, on privilégiera une acquisition rétrospective, permettant d'éditer l'ECG per-acquisition a posteriori et de « rejeter » les images acquises lors d'une extrasystole par exemple. Une méta-analyse rassemblait les données des études de coro-scanner chez des patients en arythmie complète par fibrillation auriculaire, comparées à une population de patients en rythme sinusal (5): les auteurs ne retrouvaient pas de différence significative dans le nombre de segments coronaires non diagnostiques, mais en revanche une différence significative de la dose d'irradiation, plus élevée chez les patients en arythmie. Cependant, l'âge des patients en arythmie complète était plus élevé que les patients en rythme sinusal (68 +/- 10 vs 61+/- 12 ans), signifiant aussi que le risque de développer une pathologie radio-induite n'est pas à considérer.

Les acquisitions sans injection de produit de contraste permettent essentiellement de détecter les calcifications, qu'elles soient péricardiques, valvulaires ou coronaires. L'ajout d'une synchronisation cardiaque permet l 'évaluation du score calcique, marqueur de risque établi dans la survenue d'événements cardio-vasculaires.

L'utilisation de produit de contraste iodé reste la règle pour les scanners cardiaques, permettant une opacification satisfaisante des cavités cardiaques, des gros vaisseaux médiastinaux et des coronaires.

Protocole d'acquisition type :

- Installation du patient :

  En cas d'exploration cardiaque isolée, on installera le patient de façon à ce que le cœur soit au centre de l'anneau, donc patient légèrement décalé vers la droite sur la table ; mais en cas d'exploration conjointe cœur-poumon, le patient sera centré de manière classique (symétrique) sur la table de scanner, permettant ainsi une analyse conjointe des 2 structures anatomiques. Une alternative à l'exploration conjointe cœur-poumon est la réalisation préalable au scanner cardiaque d'un hélice basse dose sur l'ensemble du thorax, permettant non seulement la détection de pathologies pulmonaires (6), mais

également la détermination de manière plus précise des niveaux d'exploration cardiaque.

- Contrôle du rythme cardiaque : un rythme cardiaque stable garantit une qualité optimale de l'acquisition cardiaque. On administre donc chez les patients rapides (>65 bpm) et avec un rythme instable des bétabloquants (en dehors de toute contre-indications : asthme, BAV 2 ou 3 non appareillés,bloc sino-auriculaire, bradycardie, phéochromocytome). Plusieurs molécules sont utilisées : aténolol (Ténormine®) qui présente l'inconvénient d'une demi-vie longue (6 à 7 h) et nécessite une surveillance du patient, mais aussi le chlorydrate d'esmolol (brévibloc®) qui a l'avantage d'une demi-vie très courte (2min) et donc ne nécessite pas de surveillance particulière ; en revanche il faudra injecter cette molécule sur la table d'examen et réaliser l'acquisition dans les suites immédiates.
- Constantes d'acquisition : elles seront adaptées à la morphologie et à l'IMC du patient, dans un souci de réduction de dose. L'utilisation d'un logiciel de modulation du miliampérage, aujourd'hui disponible sur toutes le machines, et qui détermine en fonction du scout-view les constantes à appliquer paraît nécessaire. Le kilovoltage est adapté à l'IMC, mais déterminé également en fonction de l'âge du patient. Pour les acquisitions rétrospectives, l'utilisation du « padding » permet d'optimiser les constantes d'acquisition en fonction de la phase du cycle cardiaque et de privilégier les phases en diastoel qui sont plus informatives que lors de la systole (mouvement coronaire).
- Acquisition prospective : elle sera réservée aux patients présentant un rythme cardiaque stable et < 60 bpm.
- Paramètres de reconstruction : dépendants de la technique d'acquisition, une acquisition prospective ne permettant pas une reconstruction multiphases des images.
- Protocole d'injection : On privilégiera les fortes concentrations d'iode (au moins 350 mg d'iode/ml) et des débits d'injection élevés (au moins 4,5 ml/sec). L'injection sera biphasique ou triphasique avec un bolus de sérum physiologique pour obtenir une opacification artérielle satisfaisante et des cavités cardiaques droites hypodenses, permettant une meillleure visualisation des la coronaire droite. Le protocole d'injection sera bien sûr

adapté à l'indication de l'examen. Le déclenchement de l'acquisition se fera en utilisant un logiciel de détection de bolus iodé, avec un seuil de 150 UH au niveau de l'aorte ascendante.

Données acquises = Synthèse

De nombreuses publications ont montré l'apport en scanner des développements technologiques pour l'évaluation concomitante du poumon et du cœur droit ou des artères pulmonaires.

L'interaction physiologique cœur-poumon concerne bien sûr aussi le cœur gauche. Les variations de volumes pulmonaires agissent à la fois sur le rythme cardiaque mais aussi sur la fonction. Les interactions cœur-poumon reposent sur les effets de modifications de pression intra-thoracique et des volumes pulmonaires sur le retour veineux et la fraction d'éjection ventriculaire gauche.

Le cœur gauche est impliqué également dans le cadre de la pathologie pulmonaire par le biais de l'interdépendance ventriculaire ; c'est par exemple le cas de manière physiologique lors d'une inspiration profonde, augmentant le remplissage ventriculaire droit et entrainant une diminution du remplissage du cœur gauche (7). Ainsi des volumes ventriculaires droits augmentés (secondairement à une pathologie pulmonaire par exemple) vont refouler le septum interventriculaire vers le ventricule gauche et ainsi diminuer la compliance diastolique et le volume télédiastolique ventriculaire gauche. Ce peut être le cas en cas d'embolie pulmonaire aigue ou chronique avec dilatation et défaillance ventriculaire droite.

Un certain nombre de pathologies cardiaques gauches peuvent être associées à une hypertension artérielle pulmonaire, par le biais de l'augmentation des pressions intraventriculaires ou auriculaires gauches, comme dans le cadre des régurgitations ou sténoses mitrales ou aortiques entrainant un remodelage des vaisseaux pulmonaires (8). Une étude récente a permis de déterminer sur des scanners non synchronisés l'origine cardiaque gauche ou non de l'hypertension artérielle pulmonaire : ainsi les auteurs rapportent que l'association d'une oreillette gauche dilatée (>20 mm2) et d'un ventricule droit de taille normale présente une sensibilité

de 77 % et une spécificité de 94 % en cas de dilatation artérielle pulmonaire pour le diagnostic d'hypertension artérielle pulmonaire du groupe 2 (liée à une pathologie cardiaque gauche) (9).

La bronchopathie chronique obstructive impacte également la fonction ventriculaire gauche. Une étude échocardiographique montrait un impact significatif de la sévérité de la BPCO sur la fonction diastolique ventriculaire gauche, l'altération de la fonction diastolique étant corrélée à la sévérité de la BPCO (10).

Une étude de Jorgensen publiée en 2007, chez des patients présentant un emphysème évolué retrouvait une diminution de la fraction d'éjection ventriculaire gauche expliquée par l'hypovolémie intrathoracique et une pré-charge diminuée (11).

Dans le cas de la pathologie néoplasique pulmonaire, l'impact sur le coeur gauche est largement dominé par l'envahissement loco-régional et la dysfonction que celui-ci peut entrainer.

C'est pourquoi nous nous sommes attachés à évaluer le cœur gauche dans un certain nombre de pathologies pulmonaires : néoplasiques, thromboemboliques, interstitielles.

Travaux personnels originaux

Le Coeur gauche dans la pathologie interstitielle chronique

Prévalence de la pathologie coronaire asymptomatique dans la fibrose pulmonaire idiopathique.

Cassagnes L, Gaillard V, Monge E, Faivre JB, Delhaye C, Molinari F, Petyt G, Hossein-Foucher C, Wallaert B, Duhamel A, Remy J, Remy-Jardin M.
Eur J Radiol. 2015 Jan ;84(1):163-71.

Les patients porteurs d'une fibrose pulmonaire, dans le cadre de leur prise en charge et notamment dans le cadre d'un bilan pré-greffe pulmonaire, bénéficient d'un bilan cardiologique complet (scintigraphie, échocardiographie et coronarographie). Du fait de la présence d'un état inflammatoire chronique, le risque de développement de lésions coronariennes est accru. Et il est difficile chez ces patients de déterminer l'origine de la dyspnée, résultant bien évidemment largement de la pathologie pulmonaire, mais chez qui une participation coronarienne, si elle existe, peut être traitée et prise en charge.

Nous nous sommes attachés chez ces patients à dépister l'atteinte coronarienne par scanner lors du bilan scanographique pulmonaire de leur pathologie interstitielle.

Ces données de coroscanner étaient confrontées à un bilan myocardique par scintigraphie et, le cas échéant, si ces 2 examens retrouvaient des arguments en faveur d'une pathologie coronarienne, à une coronarographie.

Nous avons évalué prospectivement par tomodensitométrie 42 patients atteints de fibrose pulmonaire avérée, en déterminant le score calcique et en analysant le coroscanner réalisé après injection.

Tous les patients ont bénéficié ensuite d'une scintigraphie myocardique stress/repos. Tous les patients présentant un score calcique > 400 et/ou une sténose coronarienne > 50 % au scanner et/ou un defect de perfusion > 5 % du myocarde étaient référrés au cardiologue pour consultation. Une coronarographie était réalisée si le patient présentait un defect de perfusion > 10 % à la scintigraphie ou une sténose significative du tronc commun ou de l'IVA. Les patients avec un passé coronarien connu étaient exclus de l'étude.

Abstract:
Introduction : du fait de l'intérêt grandissant concernant l'association entre fibrose pulmonaire idiopathique et pathologie ischémique myocardique, nous avons réalisé une étude prospective afin d'évaluer la prévalence de la pathologie coronarienne asymptomatique chez les patients porteurs de fibrose pulmonaire idiopathique.

Méthode : 44 patients porteurs d'une fibrose pulmonaire idiopathique ont bénéficier d'un dépistage non invasif de la pathologie coronarienne incluant (a) un scanner thoracique permettant le calcul du score calcique et la recherche d'une sténose coronarienne ; et (b) d'une scintigraphie de perfusion myocardique sous stress pharmacologique. Les patients avec anomalies coronaires significatives, définies par un score calcique > 400, ou une sténose coronarienne > 50 %, et/ou un defect de perfusion >5% à la scintigraphie étaient réferrés au cardiologue. Une coronarographie était réalisée en cas de défect de perfusion >10 % ou de lésion significative de l'IVA, quel que soit le résultat de la scintigraphie.

Résultats : En combinant ces 2 techniques, des anomalies significatives étaient retrouvées chez 32/42 patients (76 %). Le cardiologue : (a) n'a pas réalisé d'autres investigations chez 21 patients (anomalies scanographiques sans ischémie à la scintigraphie : 12/21 ; faux positifs de la scintigraphie : 3/21 ; insuffisance respiratoire évoluée : 6/21) ; (b) a réalisé une coronarographie chez 11 patients qui a fait retrouver des sténoses significatives chez 5 patients (5/42 ; 12 %).Dans la configuration la plus péjorative (c'est-à-dire en incluant les 6 patients chez qui des lésions coronariennes significatives étaient retrouvées mais n'avaient pas bénéficié de coronarographie du fait d'une insuffisance respiratoire évoluée), la prévalence de la pathologie coronarienne atteignait 26 % (11/42).

Conclusion :
Dans une population de patients porteurs de fibrose pulmonaire idiopathique, la prévalence de la pathologie coronarienne asymptomatique se situe entre 12 et 26 %.

European Journal of Radiology 84 (2015) 163–171

Contents lists available at ScienceDirect

European Journal of Radiology

journal homepage: www.elsevier.com/locate/ejrad

Prevalence of asymptomatic coronary disease in fibrosing idiopathic interstitial pneumonias

Lucie Cassagnes[a], Vianney Gaillard[a], Emmanuel Monge[b], Jean-Baptiste Faivre[a], Cédric Delhaye[c], Francesco Molinari[a], Grégory Petyt[d], Claude Hossein-Foucher[d], Benoit Wallaert[b], Alain Duhamel[e], Jacques Remy[a], Martine Remy-Jardin[a,*]

[a] Department of Thoracic Imaging (EA 2694), Hospital Calmette, CHRU and Univ Lille 2 Nord de France, F-59000 Lille, France
[b] Department of Pulmonology, Center of Competence for Rare Pulmonary Diseases, Hospital Calmette, CHRU and Univ Lille 2 Nord de France, F-59000 Lille, France
[c] Department of Cardiology, Cardiology Hospital, CHRU and Univ Lille 2 Nord de France, F-59000 Lille, France
[d] Department of Nuclear Medicine, Hospital Salengro, CHRU and Univ Lille 2 Nord de France, F-59000 Lille, France
[e] Department of Medical Statistics (EA 2694), Univ Lille Nord de France, F-59000 Lille, France

ARTICLE INFO

Article history:
Received 6 January 2014
Received in revised form 5 April 2014
Accepted 8 April 2014

Keywords:
Coronary arteries
Chest CT
Lung diseases
Interstitial lung disease
Atherosclerosis

ABSTRACT

Background: Because of growing body of interest on the association between fibrosing idiopathic interstitial pneumonias (f-IIP) and ischaemic heart disease, we initiated this prospective study to evaluate the prevalence of asymptomatic coronary artery disease (CAD) in patients with f-IIP.
Methods: Forty-two patients with f-IIP underwent noninvasive screening for CAD that included (a) a chest CT examination enabling calculation of the coronary artery calcium (CAC) score, then depiction of coronary artery stenosis; and (b) stress myocardial perfusion scintigraphy (MPS). Patients with significant coronary abnormalities, defined by a CAC score >400 or coronary artery stenosis >50% at CT and/or perfusion defect >5% at MPS, were referred to the cardiologist. Coronary angiography was indicated in presence of a perfusion defect >10% at MPS or significant left main or proximal left anterior descending stenosis whatever MPS findings.
Results: Combining CT and MPS, significant abnormalities were detected in 32/42 patients (76%). The cardiologist: (a) did not consider further investigation in 21 patients (CT abnormalities but no ischaemia at MPS: 12/21; false-positive findings at MPS: 3/21; poor respiratory condition: 6/21); (b) proceeded to coronary angiography in 11 patients which confirmed significant stenoses in 5 patients (5/42; 12%). In the worst-case-scenario (i.e., inclusion of 6 patients with significant coronary artery abnormalities who were not investigated due to poor respiratory condition), the prevalence of CAD reached 26% (11/42).
Conclusion: In the studied population of patients with f-IIP, asymptomatic CAD ranged between 12% and 26%.

1. Introduction

Idiopathic pulmonary fibrosis (IPF) is the most common idiopathic interstitial pneumonia and holds the worst prognosis with a median survival after diagnosis ranging from 3 to 5 years [1]. Whereas the most common cause of death in patients with IPF remains the disease itself [2], there has been a growing body of interest on the association between IPF and ischaemic heart disease in this population [3–6]. Based on autopsy findings, CAD has been reported as the immediate cause of death in 7–10% of cases [2,7,8] and as a contributing cause of death in 31% of cases [7]. During the course of the disease, the presence of CAD is difficult to recognize because episodes of shortness of breath, if suggestive of respiratory deterioration, can also represent angina equivalents [9]. Moreover, any ischaemic event might be exacerbated by hypoxia or pulmonary hypertension related to the underlying IPF, underlining the negative cascade of events that may potentially occur when the two diseases are concomitantly present [9,10]. Despite

Abbreviations: CAD, coronary artery disease; CT, computed tomography; CAC score, coronary artery calcium score; MPS, myocardial perfusion scintigraphy; f-IIP, fibrosing idiopathic interstitial pneumonia; IPF, Idiopathic pulmonary fibrosis; NSIP, nonspecific interstitial pneumonia; LM, left main coronary artery; LA, left anterior descending coronary artery; CX, circumflex coronary artery; RC, right coronary artery.

* Corresponding author at: Department of Thoracic Imaging, Hospital Calmette, Boulevard Jules Leclercq, 59037 Lille Cedex, France. Tel.: +33 3 20 44 43 11; fax: +33 3 20 44 47 20.
E-mail address: martine.remy@chru-lille.fr (M. Remy-Jardin).

http://dx.doi.org/10.1016/j.ejrad.2014.04.023
0720-048X/

such interplay in the clinical course of patients with IPF, the presence of CAD has been exclusively investigated in patients with advanced lung disease when undergoing selection for lung transplantation. Therefore, our current knowledge of the prevalence of CAD in IPF only relies on angiographic findings obtained at the time of left heart catheterization; in lung-transplant candidates, significant CAD has been reported in 28% of patients [5,9,10]. Because of similarities in the clinical behaviour of IPF and fibrotic nonspecific interstitial pneumonia (f-NSIP), both categorized as chronic fibrosing idiopathic interstitial pneumonias (f-IIP) [11], we designed our study to screen for asymptomatic CAD in an unselected population of stable f-IIP patients at the time of their annual follow-up.

2. Materials and methods

2.1. Population

Over an 18-month period (January 2011–September 2012), 64 consecutive outpatients with f-IIP were proposed to participate in a noninvasive programme for detection of asymptomatic CAD at the time of their annual follow-up. Fibrosing idiopathic interstitial pneumonia (f-IIP) was diagnosed by a multidisciplinary consensus between experienced respiratory physicians and chest radiologists ($n = 51$), completed by results of surgical lung biopsies whenever deemed necessary by the multidisciplinary approach ($n = 13$). In all cases, the diagnosis of f-IIP had been established according to the official international guidelines [12,13]. Given that all the cases had been followed for several years, perusal of subsequent correspondence ensured that no subsequent change in diagnosis had been made.

The screening programme for detection of CAD was based on noninvasive morphologic and functional evaluation of the coronary circulation (Fig. 1). The first-line examinations included (a) a chest CT examination with determination of the coronary artery calcium (CAC) score, followed by depiction of coronary artery stenosis; and (b) a stress myocardial perfusion scintigraphy (MPS). On the basis of these two investigations, the patient was referred to the cardiologist when there were CT and/or scintigraphic findings suggestive of coronary artery disease (CAD) as further described: (a) the CT criteria for CAD included a CAC score >400 or the presence of a coronary artery stenosis >50%; (b) the scintigraphic criterion for CAD was the presence of a reversible perfusion defect greater than 5% of total left ventricular volume. The cardiologist indicated coronary angiography in presence of: (a) an ischaemic mass >10% at MPS; or (b) LM or LAD proximal stenosis, whatever the results of MPS. His final decision was dictated by the patient's overall clinical situation, weighting the risks/benefits of the invasive procedure. When indicated, coronary angiography analyzed the presence and location of significant stenoses (i.e., coronary artery stenosis >50%) which could be treated by recanalization and stent deposition or proposed for surgical coronary artery bypass grafting.

Of the initial population, 22 patients were excluded for the following reasons: (a) a previous history of myocardial infarction ($n = 9$); (b) refusal to participate ($n = 5$); (c) incomplete screening programme ($n = 8$) because (c-1) chest CT examinations were only based on noncontrast CT scans (4/8) due to technical problems during the scanning session; (c-2) chest CT was the only investigation undertaken because of the onset of acute events in the course of the screening programme (4/8) (patient's death due to acute exacerbation of IPF [2/4], ischaemic neurovascular disease [1/4], and lung transplantation [1/4]). The final study group comprised 42 patients who qualified for the analysis.

Our investigation followed international [14] and national [15] recommendations concerning cardiovascular comorbidities in patients with fibrotic idiopathic international pneumonias. All

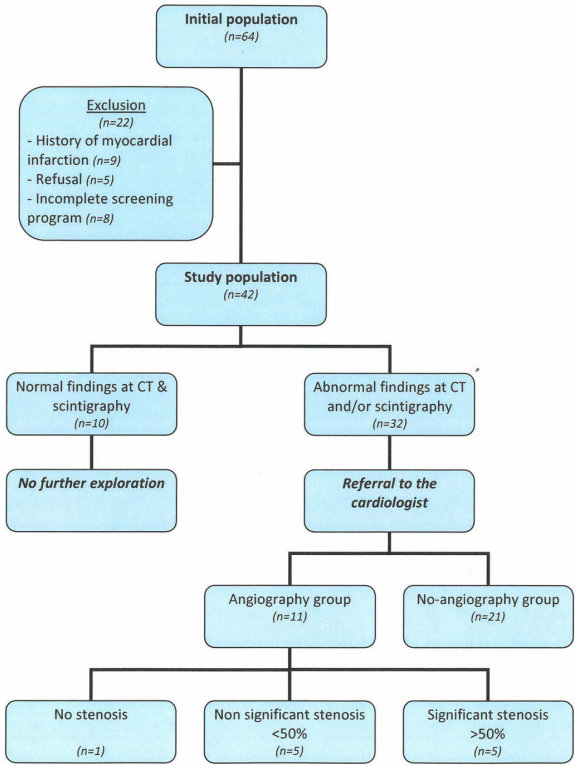

Fig. 1. Screening programme for asymptomatic CAD in the studied population of fibrosing idiopathic interstitial pneumonias (f-IIP).

patients were informed of the benefits of identifying CAD prior to lung transplantation and oral informed consent was always obtained prior to their inclusion in this screening programme. The institutional Ethics Committee considered this investigation as an observational study and allowed us to analyze patients' data with waiver of patient's informed consent. At a national level, this study was approved by the Institutional Review Board of the French Society of Pulmonology under the reference CEPRO 2012 009.

2.2. Screening programme for detection of occult CAD

2.2.1. Clinical evaluation

Each patient was evaluated for the presence of the following cardiovascular risk factors: hypertension, hypercholesterolemia, diabetes mellitus, obesity, and smoking status. In addition, treatment with glucocorticoids during the study was recorded. Hypertension was defined as arterial blood pressure $\geq$140/90 mm Hg or treatment with one or more hypertensive agents. Hypercholesterolemia was defined as a total blood cholesterol level of $\geq$2.40 g/L or treatment with one or more lipid-lowering drug. Diabetes mellitus was defined as a fasting serum glucose level $\geq$1.26 g/L or treatment with one or more oral or parenteral hypoglycaemic medications. Obesity was defined as a body mass index, BMI $\geq$ 25.0. All subjects had pulmonary function tests (PFTs) obtained at the time of CT scanning according to the guidelines of the European Respiratory Society. Forced vital capacity (FVC) and forced expiratory volume in one second (FEV_1) were measured by spirometry and plethysmography with a Jaeger-Masterlab® cabin. Single-breath diffusing capacity of the lung for carbon monoxide (DLCO: mL CO min^{-1} mm Hg^{-1}) was measured and corrected for

Table 1
Chest CT scanning protocols.

	CAC score assessment	CT angiography
Scanning mode	Prospective ECG gating	Retrospective ECG gating
Scanning parameters	• Dual-source, single energy scanning mode • 120 kV • 100 mAs/rot • Rotation time: 0.28 s	• Dual-source, single energy scanning mode • 100 kV • 450 mAs/rot • Rotation time: 0.28 s
Collimation	64 × 0.6 with z-flying spot	64 × 0.6 mm with z-flying spot
Dose modulation	• Care Dose 4D	• Care Dose 4D • ECG pulsing (full dose between 30 and 70% of R–R interval)
Reconstruction	0.75 mm/0.6 mm (kernel: B26f)	• Lung images: 1 mm/1 mm (kernel: B50f) • Mediastinal images: 1 mm/1 mm (kernel: B20f) • Coronary artery imaging: 0.75 mm/0.6 mm (kernel: B26f); R–R intervals: every 10% from 0 to 90%

haemoglobin concentration ($g\,dL^{-1}$) according to Cotes' equation: corrected (Hb) DLco = DLco × (10.2 + Hb)/(1.7 × Hb). Values were expressed as percentages of the predicted normal values calculated according to gender, weight and age [16–18].

2.2.2. Chest CT examination

2.2.2.1. Scanning protocol. The examinations were obtained without administration of beta-blockers on a dual-source CT system (Definition Flash, Siemens Healthcare, Forchheim, Germany) with a two-step protocol (Table 1). The first step consisted in a noncontrast, prospective ECG-gated mode over the cardiac cavities aimed at calculating the CAC score. During the same session, a second acquisition was performed over the entire thorax with administration of contrast material and retrospective ECG gating, aimed at assessing lung disease and depicting CAD. The injection protocol consisted of a dual-phase injection: 60 mL of a 40% contrast agent (iomeprol 400, Bracco, Milan, Italy), followed by 40 mL of diluted contrast agent (50% NaCl; 50% iodine), at a rate of 4 mL/s. For each examination, the patient's heart rate during CT scanning and the dose-length-product (DLP) were systematically recorded. The effective dose was derived from the product of the DLP and a conversion coefficient ($k = 0.017\ mSv\,mGy^{-1}\,cm^{-1}$) [19].

2.2.2.2. CAC score assessment. The coronary arteries were reviewed for the degree of calcification and were graded by Agatston score as follows: 0 = no visible calcification; 1 = trace of calcification (Agatston score 1–10), 2 = mild calcification (Agatston score 11–100), 3 = moderate calcification (Agatston score 101–400) and 4 = severe calcification (Agatston score >400) [20]. The CAC score was determined individually on the left main (LM), left anterior descending (LA), circumflex (CX), and right (RC) coronary arteries, and as total score by summing the scores of individual lesions. This evaluation was obtained using a commercial software (CaScore, version 1.1.0.10, Siemens Healthcare, Forchheim, Germany).

2.2.2.3. Analysis of coronary arteries. The coronary arteries were categorized into 15 segments according to the American Heart Association classification [21]. For each patient, the analysis of the coronary artery tree was undertaken only if the attenuation value within all proximal coronary segments was ≥200 HU. The next step consisted of an individual analysis of each coronary segment whatever its diameter, rated as assessable if the vessel lumen was completely depicted in the absence of major motion artefacts and/or dense calcification. At the level of each coronary segment, the readers recorded the presence of arterial wall abnormalities (i.e., soft plaque, calcified plaque; mixed plaque) and the any reduction in the arterial lumen, was coded as nonsignificant if <50%, or significant if >50%.

2.2.2.4. Severity of lung fibrosis. The severity of lung fibrosis was assessed using two parameters: (a) the coarseness of fibrosis using a 4-point scoring system (0, ground glass opacification alone; 1, fine intralobular fibrosis; 2, microcystic reticular pattern; and 3, macrocystic reticular pattern) on 5 levels (score ranging from 0 to 15); and (b) the grade of interstitial lung disease, depending on the relative extent of a reticular pattern or ground glass opacification (grade 1, predominant ground glass opacification; grade 2, equal proportions of ground glass opacification and a reticular pattern; and grade 3, predominant reticular pattern) on the whole CT examination as previously described [22].

2.2.2.5. Conditions of CT analysis. Image analysis was obtained by consensus between two readers with 2 years and 7 years of experience in cardiac CT at the time of initiation of this study, respectively. The radiologists were blinded to the patient's clinical data and results of other investigations. For each patient, the severity of lung fibrosis, calculation of the CAC score and identification of coronary artery stenosis were independently undertaken in separate reading sessions. The presence of significant coronary abnormalities was defined by a CAC score >400 or the presence of coronary artery stenosis >50%.

2.2.3. Stress myocardial perfusion scintigraphy

Each patient underwent stress/rest gated SPECT according to a single or two-day protocol. Fourteen patients underwent exercise testing, completed by dipyridamole injection in 6 patients and 22 patients underwent a dipyridamole stress test. Stress myocardial scintigraphy was performed after injection of 740–925 MBq Tc99m MIBI. The examinations were interpreted by consensus between two readers with 7 and 25 years of experience in nuclear medicine. Myocardial perfusion and regional wall motion were quantitatively analyzed at rest and after stress using a validated software programme (Quantitative gated SPECT; Cedars Sinai) that provided scores of ischaemic extent according to a 17-segment polar map [23]. The finding of a reversible defect ≥5% of total left ventricular volume was suggestive of myocardial ischaemia.

2.2.4. Cardiologist's evaluation

Patients with significant coronary abnormalities, defined by a CAC score >400 or coronary artery stenosis >50% at CT and/or a perfusion defect >5% at MPS, were referred to the cardiologist. Except for patients in poor general condition, conventional coronary angiography was indicated in the presence of a perfusion defect >10% at MPS or significant LM or proximal LAD stenosis whatever MPS findings. The angiographic procedure was performed by transfemoral or transradial access. The following angiographic views were systematically obtained (RAO 30°, LAO 60° cran 30°, LAO 60° caud 35°, LOA 30° cran 30°, RAO 30° caud 30°, RAO 10° cran 35°, LAO 90°), completed by additional views whenever deemed necessary by the cardiologist (RAO: right anterior oblique; LAO: left anterior oblique; cran: cranial; caud: caudal). Based on the results of this examination, patients were categorized as having significant CAD (>50% stenosis of one or more major coronary artery), nonsignificant CAD (<50% stenosis of a major vessel or disease of smaller vessels) or no disease. Coronary angiography was considered as the reference standard for diagnosis of CAD.

Table 2
Demographic characteristics of the studied population.

(a) Demographic characteristics of the studied population ($n = 42$)

Age, yrs	67.8 (±6.9) Median: 69.5
Male sex, *n* (%)	28 (66.7%)
BMI, kg/m^2	27.7 (±3.8) Median: 27.1
Familial history of CAD, *n* (%)	4 (9.5%)
Hypertension, *n* (%)	18 (42.9%)
Smoking history, *n* (%)	24 (57.1%)
Tobacco consumption, pack-years	24 (±17)
Diabetes mellitus, *n* (%)	6 (14.3%)
Obesity, *n* (%)	9 (21.43%)
Hypercholesterolemia, *n* (%)	22 (52.4%)
FVC, % pred	79.00 (±19.71)Median: 80
FEV1, % pred	75.39 (±20.53)Median: 73
DLCO, % pred	41.80 (±12.55)Median: 44
Interval of time since f-IIP diagnosis, months	32.4 (± 41.5)Median: 23.7
Fibrotic lung disease	
Idiopathic pulmonary fibrosis	*n* = 25
Idiopathic fibrotic NSIP	*n* = 17
CT severity of lung fibrosis	
-Coarseness score	
Mean ±SD (range)	8.5 ±3.7 (range: 2.4–15)
-Grade of interstitial lung disease	
Grade 1, *n* (%)	Grade 1, *n* = 13 (31%)
Grade 2, *n* (%)	Grade 2, *n* = 16 (38%)
Grade 3, *n* (%)	Grade 3, *n* = 13 (31%)
Glucocorticoids, *n*	33 (78.6%)
Immunosuppressive treatment, *n*	25 (59.5%)
Anticoagulant therapy (aspirin/AVK), n	10 (23.8%)
Beta-blockers, *n*	3 (7.1%)
Diuretics, *n*	7 (16.7%)

(b) Comparison of patients' characteristics according to the presence or absence of coronary artery abnormalities

	Patients without CAD ($n = 10$)	Patients with CAD ($n = 32$)	*p* value
Age, yrs	65.6 (±6.2) Median: 64.5	68.5 (±7.1) Median: 70	0.19[a]
Male sex, *n* (%)	4 (40%)	24 (75%)	0.05[b]
BMI, kg/m^2	28.6 (±3.6) Median: 28.7	27.4 (±3.9) Median: 26.4	0.18[a]
Familial history of CAD, *n* (%)	1 (10%)	3 (9.4%)	NA
Hypertension, *n* (%)	2 (20%)	16 (50%)	0.14[b]
Smoking history, *n* (%)	5 (50%)	19 (59.4%)	0.12[b]
Tobacco consumption, pack-years	30.2 (±12.3) Median: 20	23.5 (±13.4) Median: 20	0.45
Diabetes mellitus, *n* (%)	1 (10%)	5 (15.6%)	NA
Obesity, *n* (%)	4 (40%)	5 (15.6%)	0.18[b]
Hypercholesterolemia, *n* (%)	3 (30%)	19 (59.4%)	0.15[b]
FVC, %	84.1 (±27.2) Median: 85	77.3 (±16.9) Median: 79	0.28[a]
FEV1, %	81.5 (±23.2) Median: 83.5	73.4(±19.6) Median: 69	0.28[a]
DLCO, %	42.2(±13.9) Median: 46	41.7 (±12.4) Median: 43	0.96[a]
Interval of time since f-IIP diagnosis, months	21 (± 20.4) Median: 10.3	35.9 (± 45.9)Median: 25.1	0.43[a]
CT severity of lung fibrosis			
-Coarseness score			
Mean ±SD, median	9.3 ±3.6, med = 9	8.4 ±3.8, med = 8.5	0.62[a]
-Grade of interstitial lung disease			
Grade 1, *n* (%)	3 (30%)	10 (31%)	
Grade 2, *n* (%)	3 (30%)	13 (41%)	
Grade 3, *n* (%)	4 (40%)	9 (28%)	0.89[b]
Glucocorticoids, *n*	8 (80%)	25 (78.1%)	1[b]
Immunosuppressive treatment, *n*	6 (60%)	19 (59.4%)	1[b]
Antithrombotic therapy (aspirin/AVK), *n*	0 (0%)	10 (31.25%)	0.08[b]
Beta-blockers, *n*	1 (10%)	2 (6.2%)	NA
Diuretics, *n*	1 (10%)	7 (18.75%)	1[b]

Abbreviations: (a) f-IIP: fibrosing idiopathic interstitial pneumonia; med: median; FVC: forced vital capacity; FEV1: forced expiratory volume in one second; DLCO: diffusing capacity of the lung for carbon monoxide; % pred: percentage of predicted value. (b) FVC: forced vital capacity; FEV1: forced expiratory volume in one second; DLCO: diffusing capacity of the lung for carbon monoxide NA: not applicable; CAD: coronary artery disease.
(a) NB: Numerical variables are expressed as means with standard deviation. (b) NB: Numerical variables are expressed as means with standard deviation. Patients with CAD referred to patients with abnormal findings at CT (CAC score >400 or coronary artery stenosis >50%) and/or MPS (perfusion defect >5%).

[a] Wilcoxon unpaired test.
[b] Fischer's exact test.

Description of CT findings at the level of abnormal coronary artery segments ($n = 141$).

		CA stenosis			
		No stenosis	Nonsignificant stenosis (<50%)	Significant (>50%) 50–99% stenosis	Stenosis Occlusion
Type of coronary artery lesions	Soft plaques ($n = 4$)	0	4	0	0
	Soft and calcified plaques ($n = 21$)	0	11	9	1
	Calcified plaques ($n = 116$)	2	96	17	1

Note: Considering the 28 significant stenoses identified on CT angiograms, 27 of them were identified on proximal or mid coronary segments.
Abbreviations: CA: coronary artery.

Table 4
Description of coronary artery lesions on CT examinations in the studied population ($n = 42$).

	Absence of CA stenosis $n = 6$	Nonsignificant CA stenosis (<50%) $n = 21$	Significant CA stenosis (>50%) $n = 15$
CAC score = 0 ($n = 4$)	4	0	0
CAC score < 400 ($n = 22$)	2	16	4
CAC score > 400 ($n = 16$)	0	5	11

Abbreviations: CAC: coronary artery calcium; CA: coronary artery.

2.2.5. Significance of CAD throughout the manuscript according to current guidelines

2.2.5.1. Clinical context (from Ref. [24]). Stable coronary artery disease is generally characterized by episodes of reversible myocardial demand/supply mismatch, related to ischaemia or hypoxia, which are usually inducible by exercise, emotion or other stress and reproducible – but, which may also be occurring spontaneously. Such episodes of ischaemia/hypoxia are commonly associated with transient chest discomfort (angina pectoris). SCAD (suspected coronary artery disease) also includes the stabilized, often asymptomatic, phases that follow an ACS (Acute Coronary Syndrom).

2.2.5.2. CT criteria (from Ref. [25]). It used MSCT as a diagnostic test for obstructive CAD, with >50% diameter stenosis selected as the cut-off criterion for significant CAD, using conventional invasive angiography as the reference standard.

2.2.5.3. Scintigraphic criteria (from Ref. [26]). Less than 5% ischaemic myocardium was considered minimal ischaemia; 5–9% ischaemic myocardium was considered mild ischaemia, and >10% ischaemic myocardium was considered moderate to severe ischemia. "Our findings suggest a treatment target of >5% ischaemia reduction with OMT (optimal medical therapy) with or without coronary revascularization."

2.3. Statistical analysis

Statistical analysis was performed with commercially available software (SAS Institute, Cary, N.C. 25513). Results were expressed as means, standard deviations and medians for continuous variables and as frequencies and percentages for categorical variables. Comparative analyses were obtained using the chi-square test for categorical data; when not applicable because of the sample size, the Fisher's exact test was used. For numerical variables, we used the unpaired Wilcoxon test. *P* values inferior to 0.05 were considered statistically significant.

3. Results

3.1. Population characteristics ($n = 42$) (Table 2)

Our study group comprised 25 patients with IPF and 17 patients with idiopathic fibrotic NSIP. The diagnosis of f-IIP required surgical lung biopsy in 13 patients. Using DLCO as an index of lung disease severity, 10 patients had low DLCO values (i.e., below lower limit of normal but >50% predicted); 22 patients had marked DLCO reduction (i.e., between 35% and 50% predicted) and 9 patients had severe DLCO reduction (i.e., <35% predicted).

3.2. CT detection of CAD ($n = 42$)

3.2.1. CAC scores

The median value of the CAC score of the studied population was 274.5 (range: 0–4769). Regarding the depiction of CAD: (a) 26 patients had a CAC score <400 (median value: 61.0; range: 0–393); (b) 16 patients had a CAC score >400 (median value: 1114; range: 447–4769).

3.2.2. Analysis of coronary arteries

The mean heart rate of the studied population was 80.9 ± 12.7 bpm (range: 56–100). Considering 15 coronary segments per patient, a total of 630 segments were analyzed: (a) 77% (486/630) were rated as analyzable; (b) among them, 141 segments (141/486; 29.0%) showed coronary artery lesions whose

Table 5
Summary of CT and MPS abnormalities in the studied population ($n = 42$).

		Myocardial Normal findings Perfusion defects <5% $n = 20$	Perfusion Abnormal Perfusion defects between 5 and 10% $n = 8$	Scintigraphy Findings Perfusion defects >10% $n = 14$
CT findings	Absence of CAD (CAC = 0 and no stenosis) ($n = 4$)	1	1	2
	Nonsignificant CAD (CAC < 400; no stenosis or stenosis <50%) ($n = 18$)	9	3	6
	Significant CAD (CAC > 400; stenosis >50%) ($n = 20$)	10	4	6

Abbreviations: CAD: coronary artery disease; CT: computed tomography; MPS: myocardial perfusion scintigraphy.

Table 6
CT, MPS and coronary angiography results in the 11 patients who were referred to the cardiologists and underwent coronary angiography.

Patients	CAC score	CTA Presence of significant CAD	MPS findings	Coronary angiography Presence of significant CAD
Patient 1	2405	+ (segment 7)	>10% (inferior and anterior)	+ (segment 7)
Patient 2	266	+ (segments 6, 7, 9)	5–10% (inferior and anterior)	+ (segments 6, 7)
Patient 3	4769	+ (segment 1)	5–10% (inferior and lateral)	+ (segments 2, 3, 6, 12)
Patient 4	902	+ (segments 1, 6, 7)	>10% (anterior)	+ (segments 1, 6, 7, 11)
Patient 5	2709	+ (segments 2, 5, 6, 7, 10, 11)	>10% (anteroseptal)	+ (segments 6, 7, 10, 11)
Patient 6	95.8	–	>10% (anteroseptal)	–
Patient 7	334	+ (segment 11)	5–10% (inferior and lateral)	–
Patient 8	586	–	>10% (inferior)	–
Patient 9	0	–	>10% (inferior)	–
Patient 10	319	+ (segments 6, 7)	–	–
Patient 11	117	+ (segment 2, 6)	>10% (inferior)	–

severity is summarized in Table 3. When considering 10 coronary segments per patient (i.e., proximal and mid coronary segments), 87% (364/420) were rated as analyzable. At a patient level, CT angiography showed no stenosis in 6 patients, nonsignificant stenosis in 21 patients and significant stenosis in 15 patients. Among the 15 patients with significant coronary artery stenosis, the extent of CAD was as follows: (a) one-vessel disease ($n = 9$); (b) 2-vessel disease ($n = 4$); (c) 3-vessel disease ($n = 2$).

3.2.3. CT detection of CAD

On the basis of CT findings (Table 4): (a) 4 patients had normal coronary arteries (CAC score = 0; no stenosis); (b) 18 patients had CT findings which did not justify further evaluation (CAC score <400; no significant coronary artery stenosis); and (b) 20 patients were considered to have CT features of CAD based on a CAC score >400 ($n = 16$) and/or significant coronary artery stenosis (>50%) ($n = 15$). The mean DLP of CT examinations was 895.54 ± 322.15 mGy cm (range: 252–1513) (median: 807). The mean effective dose was 15.22 ± 5.48 mSv (range: 4.28–25.72) (median value: 13.72).

3.3. Detection of perfusion defects by stress MPS (n = 42)

Stress MPS showed: (a) no perfusion abnormality (0–5%) in 20 patients; (b) perfusion defects in 22 patients, including 8 patients with perfusion defects between 5 and 10%; and 14 patients with perfusion defects >10%. Table 5 summarizes the abnormal findings on CT and MPS in the studied population. The average radiation dose of MPS varied between 7.5 and 9.5 mSv.

3.4. CAD depiction based on the combined analysis of CT and myocardial perfusion scintigraphy

Combined analysis of CT and myocardial perfusion scintigraphy led to the depiction of 10 patients without CAD (i.e., normal coronary artery CT angiogram and no perfusion defects or defects <5%) and 32 patients with coronary artery abnormalities (CAC >400 or significant stenosis; $n = 20$, and/or perfusion defects >5%; $n = 21$) who were referred to the cardiologist. As shown in Table 2b, no significant difference was found between these two subgroups of patients when comparing (a) the mean interval of time between IPF diagnosis and screening for CAD ($p = 0.43$); (b) the mean scores ($p = 0.62$) and grades ($p = 0.89$) of lung disease on CT images; and (c) the mean values of DLCO ($p = 0.96$), FVC ($p = 0.28$) and FEV1 ($p = 0.28$).

3.5. Cardiologist's management

The cardiologist: (a) did not consider further investigation in 21 patients (CT abnormalities but no ischaemia at MPS: 12/21; false-positive findings at MPS: 3/21 [very low calcium score; no significant stenosis at CTA; hypoperfusion exclusively located in the inferior wall that was considered to correspond to artefacts]; poor respiratory condition at the time of evaluation: 6/21); (b) proceeded to coronary angiography ($n = 11$): 5 patients were categorized as having significant CAD (need for an intervention on major vessel with >50% lesion); 5 patients had nonsignificant CAD (<50% occlusion of major vessel or disease of smaller vessels) and 1 patient had no coronary abnormality. Table 6 summarizes the findings at CT, MPS and invasive coronary angiography for the 11 patients who underwent coronary angiography. Fig. 2 illustrates the findings at CT, MPS and invasive coronary angiography in one of these patients (i.e., patient $n = 5$; Table 6). On the basis of coronary angiography results, the prevalence of asymptomatic CAD was 12% (5/42). Considering that 6 patients could not undergo further investigation due to poor respiratory condition, the prevalence of asymptomatic CAD in the worst-case scenario was 26% (11/42).

In the angiography group, surgery or stent placement was performed in the 5 patients with significant CAD while the remaining 6 patients were treated medically. In the no-angiography group ($n = 21$), 16 patients received medical treatment. A total of 27 patients (27/42; 64% of the studied population) had therapeutic modifications induced by the screening programme.

Regarding demographic characteristics of the two subgroups, the angiography group ($n = 11$) did not significantly differ from the no-angiography group ($n = 21$) except for a higher frequency of hypertension (81.8% vs 33.33%; $p = 0.0092$), a higher level of total blood cholesterol (2.22 ± 0.43 [median: 2.02] vs 1.8 ± 0.27 [median: 1.75]; $p = 0.0070$) and HDL (0.85 ± 0.42 [median: 0.63] vs 0.55 ± 0.14 [median: 0.54]; $p = 0.0310$). No significant differences were found between patients of the angiography and no-angiography groups when comparing (a) the distribution of grades ($p = 0.1881$) and mean scores ($p = 0.20$) of lung infiltration; (b) the mean values of values of DLCO ($p = 0.94$), FVC ($p = 0.23$) and FEV1 ($p = 0.37$).

4. Discussion

To our knowledge, this is the first study investigating the prevalence of asymptomatic CAD in a population of unselected f-IIP patients. Although coronary angiography is generally accepted as the clinical gold standard for diagnosing the presence of CAD, it was not possible to use it as a screening test in asymptomatic patients due to its highly invasive nature. On the basis of two screening tests known for their noninvasiveness and high negative predictive values, 12% (5/42) of our population was diagnosed with silent significant CAD. However, this percentage reached 26% (11/42) when including patients with CT and/or scintigraphic criteria who could not undergo coronary angiography due to poor respiratory conditions. These values are in the range of that previously reported by Nathan et al. [9] in patients with more advanced lung disease. From their study group of 73 IPF patients referred for pre-transplant

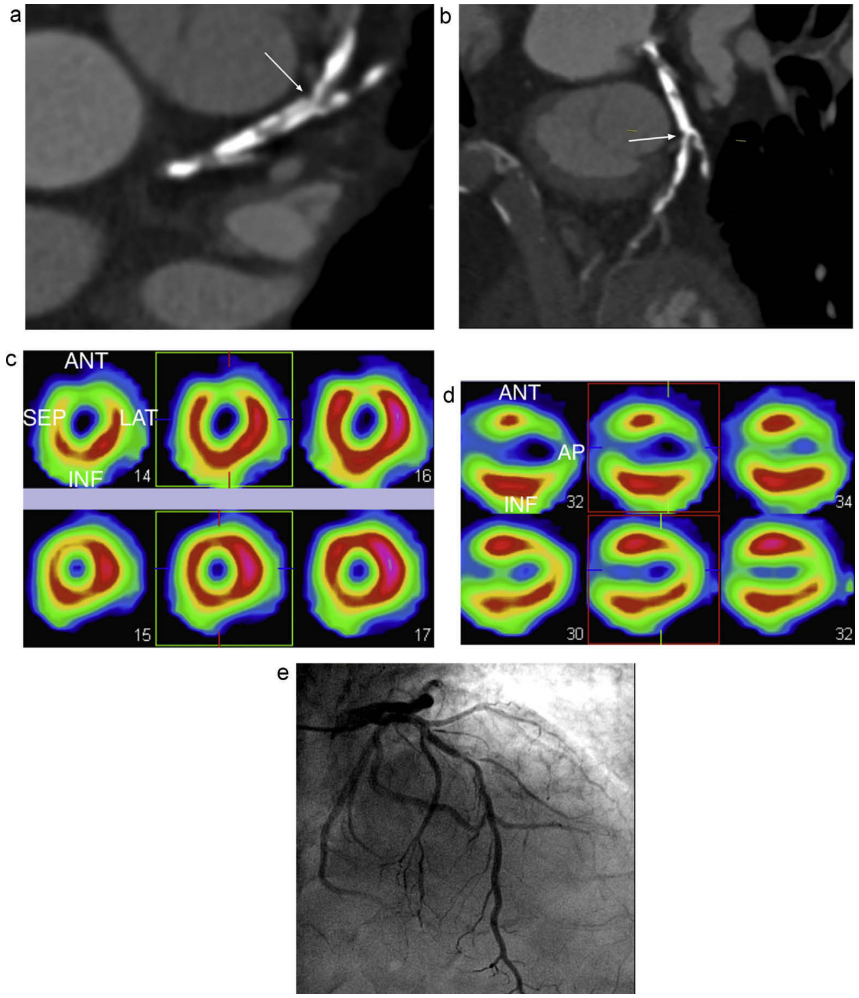

Fig. 2. 72-year old male patient with stable idiopathic pulmonary fibrosis (CAC score: 2709). CT angiographic examination: oblique transverse CT section (a) and curved MPR (b) centred on mid LAD, showing massive calcifications and mid LAD stenosis (arrow). Note the additional presence of stenosis at the level of the origin of the second diagonal branch. Myocardial perfusion scintigraphy (MPS): short axis (c) and vertical long axis (d) views. This patient underwent an exercise test and reached a peak heart rate of 129 bpm (87% predicted heart rate) without ECG abnormality. Stress and rest images show a large anteroseptal ischaemia, corresponding to 15% of the myocardial mass. (e) Invasive coronary angiography (LAO 10, cranial 40). Angiographic confirmation of mid LAD stenosis (arrow). Note the additional presence of stenosis at the origin of the second diagonal branch.

evaluation, 52 patients had an unknown CAD status at the time of referral; 11 of them (11/52; 21.2) had significant coronary stenosis at coronary angiography. The pathogenesis of CAD in IPF patients remains largely debated. Izbicki et al. suggested that the inflammatory process in pulmonary fibrosis could eventually involve the coronary arteries as a part of a systemic inflammatory disease, rather than being an idiopathic process confined to the lungs [5]. Alternatively, it has been postulated that IPF and acute coronary syndromes share common etiologic factors, most notably cigarette smoking. In keeping with this hypothesis, it is interesting to note that the prevalence of CAD in f-IIP patients with severe lung disease is in the range of that reported in COPD. In a large cohort of 1664 COPD patients, Divo et al. [27] have recently reported a 30% prevalence of CAD.

In contrast to a recent study detecting CAD only on the basis of CAC scores [10], our screening programme for subclinical atherosclerosis was based on the complementarity between CT and myocardial perfusion scintigraphy. At the time of the patients' referral for follow-up, we modified the CT scanning mode to provide comprehensive cardiothoracic information. Using CAC, it was possible to depict patients with atherosclerosis owing to the close correlation between extent of CAC and atherosclerotic plaque burden. The anatomical characteristics of atherosclerosis were then provided with coronary CTA which allowed us to assess the location, severity and characteristics of atherosclerotic plaques. Because of well-known limitations for CAC and coronary CTA to diagnose obstructive CAD [24–26], CT morphological evaluation was completed by perfusion scintigraphy to depict flow-limiting coronary stenosis. On the basis of this combination, 32 patients were referred to the cardiologist. It should be underlined that this stratification of our study group could not be predicted by the clinical, biological and/or pulmonary functional presentation

at the time of their annual follow-up. This lack of predictive factors has already been pointed out by Izbicki et al. Investigating the incidence of CAD in lung-transplantation candidates with emphysema and lung fibrosis, these authors found that the tendency to develop significant CAD among patients with fibrosis as compared with emphysema could not be predicted by the measurement of traditional risk factors [5].

Regarding the clinical benefits of this screening programme for our population, one should underline that 5 patients underwent coronary revascularization for significant CAD and 27 patients, i.e., 64% of the study group, were prescribed statins and/or beta-blockers. In the absence of specific attention to CAD, these patients would not have received these medications. These findings tend to confirm that the presence of a serious lung disease might distract medical attention from routine cardiovascular care, and that primary and secondary prevention interventions are often neglected in IPF patients [3]. Although not investigated in the present study, one might expect that an early detection of CAD in IPF might improve patients' survival, as an impact as the presence of CAD has been shown to be associated with a worse outcome [9], further reinforced by the high frequency of atypical angina [28]. The presence of underlying CAD is also important to investigate as IPF patients are potential candidates for lung transplantation. Whereas no longer considered as an absolute contraindication for lung transplantation, CAD remains an important potential complicating factor for surgical candidates [5,29,30]. Despite the fact that combined coronary artery bypass and bilateral lung transplantation has been described [29], it would be more suitable to detect and treat CAD before end-stage lung disease. As recently recommended by guidelines for lung transplantation [31], it would allow an orderly process of assessment, management of areas of concern, and patient education before active listing. This is further reinforced by the impossibility to predict the outcome of IPF patients, and thus to differentiate patients with a slowly progressive decline in lung function from those with rapidly progressive IPF [32,33]. It has been shown that a gradual progressive decline does not occur in many patients, thereby supporting the need for early referral for lung transplantation [34]. It should be underlined that our approach only searched for flow-limiting coronary stenosis and myocardial ischaemia. The prognosis of CAD, however, is more closely related to atherosclerotic plaque burden and stability than the extent of a particular stenosis. As appropriate preventive strategies can be instituted at this stage, specific evaluation of this preclinical and pre-flow limiting phase of CAD in IPF would also be clinically relevant.

Several limitations in our study should be noted. Firstly, our study group included a small cohort of patients which is directly linked to IPF incidence. Subsequently, our findings have to be confirmed in larger populations. Secondly, we included two conditions, IPF and NSIP which have different clinical courses. However, we limited the NSIP group to fibrotic NSIP which does not represent major bias according to the potential overlap between the two subgroups. Thirdly, no attempt was made to compare the respective impact of CT and scintigraphy in the depiction of CAD. This was a direct consequence of our study design in which invasive coronary angiography could not be systematically performed in asymptomatic patients.

In the studied population of patients with stable f-IIP, asymptomatic CAD ranged between 12% and 26%.

Conflicts-of-interest

For each author, no significant conflicts of interest exist with any companies or organizations whose products or services are mentioned in this article.

Conception and design: M.R.J., B.W., C.D., C.H.F.

Analysis and interpretation: B.W., E.M., L.C., V.G., J.B.F., F.M., G.P., A.D.

Drafting the manuscript for important intellectual content: M.R.J., B.W., J.R.

References

[1] American Thoracic Society/European Respiratory, Society. Idiopathic pulmonary fibrosis: diagnosis and treatment: international consensus, statement. Am J Respir Crit Care Med 2000;161:646–64.

[2] Olson AL, Swigris JJ, Lezotte DC, Norris JM, Wilson CG, Brown KK. Mortality from pulmonary fibrosis increased in the United States from 1992 to 2003. Am J Respir Crit Care Med 2007;176:277–84.

[3] Hubbard RB, Smith C, Le Jeune I, Gribbin J, Fogarty AW. The association between idiopathic pulmonary fibrosis and vascular disease. A population-based study. Am J Respir Crit Care Med 2008;178:1257–61.

[4] Kizer JR, Zisman DA, Blumenthal NP, Kotloff RM, Kimmel SE, Strieter RM, et al. Association between pulmonary fibrosis and coronary artery disease. Arch Intern Med 2004;164:551–6.

[5] Izbicki G, Ben-Dor I, Shitrit D, Bendayan D, Aldrich TK, Kornowski R, et al. The prevalence of coronary artery disease in end-stage pulmonary disease: is pulmonary fibrosis a risk factor? Respir Med 2009;103:1346–9.

[6] Ponnuswamy A, Manikandan R, Sabetpour A, Keeping IM, Finnerty JP. Association between ischaemic heart disease and interstitial lung disease: a case-control study. Respir Med 2009;103:503–7.

[7] Daniels CE, Yi ES, Ryu JH. Autopsy findings in 42 consecutive patients with idiopathic pulmonary fibrosis. Eur Respir J 2008;32:170–4.

[8] Panos RJ, Mortenson RL, Niccoli SA, King Jr TE. Clinical deterioration in patients with idiopathic pulmonary fibrosis. Am J Med 1990;88:396–404.

[9] Nathan SD, Basavaraj A, Reichner C, Shlobin OA, Ahamd S, Kiernam J, et al. Prevalence and impact of coronary artery disease in idiopathic pulmonary fibrosis. Respir Med 2010;104:1035–41.

[10] Nathan SD, Weir N, Shlobin OA, Urban BA, Curry CA, Basavaraj A, et al. The value of computed tomography scanning for the detection of coronary artery disease in patients with idiopathic pulmonary fibrosis. Respirology 2011;16:481–6.

[11] Travis WD, Costabel U, Hansell DM, King Jr TE, Lynch DA, Nicholson AG, et al. An official ATS/ERS statement: update of the international multidisciplinary classification of the idiopathic interstitial pneumonias. Am J Respir Crit Care Med 2013;188:733–48.

[12] Raghu G, Collard HR, Egan JJ, Martinez FJ, Behr J, Brown KK, et al. An official ATS/ERS/JRS/ALAT statement: idiopathic pulmonary fibrosis: evidence-based guidelines for diagnosis and treatment. Am J Respir Crit Care Med 2011;183:788–824.

[13] Travis WD, Hunninghake G, King Jr TE, Lynch DA, Colby TV, Galvin JR, et al. Idiopathic nonspecific interstitial pneumonia. Report of an American Thoracic Society project. Am J Crit Care Med 2008;177:1338–47.

[14] Fell CD. Idiopathic pulmonary fibrosis: phenotypes and comorbidities. Clin Chest Med 2012;33:51–7.

[15] Cottin V, Crestani B, Valeyre D, Wallaert B, Cadranel J, Dalphin JC, et al. French practical guidelines for the diagnosis and management of idiopathic pulmonary fibrosis from the National Reference and Competence Centers for Rare Diseases and the French Society of Pulmonology. Rev Mal Respir 2013;30:879–902.

[16] Standardized lung function testing. Official statement of the European Respiratory, Society. Eur Respir J Suppl 1993;16:1–100.

[17] Stocks J, Quanjer PH. Reference values for residual volume, functional residual capacity and total lung capacity. ATS Workshop on Lung Volume Measurements. Official Statement of the European Respiratory Society. Eur Respir J 1995;8:492–506.

[18] Pellegrino R. Interpretative strategies for lung function tests. Eur Respir J 2005;26:948–68.

[19] Huda W, Odgen KM, Khorasani MR. Converting dose-length product to effective dose at CT. Radiology 2008;248:995–1003.

[20] Agatston AS, Janowitz WR, Hildner FJ, Zusmer NR, Viamonte Jr M, Detrano R. Quantification of coronary artery calcium using ultrafast computed tomography. J Am Coll Cardiol 1990;15:827–32.

[21] Austen WG, Edwards JE, Frye RL, Gensini GG, Gott VL, Griffith LS, et al. Reporting system on patients evaluated for coronary artery disease: Report of the Ad Hoc Committee for Grading of Coronary Artery Disease, Council on Cardiovascular Surgery, American Heart Association. Circulation 1975;51(Suppl. 4):5–40.

[22] Desai SR, Veeraraghavan S, Hansell DM, Nikolakopolou A, Goh NS, Nicholson AG, et al. CT features of lung disease in patients with systemic sclerosis: comparison with idiopathic pulmonary fibrosis and nonspecific interstitial pneumonias. Radiology 2004;232:560–7.

[23] Berman DS, Abidov A, Kang X, Hayes SW, Friedman JD, Sciammarella MG, et al. Prognostic validation of a 17-segment score derived from a 20-segment score for myocardial perfusion SPECT interpretation. J Nucl Cardiol 2004;11:414–23.

[24] Montalescot G, Sechtem U, Achenbach S, Andreotti F, Arden C, Budaj A, et al. 2013 ESC guidelines on the management of stable coronary artery disease. Eur Heart J 2013;34:2949–3003.

[25] Hamon M, Biondi-Zoccai GG, Malagutti P, Agostoni P, Morello R, Valgimigli M. Diagnostic performance of multislice spiral computed tomography of coronary

arteries as compared with conventional invasive coronary angiography: a meta-analysis. J Am Coll Cardiol 2006;48:1896–910.
[26] Shaw LJ, Berman DS, Maron DJ, Mancini GB, Hayes SW, Hartigan PM, et al. Optimal medical therapy with or without percutaneous coronary intervention to reduce ischemic burden. Circulation 2008;117:1283–91.
[27] Divo M, Cote C, de Torres JP, Casanova C, Marin JM, Pinto-Plata V. Comorbidities and risk of mortality in patients with chronic obstructive pulmonary disease. Am J Crit Care Med 2012;186:155–61.
[28] Diamond GA, Forrester JS. Improved interpretation of a continuous variable in diagnostic testing: probabilistic analysis of scintigraphic rest and exercise left ventricular ejection fractions for coronary disease detection. Am Heart J 1981;102:189–95.
[29] Lee R, Meyers BF, Sundt TM, Turlock EP, Patterson GA. Concomitant coronary artery revascularization to allow successful lung transplantation in selected patients with coronary artery disease. J Thorac Cardiovasc Surg 2002;124:1250–1.
[30] Patel VS, Palmer SM, Messier RH, Davis RD. Clinical outcome after coronary artery revascularization and lung transplantation. Ann Thorac Surg 2003;75:372–7.
[31] Orens JB, Estenne M, Arcasoy S, Conte JV, Corris P, Egan JJ, et al. Internationa guidelines for the selection of lung transplant candidates: 2006 update – a consensus report from the pulmonary scientific council of the Internationa Society for Heart and Lung Transplantation. J Heart Lung Transplant 2006;25 745–55.
[32] Ley B, Collard HR, King TE. Clinical course and prediction of survival in idiopathic pulmonary fibrosis. Am J Respir Crit Care Med 2011;183:431–40.
[33] Barlo NP, van Moorsel CHM, van den Bosch JMM, Grutters JC. Predicting prognosis in idiopathic pulmonary fibrosis. Sarcoidosis Vasc Diffuse Lung Dis 2010;27:85–95.
[34] Martinez FJ, Safrin S, Weycker D, Starko KM, Bradford WZ, King Jr TE, et al. The clinical course of patients with idiopathic pulmonary fibrosis. Ann Intern Med 2005;142:963–7.

Conclusion :

Nous avons pu mettre en évidence une prévalence non négligeable de la pathologie coronarienne chez les patients porteurs de fibrose pulmonaire idiopathique, la dyspnée pouvant donc être chez eux plurifactorielle. Le pronostic d'un patient atteint de fibrose pulmonaire est évalué en fonction de l'importance de la dyspnée, des EFR, de la saturation percutanée en oxygène en fin de test de marche, mais aussi de la présence ou non de signes d'hypertension pulmonaire et des lésions scanographiques. La recherche de comorbidités (pathologies cardio-vasculaires, maladie veineuse thromboembolique, diabète, dépression) ne fait pas aujourd'hui partie des recommandations mais elle est proposée dans la prise en charge de ces patients (12), et ce d'autant plus que plusieurs études ont montré la fréquence élevée de comorbidités notamment liées au tabagisme (13).

Le caractère inflammatoire chronique de la pathologie pulmonaire interstitielle est également un facteur de développement de la coronaropathie (14).

La possibilité de traitement et de prise en charge de cette coronaropathie chez des patients pour lesquels le traitement curatif de la fibrose pulmonaire (en dehors de la transplantation pulmonaire) n'est pas possible, pourrait permettre une amélioration de la tolérance à l'effort.

Plus largement, la détection et la prise en charge des comorbidités chez ces patients permet notamment d'augmenter leur tolérance à l'effort, alors que le traitement curatif de la pathologie interstitielle pulmonaire n'est pas possible.

Le Coeur gauche dans la pathologie obstructive chronique :

Left atrial volume in chronic obstructive pulmonary disease.

Cassagnes L, Pontana F, Molinari F, Faivre JB, Santangelo T, Algeri E, Duhamel A, Remy J, Remy-Jardin M.

J Thorac Imaging. 2014 Jul;29(4):233-9.

On sait que la BPCO est associée à une augmentation de la prévalence de la coronaropathie, mais la bronchopathie chronique obstructive chez les fumeurs se traduit par une destruction parenchymateuse avec développement de l'emphysème, et une bronchopathie isolée ou associée à l'emphysème. Nous avons réalisé une étude rétrospective sur des données acquises prospectivement dans une population de patients fumeurs. Le but de notre étude était d'étudier la corrélation avec la sévérité de l'emphysème, donc la diminution du retour veineux pulmonaire par destruction capillaire, et le volume indexé de l'oreillette gauche. Le volume de l'oreillette gauche impactant le remplissage ventriculaire gauche et donc la fonction diastolique ventriculaire gauche.

Abstract :

Objectif :

Le but de cette étude était d'évaluer le volume auriculaire gauche chez des patients fumeurs corrélé à l'importance de l'emphysème, en cherchant à prouver indirectement la réduction du retour veineux pulmonaire secondaire à la destruction capillaire.

Matériel et méthodes :

121 patients fumeurs ont bénéficié d'un angioscanner avec pitch élevé et haute résolution, permettant la quantification de l'emphysème, du volume pulmonaire total, et de la mesure du volume de l'oreillette gauche indexé à la surface corporelle.

Résultats :

Les phénotypes scanographiques étaient les suivants : emphysème prédominant (groupe 1, n = 57), atteinte bronchique prédominante (groupe 2, n= 30), atteinte mixte emphysème et bronchopathie (groupe 3, n= 15), absence de signes scanographiques de BPCO (groupe 4, n= 19). Une corrélation négative a été retrouvée entre le volume indéxé de l'oreillette gauche et le pourcentage d'emphysème : (a) dans la population complète de l'étude (P=0.032; r = -0.19); (b) dasn le groupe 1(P=0.0163; r = -0.32); et (c) dans les groupes 1 et 3 analysés conjointement (P=0.0492; r = -0.23). Une correlation négative était retrouvée entre le volume indéxé de l'oreillette gauche et le volume pulmonaire total dans la population complete de l'étude (P=0.039; r = -0.19) et dans le groupe 1 (P=0.048; r = -0.26), alors qu'aucune correlation n'était trouvée dans le groupe 2 (P=0.44; r = -0.15), le groupe 3 (P=0.52; r = -0.17), et les groupes 1 et 3 analysés conjointement (P=0.14; r = -0.17).

Conclusion:

Le volume indéxé de l'oreillette gauche, impactant la pré-charge ventriculaire gauche, est corrélé à la sévérité de l'emphysème.

Left Atrial Volume in Chronic Obstructive Pulmonary Disease

Lucie Cassagnes, MD,† François Pontana, MD,* Francesco Molinari, MD,* Jean-Baptiste Faivre, MD,* Teresa Santangelo, MD,* Emmanuela Algeri, MD,* Alain Duhamel, MD,‡ Jacques Remy, MD,* and Martine Remy-Jardin, MD, PhD**

Purpose: The aim of the study was to evaluate left atrial (LA) volume in smokers according to the severity of emphysema, with the objective of providing indirect evidence of reduced pulmonary venous return due to capillary destruction.

Materials and Methods: A total of 121 smokers underwent a high-pitch and high–temporal resolution computed tomography (CT) angiographic examination, enabling quantification of emphysema, total lung volume, and LA volume measurements normalized to body surface area.

Results: The CT phenotypes were as follows: emphysema predominant (group 1; n = 57); airway predominant (group 2; n = 30); a mixed pattern of emphysema and airway disease (group 3; n = 15); and absence of bronchopulmonary CT abnormalities (group 4; n = 19). A negative correlation was found between the indexed LA volume and the percentage of emphysema: (a) in the overall study group ($P = 0.032$; $r = -0.19$); (b) in group 1 ($P = 0.0163$; $r = -0.32$); and (c) in groups 1 and 3 when analyzed together ($P = 0.0492$; $r = -0.23$). A negative correlation was found between the indexed LA volume and the total lung volume in the overall study group ($P = 0.039$; $r = -0.19$) and in group 1 ($P = 0.048$; $r = -0.26$), whereas no correlations were found in group 2 ($P = 0.44$; $r = -0.15$), group 3 ($P = 0.52$; $r = -0.17$), and groups 1 and 3 analyzed as a whole ($P = 0.14$; $r = -0.17$).

Conclusions: The indexed LA volume, impacting left ventricular preload, is correlated to the severity of emphysema.

Key Words: dual-source computed tomography, left atrium, left ventricular function, smokers, emphysema

(*J Thorac Imaging* 2014;29:233–239)

Whereas abnormal left ventricular (LV) systolic function in the absence of coronary artery disease is rarely encountered in chronic obstructive pulmonary disease (COPD), LV diastolic dysfunction is a frequently reported echocardiographic observation.[1–5] Mostly studied in patients with moderate to severe COPD, the LV of emphysema patients is hypovolemic, manifesting in small LV end-diastolic dimensions, concomitantly observed with modifications of the LV filling dynamics.[1,3,5–7] The low LV preload in stable COPD patients has recently been linked to decreased intrathoracic blood volume measured on magnetic resonance studies in patients with severe emphysema.[6]

Two mechanisms have been proposed to explain the intrathoracic hypovolemia in severe COPD, namely a decreased compliance of the pulmonary vascular bed due to the hyperinflated lungs and a destruction of the capillary bed by the emphysematous disease.[1,6] In a recent study investigating a large cohort of patients with mild emphysema, Barr et al[8] also observed impaired LV filling and related the limited LV flow to the subclinical loss of lung parenchyma and pulmonary capillary bed. Because the left atrium (LA) collects the pulmonary venous return, we hypothesized that a reduction in the intrathoracic blood volume due to emphysematous lung destruction would affect the LA volume, which, in turn, could provide indirect evidence of reduced LV diastolic dysfunction in COPD patients.

The main objective of this study was thus to search for a negative correlation between severity of emphysema and LA volumes in an unselected population of smokers referred for chest computed tomography (CT) angiographic examinations. Were this hypothesis to be verified, the LA could become an additional area of interest on chest CT examinations in COPD populations.

MATERIALS AND METHODS

Population

Our study group was drawn from a population of 133 consecutive smokers who underwent a high–temporal resolution, high-pitch CT angiographic (CTA) examination of the chest, that is, the standard CTA protocol in our institution, during a 4-month period (December 2010 to March 2011). Chest CT examinations had been indicated for (a) evaluation of respiratory symptoms such as progressive worsening of dyspnea and atypical chest pain, (b) suspicion of chest radiographic abnormality, and (c) presurgical evaluation of small-sized lung nodules with high probability of malignancy. In these situations, chest CT examinations were obtained with injection of contrast material, using the standard protocol in our department for chest imaging with dual-source CT technology—that is, a high–temporal resolution and high-pitch protocol, which will be described in the following section of this manuscript. For the purpose of the present study, we excluded 12 patients with a previous history of coronary artery disease (n = 3), known valvular heart disease (n = 2), dilated cardiomyopathy (n = 1), congenital heart disease (n = 1), or atrial tachyarrhythmia (n = 5), leading to a final study group of 121 patients. This cohort represented an unselected population of consecutive smokers free of clinical cardiovascular disease. All patients were scanned during clinical workup with interpretation of CT examinations during the course of our clinical activity;

From the Departments of *Thoracic Imaging; ‡Medical Statistics, Hospital Calmette (EA 2694), Univ Lille Nord de France, Lille; and †Department of Radiology, University Centre of Gabriel Montpied, University of Clermont-Ferrand, Clermont-Ferrand, France.

The authors declare no conflicts of interest.

Reprints: Martine Remy-Jardin, MD, PhD, Department of Thoracic Imaging, Hospital Calmette, Boulevard Jules Leclercq, 59037 Lille cedex, France (e-mail: martine.remy@chru-lille.fr).

storage of data sets on external disks enabled their retrospective analysis. Pulmonary function tests, performed within 2 months of CT examinations, were available for 105 patients, all of whom were inpatients, and were not available for the remaining 16 patients, who had been referred as outpatients. On the basis of the available pulmonary function tests, the mean (± SD) forced expiratory volume in 1 second (FEV_1) was 67.46% (± 25.15%) of predicted values (range, 13% to 113%), and the mean FEV_1/forced vital capacity ratio was 59.66 (± 16.73) (range, 21.15 to 90.58). The study was approved by the local ethics committee with a waiver of patients' informed consent in agreement with national regulations.

CT Examination

Chest CTAs were obtained on a dual-source CT system (Definition Flash; Siemens, Germany).

Acquisition Parameters

The acquisition parameters included: (a) a dual-source, single-energy protocol with a temporal resolution of 75 ms and a pitch of 3.0; (b) a craniocaudal acquisition after deep inspiration; (c) detector collimation: $64 \times 2 \times 0.6$ mm by means of a z-flying focal spot; (c) a kilovoltage of 100 kV (reference milliamperage: 90 mAs) for patients with a body weight of < 80 kg; and a kilovoltage of 120 kV (reference milliamperage: 90 mAs) for patients with a body weight between 80 and 100 kg; (d) systematically obtained examinations with automatic adjustment of the milliamperage according to the patient's size (Care Dose 4D; Siemens Medical Solutions, Germany), without administration of β-blockers.

Injection Parameters

The injection protocol consisted of the administration of 120 mL of a 35% iodinated contrast agent (iohexol; Omnipaque 350; Amersham Health, Carrigtohill, Ireland) at a flow rate of 4 mL/s, using a dual-headed pump injector (Stellant Medrad France, Rungis, France) without saline flush. The threshold of the bolus tracking system (Care Bolus; Siemens Healthcare, Forchheim, Germany) was set at 150 HU, with the region of interest positioned within the descending aorta.

Reconstructions

For the overall chest CT evaluation, the reconstructed images consisted of 1-mm-thick lung and mediastinal images, reconstructed with standard reconstruction kernels (mediastinal images: soft reconstruction kernel [B20f]; lung images: high–spatial resolution algorithm [B50f]) with a field of view adapted to the patient's size. All images were viewed in both mediastinal (window width, 450 HU; window center, 50 HU) and lung parenchymal (window width, 1600 HU; window center, −600 HU) window settings. An automated quantification of lung volumes and emphysematous lesions was obtained using a dedicated software as described later. For the purpose of assessing LA volumes, cross-sectional images were reconstructed from the carina to the cardiac base with a slice thickness of 0.75 mm at 0.6 mm intervals, a small field of view, and a soft-tissue convolution kernel (B26f). The images were transferred to an off-line computer workstation (Leonardo workstation; Siemens Medical Solutions) for postprocessing in a standardized manner using a dedicated cardiac CT visualization software (Circulation; Siemens Medical Solutions). Postprocessing was then realized using the Inspace software on a Syngo MMWP workstation (Siemens Healthcare).

CT Parameters Analyzed

Scanning Conditions

We systematically recorded the duration of data acquisition, *z*-axis coverage, and patient radiation dose, using the dose-length product in mGy.cm calculated by the CT computer. On lung inspiratory scans, we recorded the presence of cardiac and/or respiratory motion artefacts to provide information on the overall quality of lung images before quantitative analyses.

Smoking-related CT Features

Visual analysis of lung images led the readers to evaluate the presence of smoking-related CT changes, that is, emphysema, bronchial wall thickening, bronchiectasis (further categorized as central airway disease), centrilobular micronodules, bronchiolectasis, and tree-in-bud pattern (further described as small-airway disease). Depending on the predominant abnormality observed on a given CT examination and following the current stratification of COPD populations,[9] each patient was classified into one of the following subgroups: emphysema predominant (group 1) (Fig. 1); airway disease predominant (group 2) (Fig. 2); presence of both airway disease and emphysema with no predominance of either abnormality (group 3); or no bronchopulmonary CT abnormality (group 4).

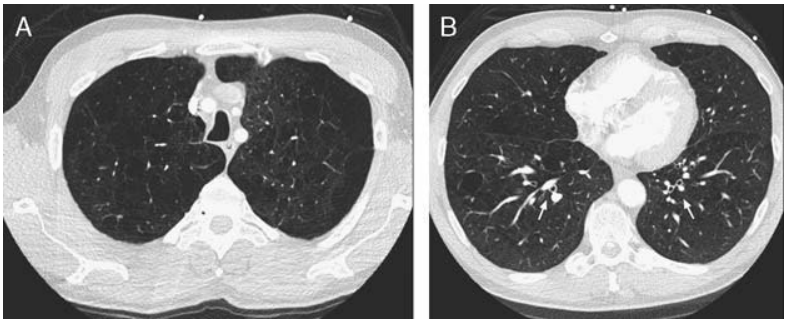

FIGURE 1. A 58-year-old male smoker (38 pack-years) illustrating the CT phenotype of "emphysema predominance." Transverse CT sections (1 mm thick) obtained at the level of the upper (A) and lower (B) lung zones showing marked emphysematous destruction with an upper-lobe predominance and mild bronchial wall thickening (arrows, B).

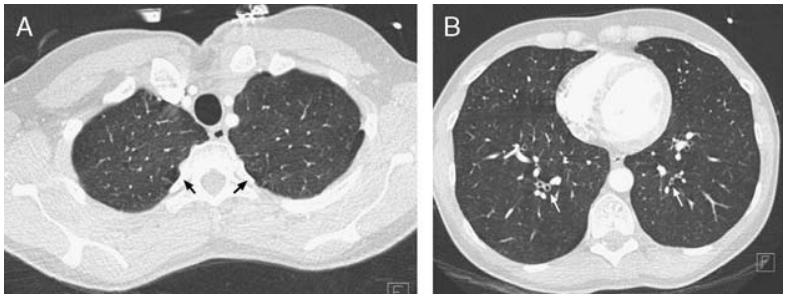

FIGURE 2. A 41-year-old female smoker (18 pack-years) illustrating the CT phenotype of "airway disease predominance." Transverse CT sections (1 mm thick) obtained at the level of the upper (A) and lower (B) lung zones showing marked bronchial wall thickening (white arrows, B) and a few bullae (black arrows, A) in the apices.

Marker of Right Ventricular (RV) Dysfunction

The ratio of the RV to LV short-axis diameters (RV/LV) was calculated by measuring the minor axes of the RV and LV of the heart in the transverse plane at their widest points between the inner surface of the free wall and the surface of the interventricular septum.[10] An RV/LV ratio >1 was indicative of RV dysfunction with deviation of the interventricular septum toward the LV.

Quantitative Analysis

The LA volume was obtained after automatic contouring of the atrial cavity by using Inspace software and manual exclusion of the pulmonary veins. The LA appendage was systematically included in the final volume. All measurements were normalized for body surface area (ie, atrial indices).

An automated quantification of lung volumes and emphysematous lesions was obtained as further described. Image data sets, consisting of contiguous 1-mm-thick inspiratory lung CT scans, reconstructed with a soft kernel (B20), were sent to a research workstation (Syngo MMWP version 2007-A; Siemens Forchheim) running MevisPulmo software, version 3.0 (MeVis Bremen, Germany). Automated lobar quantification of emphysema consisted of a multi-step process.[11]

(1) Segmentation of the overall airspace by applying an upper threshold of -400 HU, followed by an automated segmentation of the tracheobronchial tree up to the segmental level.
(2) Lobar segmentation allowing automated delineation of each of the 5 pulmonary lobes. A colored mask was superimposed on the CT images, with a different color for each lobe. By scrolling through the multiplanar images, it was possible to evaluate whether the automated lobar segmentation was adequate. If necessary it was possible to manually correct the lobar limits displayed by the software.
(3) Low-attenuation area segmentation using an upper threshold of -960 HU.[12]
(4) Final display of quantification results in a table indicating for the whole lung, the right and left lung and each of the 5 lobes, the absolute and relative volume, and the low-attenuation area proportion representing the emphysema score.

Conditions of Image Analysis

The smoking-related CT features and measurements of RV and LV diameters were determined by consensus between 2 readers (L.C., a senior cardiovascular radiologist with 10 y of experience in reading CT scans; and J.-B.F., a senior cardiovascular radiologist with 10 years of experience in chest CT imaging) without information on the subjects' clinical status. The cardiovascular radiologist then undertook the objective quantification of emphysema and LA volumetric analysis.

Statistical Analysis

The study design was conducted as follows: (a) the main purpose of this study was to search for relationships between the severity of emphysema, expressed as a percentage of lung volume affected by lung destruction, and the volume of the LA, the latter being indexed to the body surface area; (b) at the time of initiation of this study, there were no specific data in the literature enabling us to calculate the sample size; consequently, we did not compute a sample size on the basis of an effect size defined a priori; (c) considering that emphysema is a frequent finding in the populations of smokers regularly referred to our department, we designed this investigation as an observational study over a 4-month period. This interval of time was considered to be sufficient to investigate a wide range of emphysematous lesions and, thus, to be compatible with the main objective of this study.

Statistical analysis was performed with commercially available software (SAS Institute, Cary, NC; version 9.1). Results were expressed as means, SDs, medians, and ranges for continuous variables and as frequencies and percentages for categorical variables. For continuous variables, comparisons of groups were performed using the Kruskal-Wallis test. All post hoc comparisons were adjusted using the Bonferroni correction. Depending on the sample size, the relationships between continuous variables were assessed by the Pearson correlation coefficient or the Spearman correlation coefficient. The statistical significance was defined as $P < 0.05$.

RESULTS

Population Characteristics

The study population included 89 male and 32 female patients with the following characteristics: (a) mean (± SD) age: 56.38 (± 12.59) years (range, 26 to 88 y); (b) mean (± SD) body mass index: 22.85 (± 4.44) kg/m^2 (range, 13.74 to 35.26 kg/m^2); (c) mean (± SD) body surface area: 1.77 (± 0.21) m^2 (range, 1.19 to 2.39 m^2); (d) mean (± SD) cigarette consumption: 41.85 (± 28.20) pack-years (range, 3 to 140); (e) mean (± SD) heart rate: 76.02 (± 17.52) bpm (range, 47 to 139 bpm). The scanning conditions were

characterized by: (a) a mean (± SD) *z*-axis coverage of 337.67 (± 27.39) mm (range, 263 to 402 mm); (b) a mean duration of data acquisition of 0.78 (± 0.07) seconds (range, 0.58 to 0.93); and (c) a mean (± SD) dose-length product of 102.34 (± 24.97) mGy.cm (range, 30 to 191 mGy.cm).

The overall image quality of lung images was deemed acceptable for depiction and quantification of emphysema: (a) mild respiratory motion artefacts were depicted in the lower lung zones in 2 patients (2/121; 1.6%); (b) minimal motion artifacts were depicted around the cardiac cavities in 7 patients (7/121; 5.8%).

Regarding quantitative data in the overall study group: (a) the median value of emphysema was 3.2% (range, 0% to 58%); (b) the mean (± SD) value of the total lung volume (TLV) was 5935.6 (± 1343.5) mL (range, 1982 to 9464 mL); and (c) the mean (± SD) indexed LA volume was 43.2 (± 12.6) mL/m^2 (range, 22.4 to 83.1 mL/m^2). The RV/LV ratio was <1.0 in 104 patients and >1 in 17 patients.

The study population was divided into 4 subgroups according to the smoking-related CT phenotypes, including 57 patients in group 1 (ie, emphysema predominant), 30 patients in group 2 (ie, airway disease predominant), 15 patients in group 3 (ie, airway disease and emphysema with no predominance of either abnormality), and 19 patients in group 4 (ie, no bronchopulmonary abnormalities). As shown in Table 1, there was a statistically significant difference in the mean percentage of emphysema ($P < 0.0001$) and TLV ($P = 0.0007$) between groups. A detailed analysis of intergroup differences is summarized in Graph 1: (a) regarding the percentage of emphysema, it was significantly higher (a1) in group 1 compared with group 2 ($P = 0.0001$); and (a2) in group 3 compared with group 2 ($P = 0.0102$); (b) the TLV in group 1 was significantly higher than that of group 2 ($P = 0.0108$) and group 4 ($P = 0.0036$).

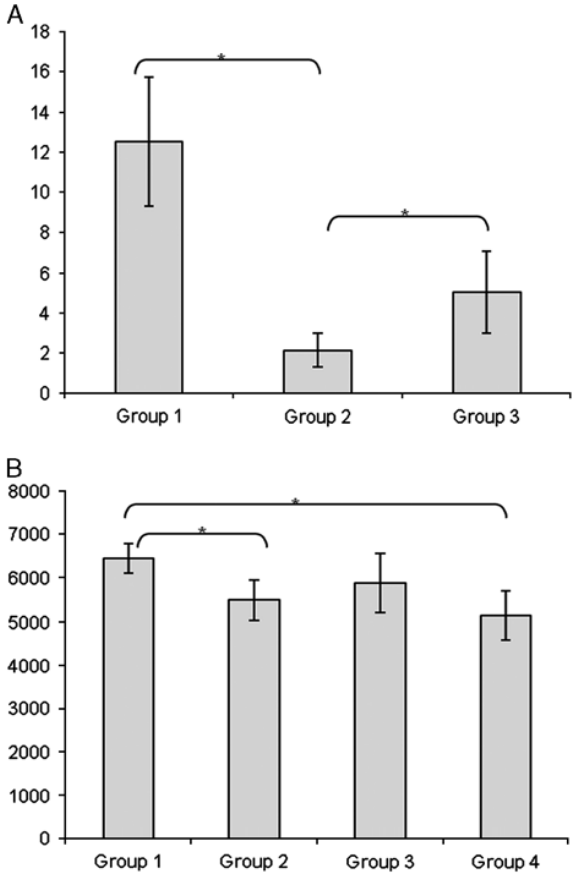

GRAPH 1. Group-by-group comparisons of quantitative CT findings in the study population. A, Comparison of the severity of emphysema (expressed as percentages). Post hoc comparisons were adjusted using the Bonferroni correction. *$P<0.05$. B, Comparison of the TLV (expressed in mL). Post hoc comparisons were adjusted using the Bonferroni correction. *$P<0.05$.

Correlations Between LA Volume and Severity of Emphysema

Overall Percentage of Emphysema

We found a negative correlation between the indexed LA volume and the overall percentage of emphysema: (a) in the entire study group ($P = 0.032$; $r = -0.19$); (b) in group 1 ($P = 0.0163$; $r = -0.32$); and (c) in group 1 and group 3 when analyzed together ($P = 0.0492$; $r = -0.23$). No correlation was found between the indexed LA volume and the percentage of emphysema in group 2 ($P = 0.931$; $r = 0.02$) and group 3 ($P = 0.3147$; $r = 0.28$) (Figs. 3, 4).

Lobar Percentage of Emphysema

We found a negative correlation between the indexed LA volume and the percentage of emphysema in the right

TABLE 1. Quantitative Findings in the Study Population Stratified by Smoking-related CT Features

	Group 1 Emphysema Predominant n = 57	Group 2 Airway Disease Predominant n = 30	Group 3 Presence of Emphysema and Airways Disease n = 15	Group 4 No Bronchopulmonary Abnormality n = 19	*P*
Emphysema (%)					
Mean ± SD	12.5 ± 12.1	2.1 ± 2.3	5.1 ± 3.7	1.3 ± 0.8	< 0.0001
Range	0.3-58	0-9.6	0.3-12.1	0.2-2.8	
Median	8.1	1.4	3.9	0.9	
TLV (mL)					
Mean ± SD	6447.3 ± 1296.4	5491.7 ± 1219.2	5886.3 ± 1241.7	5140.3 ± 1176.1	0.0007
Range	4138-9464	1982-8243	4004-8113	3032-7386	
Median	6449	5547	5797	4822	

Comparisons were obtained using the Kruskal-Wallis test.

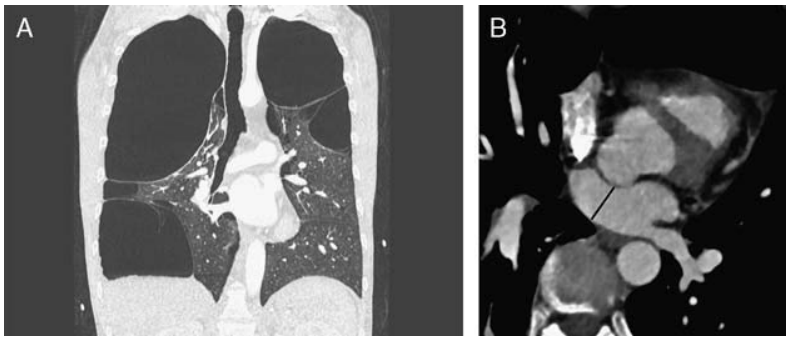

FIGURE 3. A 27-year-old male smoker (10 pack-years), referred as a potential candidate for surgical resection of bullae. A, Coronal view of the lungs obtained at the level of the carina, illustrating the severity of emphysematous destruction found to predominate in the right lung (quantitative estimation of emphysema: 58%). The indexed LA volume was 34.11 mL/m^2. B, Cross-section (magnified view), obtained at the level of the aortic root. The small LA volume can be visually suspected when observing the reduced anteroposterior LA diameter (black line).

upper and right middle lobes ($P = 0.03$; $r = -0.29$) in group 1. A similar trend was observed in the overall study group but without reaching statistical significance ($P = 0.0586$). No significant results were found when analyzing groups 1 and 3 together.

Correlations Between LA Volume and Lung Volume

We found a negative correlation between the indexed LA volume and the TLV: (a) in the overall study group ($P = 0.0388$; $r = -0.19$); (b) in the emphysema group (group 1; $P = 0.0483$; $r = -0.26$). No correlations were found in the airway-predominant group (group 2; $P = 0.5544$; $r = -0.11$) or in group 3 patients with both emphysema and airway disease ($P = 0.5159$; $r = -0.18$); no correlations were found when evaluating group 1 and group 3 patients altogether ($P = 0.1439$; $r = -0.17$).

Analysis of Correlations in the Absence of RV Dilatation

After exclusion of 17 patients with an RV/LV ratio >1, the remaining population comprised 104 patients with an RV/LV ratio <1. In this subgroup, we found a negative correlation between the indexed LA volume and (a) the overall percentage of emphysema ($P = 0.02$; $r = -0.23$); (b) the percentage of emphysema in the right upper and right middle lobes ($P = 0.03$; $r = -0.20$); and (c) the TLV ($P = 0.04$; $r = -0.197$).

Categorizing the 104 patients with an RV/LV ratio <1 according to their smoking-related CT features, correlations were only found in the subgroup of patients with emphysema-predominant CT findings. We observed a negative correlation between the indexed LA volume and overall percentage of emphysema ($P = 0.0086$; $r = -0.39$) and between the indexed LA volume and the percentage of emphysema in the right upper and right middle lobes ($P = 0.0156$; $r = -0.36$), whereas no correlation was found between the indexed LA volume and TLV ($P = 0.0637$; $r = -0.28$).

DISCUSSION

To our knowledge, this is the first study, based on quantitative CT information, demonstrating that an increasing severity of emphysema in patients free of cardiovascular disease is associated with a decreasing volume of the LA. In the present investigation, a negative correlation was found between the indexed LA volume and the percentage of emphysema in the overall study group in whom the median value of emphysema was 3.2%. Similar findings were observed in all CT phenotypes showing emphysematous lesions, namely in group 1 and in groups 1 and 3 when analyzed together. Because altered RV function can affect LA filling during the ventricular systole,[1] we also

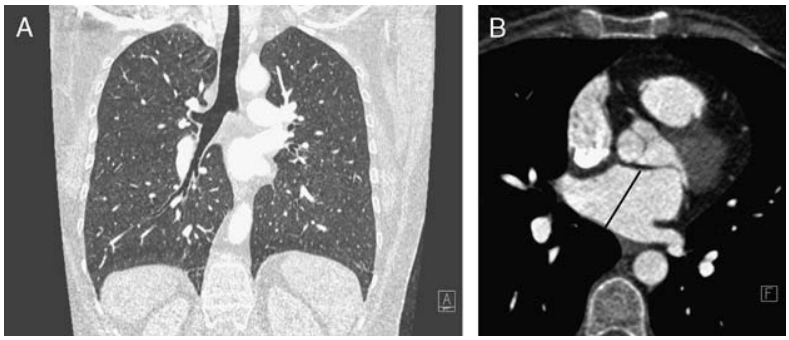

FIGURE 4. A 46-year-old female smoker (40 pack-years), referred for progressive worsening of dyspnea. A, Coronal view of the lungs illustrating the normal appearance of lung parenchyma. The indexed LA volume was 41.61 mL/m^2. B, Cross-section (magnified view), obtained at the level of the aortic root, illustrating the usual appearance of the LA. Note the larger anteroposterior LA diameter (black line) compared with Figure 3B.

evaluated the relationships between the extent of emphysema and LA volume after exclusion of 17 patients with an RV/LV ratio >1. Focusing on the remaining 104 patients with no enlargement of the RV, a negative correlation between the severity of emphysema and LA volumes was still observed, reinforcing the results observed in the entire study group.

Because there are well-established links between lung hyperinflation and heart size in COPD,[5,6] we also analyzed the relationships between LA volume and lung volumes. A negative correlation was found between the LA volume and lung volumes in the overall population and in the subgroup of patients with emphysema-predominant CT changes. However, this link was not observed in the other subgroups, especially in group 3 whose lung volumes did not differ from those of group 1. These findings suggest that the LA volume is more influenced by the severity of lung destruction than by lung hyperinflation.

On the basis of such correlations, a small LA volume secondary to lung capillary bed destruction would be a logical explanation for the low LV end-diastolic volumes observed in emphysema patients. It could then provide the missing link between reduced LV end-diastolic volumes and the reduced preload of COPD patients, mostly studied in patients with severe emphysema[5–7] but also recently reported in patients with mild emphysema.[8] Although the feasibility of diastolic function assessment with cardiac CT has been recently reported,[13] this information is not available in the conditions of routine clinical practice, in which most patients are referred for chest, and not cardiac, CT. Because a reduced blood volume in the LA may worsen the hemodynamic conditions of LV filling,[1,3,5,6] LA volumetric analysis could be proposed as an indirect means to suspect LV diastolic dysfunction. In the specific subset of patients with COPD, Watz et al[4,5] have already shown that diastolic dysfunction is an independent predictor of reduced physical capacity in daily life. Moreover, early recognition and appropriate therapy of diastolic dysfunction in COPD is advisable to prevent further progression to diastolic heart failure and death as proposed in other populations.[14] Because aging has been shown to increase LA size after the patients become older than 50 years,[15] our findings are particularly relevant when scanning COPD patients, mostly seen in this age category.

This study has several limitations that need to be addressed. Firstly, we did not take the LA phasic function into consideration, which would have required retrospective electrocardiography (ECG)-gated CT acquisitions.[16,17] However, even under such scanning conditions, measurement errors for the LA volumes estimated with cardiac multidetector CT have recently been reported.[18] It is important to emphasize that the size of the LA varies during the cardiac cycle[19–21] and that LA performance varies with age,[20] resulting in great variability of LA dynamics among individuals. Therefore, our scanning conditions provide a snapshot of LA morphology in the most favorable scanning conditions for non–ECG-gated cardiothoracic imaging—that is, combining high pitch and high temporal resolution. The simplicity of this scanning mode and calculation of the LA volume make this approach easily applicable in routine clinical practice. Because most clinical CT examinations of the chest continue to be performed without ECG gating, Huckleberry et al[22] have also proposed this scanning mode to detect left-sided cardiac chamber enlargement. Secondly, lung volumes were not indexed to the patient's size, and our population was stratified according to CT phenotypic characteristics and not functional variables, which limits some observations regarding the role of lung hyperinflation. Thirdly, CT quantification of emphysema was obtained on contrast-enhanced CT examinations, although it is usually performed on noncontrast CT examinations. Technically feasible, this approach has recently been found to minimize the emphysematous lesions.[23] Despite a median value of 3.2% of emphysema in our study group, that is likely to have been underestimated in our scanning conditions, the amount of quantified emphysema was found to be correlated to LA volumes. Lastly, we did not investigate whether the reduced LA volumes observed in our population were associated with LV diastolic dysfunction, the ultimate objective of such a morphologic analysis. This would have required a substantial modification of the conditions of routine clinical practice in which echocardiography is not systematically indicated in the management of smokers. Moreover, although echocardiography is the most commonly used diagnostic modality for assessing LA volume in daily clinical situations, volume measurement may be difficult to obtain in emphysematous patients and may be inaccurate due to the complex shape of the LA.[1,24]

In summary, this study shows that the indexed LA volume is correlated to the severity of lung destruction in smokers.

REFERENCES

1. Boussuges A, Pinet C, Molenat F, et al. Left atrial and ventricular filling in chronic obstructive pulmonary disease. An echocardiographic and Doppler study. *Am J Respir Crit Care Med*. 2000;162:670–675.
2. Rutten FH, Vonken EJ, Cramer MJ, et al. Cardiovascular magnetic imaging to identify left-sided chronic heart failure in stable patients with chronic obstructive pulmonary disease. *Am Heart J*. 2008;156:506–512.
3. Funk GC, Lang I, Schenk P, et al. Left ventricular diastolic dysfunction in patients with COPD in the presence or absence of elevated pulmonary arterial pressure. *Chest*. 2008;133:1354–1359.
4. Watz H, Waschki B, Boehme C, et al. Extrapulmonary effects of chronic obstructive pulmonary disease on physical activity: a cross-sectional study. *Am J Respir Crit Care Med*. 2008;177:743–751.
5. Watz H, Waschki B, Meyer T, et al. Decreasing cardiac chamber sizes and associated heart dysfunction in COPD. Role of hyperinflation. *Chest*. 2010;138:32–38.
6. Jorgensen K, Muller MF, Nel J, et al. Reduced intrathoracic blood volume and left and right ventricular dimensions in patients with severe emphysema: an MRI study. *Chest*. 2007;131:1050–1057.
7. Jorgensen K, Houltz E, Westfelt U, et al. Left ventricular performance and dimensions in patients with severe emphysema. *Anesth Analg*. 2007;104:887–892.
8. Barr RG, Bluemke DA, Ahmed FS, et al. Percent emphysema, airflow obstruction, and impaired left ventricular filling. *N Engl J Med*. 2010;362:217–227.
9. Patel BD, Coxson HO, Pillai SG, et al. Airway wall thickening and emphysema show independent familial aggregation in chronic obstructive pulmonary disease. *Am J Respir Crit Care Med*. 2008;178:500–505.
10. van der Meer RW, Pattynama PMT, van Strijen MLJ, et al. Right ventricular dysfunction and pulmonary obstruction index at helical CT: prediction of clinical outcome during 3-month follow-up in patients with acute pulmonary embolism. *Radiology*. 2005;235:798–803.

11. Revel MP, Faivre JB, Remy-Jardin M, et al. Automated lobar quantification of emphysema in patients with severe COPD. *Eur Radiol*. 2008;18:2723–2730.
12. Madani A, De Maertelaer V, Zanen J, et al. Pulmonary emphysema: radiation dose and section thickness at multidetector CT quantification—comparison with macroscopic and microscopic morphometry. *Radiology*. 2007;243:250–257.
13. Boogers MJ, van Werkhoven JM, Schuijf JD, et al. Feasibility of diastolic function assessment with cardiac CT: feasibility study in comparison with tissue Doppler imaging. *J Am Cardiovasc Imaging*. 2011;4:246–256.
14. Mandinov L, Eberli FR, Seiler C, et al. Diastolic heart failure. *Cardiovasc Res*. 2000;45:813–825.
15. Pan NH, Tsao HM, Chang NC, et al. Aging dilates atrium and pulmonary veins: Implications for the genesis of atrial fibrillation. *Chest*. 2008;133:190–196.
16. Yamanaka K, Fujita M, Doi K, et al. Multislice computed tomography accurately quantifies left atrial size and function after the MAZE procedure. *Circulation*. 2006;114:I5–I9.
17. Kühl JT, Kofoed KF, Moller JE, et al. Assessment of left atrial volume and mechanical function in ischemic heart disease: a multislice computed tomography study. *Int J Cardiol*. 2010; 145:197–202.
18. Gweon HM, Kim SJ, Kim TH, et al. Evaluation of left atrial volumes using multidetector computed tomography: comparison with echocardiography. *Korean J Radiol*. 2010;11:286–294.
19. Braunwald E, Frahm C. Studies on Starling's law of the heart, IV. Observations on the hemodynamic functions of the left atrium in man. *Circulation*. 1961;24:633–642.
20. Spencer KT, Mor-Avi V, Gorcsan IJ, et al. Effects of aging on left atrial reservoir, conduit, and booster pump functiona multi-institution acoustic quantification study. *Heart*. 2001;85: 272–277.
21. Jarvinen V, Kupari M, Hekali P, et al. Assessment of left atrial volumes and phasic function using cine magnetic resonance imaging in normal subjects. *Am J Cardiol*. 1994;73:1135–1138.
22. Huckleberry J, Haltom S, Issac T, et al. Accuracy of non-ECG-gated computed tomography angiography of the chest in assessment of left-sided cardiac chamber enlargement. *J Thorac Imaging*. 2012;27:354–358.
23. Heussel CP, Kappes J, Hantusch R, et al. Contrast-enhanced CT-scans are not comparable to non-enhanced scans in emphysema quantification. *Eur J Radiol*. 2010;74:473–478.
24. Koka AR, Gould SD, Owen AN, et al. Left atrial volume: comparison of 2D and 3D transthoracic echocardiography with ECG-gated CT angiography. *Acad Radiol*. 2012;19:62–68.

Conclusion

Nous avons donc retrouvé une corrélation négative entre le volume de l'oreillette gauche et l'importance de l'emphysème, ceci impactant la pré-charge ventriculaire gauche et donc la fonction diastolique ventriculaire gauche.

Depuis ce travail, une étude récente de Mahabadi et al publiée dans JACC : cardiovascular imaging (15) évaluait plusieurs paramètres sur des scanners non injectés réalisés pour mesure du score calcique. Les auteurs ont également mesuré l'oreillette gauche. Le suivi de ces patients pendant 10 ans ont fait retrouver une association significative entre le volume de l'oreillette gauche et la survenue d'événements cardio-vasculaires ; avec un volume d'oreillette gauche significativement plus important chez les patients qui ont présenté un evenement cardiovasculaire. Les auteurs proposent donc d'intégrer de nouvelles mesures au score calcique dans l'évaluation du risque cardio-vasculaire : taille de l'oreillette gauche, graisse épicardique et calcifications aortiques thoraciques.

De même, une évaluation retrospective du volume de l'oreillette gauche chez 756 patients présentant une embolie pulmonaire aigue publiée dans Chest en 2016 par Aviram et al, (16) retrouvait une corrélation significative entre un volume diminué d'oreillette gauche et le taux de mortalité ; un volume d'oreillette gauche diminué étant lié au taux de mortalité le plus important, comparativement aux volumes de toutes les autres cavités cardiaques.

Le volume de l'oreillette gauche, souvent négligé sur les scanners apparaît pourtant corrélé non seulement au taux d'emphysème, mais apparaît également comme un indicateur de survenue d'événements cardio-vasculaires et de mortalité dans l'embolie pulmonaire aigue ; son évaluation paraît donc légitime chez les patients porteurs de pathologies pulmonaires ou cardiaques.

Acute Pulmonary Embolism: evaluating middle-term mortality with multidetector computed tomography: a retrospective cohort study

N. Dublanchet, F. Moustafa, N. Vincent, J. Raconnat, P. Chabrot, L. Boyer, J. Schmidt, L. Cassagnes.

Article Soumis Diagnostic & Interventional Imaging

Il est connu désormais qu'une inversion du rapport VD/VG dans le cadre de l'embolie pulmonaire aigue est un facteur de mauvaise tolérance hémodynamique, associé à une surmortalité à 3 mois. Nous avons étudié ce même paramètre sur une série de 228 patients avec évaluation de la surmortalité à 1 an. Notre série a permis de retrouver une surmortalité significative même à distance de l'épisode aigu en cas d'inversion du rapport VD/VG. Ceci objective bien sûr la défaillance ventriculaire droite, mais cette défaillance, une fois l'épisode aigu passé, reste significative. On peut aussi se poser la question du retentissement sur le ventricule gauche, qui présente alors un obstacle à la pré-charge par le biais de l'interaction interventriculaire.

t àn à

d9mS8C6D(f69

b9I j7C1 a8j(C 46j1 89b(SC b(E6C jb OYIT89D(f69 2C9mS(D6jb(SC OS8(mC H2bj6HC I6 S j7b9E(8IDb99CS(9(mbj 4bSjC Sb448Sm 2C9mS(D6jC Eb6DPC 2C9mS(D6jC OS8(mC Im69 TbDm6S SCD8996 Cm(9CH4C9Cb9mC C1 8Sbj(mH F 1 8(I 1 b(I I8 9 ShjC 4SHO(DmTOC 1 8Sbj(mH F 1 8(I 1 8(I Cm b9 SCIm C(9D8996 r C O(b1 èmSC O6 mS89D bSmHS(Cj 46j1 89b(SC Cm I8 9 Sbm(8 4bS Sb448Sm b6 O(b1 èmSC OC j7b8SmC bIDC9Cb9mC 4O6m HEbjC1 C9m VmSC 69 4SHO(DmO6SOC jb 1 8Sbj(mH F 1 8YC9 mC6S1 C

P acCD(mT

r 7acCD(mT4S(9D(4bj OC 98mSC Hm6OC Hmb(mO7H2bj6CSjb 2bjO6S 4S898Im() 6C O6 O(b1 èmSC bSmHS(Cj 46j1 89b(SC O6 Sb448Sm é 8 CmO6 Sb448SmU U° C9 D864CI bMbjCI I6 Sjb 1 8Sbj(mH F 1 8YC9 mC6S1 C CHT(9(C F Cm 1 8(I r 7acCD(mTICD89Cb(SC Hmb(mOC SHbj(ICS jb 1 V1 C b9bjYIC b4SeI CMD6jI(89 CCI 4bm(C9mh 48Sm6S CC 4bmR8j8E(C 46j1 89b(SC DRS89() 6C

e bmHS(Cj 1 HmR8CC

: 86I b289I H2bj6H SHmS8I4 CD(f2C1 C9m 4bm(C9mh 4SHIC9mb9m 69C C1 a8j(C 46j1 89b(SC b(E6C D89T(S1 HC 4bS b9E(8IDb99CS r C Sb448SmU U° b2CD 69C 2bjO6S IC6(j OC jC O(b1 èmSC bSmHS(Cj 46j1 89b(SC 2bjO6S IC6(j OC 1 1 CmjC Sb448Sm é 8SmC 2bjO6SIC6(j F Hmb(C9m6m(j(IHI 486SH2bj6CSjO6S2bjO6S4S898Im() 6C

n HI6 jmb.mh

r 7LEC 1 8YC9 Hmb(mOC x b9I I 9 Sb448SmU U° Hmb(mD8SSHjH b2CD 69 mb6MOC 1 8Sbj(mH b6E1 C9mH F 1 8(I 4 1 8(I 4 Cm b9 4 1 b(I b6II(b2CD jb 1 8Sbj(mH F 1 8(I DRC- jCI 4bm(C9mh Ib 9I 4bmR8j8E(C 46j1 89b(SC DRS89() 6C 4

I 9 O(b1 èmSC é 1 1 CIm D8SSHjH F 69 mb6MOC 1 8Sbj(mH 4j6I (1 48Sb9mF 1 8(I 4 Cm b9 4 I 9 Sb448Sm é 8 97Hmb(m 4bI D8SSHjH F 69C I6 S1 8Sbj(mH

89D6jI(89

RC- jCI 4bm(C9mh 4SHIC9mb9m69C C1 a8j(C 46j1 89b(SC b(E6C 69 Sb448SmU U° bM CIm69 T8Sm4SHO(DmO6SOC jb 1 8Sbj(mH F 1 8YC9 mC6S1 C I4 HD(bjC1 C9m DRC- jCI 4bm(C9mh Ib 9I 4bmR8j8E(C 46j1 89b(SC DRS89() 6C 1 b(I HEbjC1 C9m486S4SHO(SC 69C 1 8Sbj(mH4SHD8DC

ABSTRACT

BACKGROUND
In acute pulmonary embolism (PE), right ventricular (RV) dysfunction is a powerful and independent predictor of one-month mortality, but its role as a predictor of 3-month, 6-month and one-year mortality is unknown.

OBJECTIVES
The main objective of this study was to assess the prognostic value of PA diameter, PA/Ao and RV/LV axial views on mid-term mortality (defined at one, three, six and twelve months). The secondary objective was to repeat the analysis after excluding patients presenting chronic pulmonary disease (CPD).

METHODS
We retrospectively evaluated 228 consecutive patients with acute PE confirmed by chest CT. RV/LV ratios (with a 0.9 cut-off value), PA diameter (cut-off value of 30 mm) and PA/Ao ratio (cut-off value of 1) were used to evaluate their prognostic value.

RESULTS
Mean age was 66.9 ± 21.2 years. RV/LV>0.9 correlated with increased mortality rate at 3 months (p=0.037), 6 months (p=0.046) and one year (p=0.027), and with one-month mortality in patients without CPD (p=0.036). PA>30mm pointed to higher mortality at 6 months (p=0.038) and one year (p=0.038). PA/Ao>1 did not correlate to mortality rates.

CONCLUSION
In patients presenting acute PE, RV/LVax>0.9 is a strong predictor of midterm mortality, especially in patients without chronic pulmonary disease, but also a predictor of early mortality.

KEYWORDS
Acute pulmonary embolism, Prognosis, Mortality, Computed tomography,
Right ventricular dysfunction.

INTRODUCTION

Overall 30-day mortality rate in acute pulmonary embolism (PE) is over 10% [1]–[3], secondary to hemodynamic failure : RV dysfunction and hematosis disruption [4]–[6]. Acute PE requires initial risk stratification to make therapeutic decision. CT angiography has become the first-line noninvasive approach to explore pulmonary circulation and diagnose PE [7]. CT also serves to assess RV failure and predict pulmonary hypertension (PHT). RV failure is suspected by right-to-left ventricle diameter ratio measured on axial views (RV/LVax) [8]–[12] with a cutoff value defined as RV/LVax>0.9 [8]. This value has been previously shown to correlate with a higher 30-day mortality, but its role as a predictor of mortality over the first year after acute PE has not been yet proven [13]. Some studies have found that this same ratio measured on four-chamber reconstructed views is a predictor of 30-day mortality [14]. A main pulmonary artery (PA) diameter higher than 30 mm is a parameter put forward for PHT assessment after acute PE [15]–[19] but is not constantly associated with early mortality after acute PE [9], [11]. The ratio between PA diameter and ascending aorta (Ao) diameter (PA/Ao), with a cutoff value defined as PA/Ao>1, is also proposed to identify PHT but does not correlate to a higher mortality during early hospital course [11].

Echocardiography is an important risk stratification tool in acute PE,as it assesses RV diameter, LV diameter and RV dysfunction. [5], [20]–[22]. However, echocardiographic findings are associated with a high inter-observer variability, whereas CT axial images analysis is not. The RV may be difficult to evaluate with the transthoracic approach. In most patients presenting acute PE, echocardiography has a lower diagnostic value than CT [7].

Contrast-enhanced CT is already the first-line PE imaging test for diagnosis according to European Task Force Guidelines on PE [7]. CT could offer useful prognostic value through its ability to assess RV dysfunction combined with its high positive diagnostic value.

In this study, we retrospectively evaluated the prognostic value of RV/LVax>0.9, PA diameter>30 mm and PA/Ao>1 evaluated on CT angiography on 30-day, 3-month, 6-month and one-year mortality rates in 228 consecutive patients admitted to our emergency department for acute PE.

MATERIALS AND METHODS

Population

We retrospectively identified a cohort of 228 patients admitted to our emergency department between January 2007 and December 2009 with acute PE confirmed by contrast-enhanced CT performed during the first 24 hours of hospital course.

Eligible patients were screened from our hospital computer database based on all keyword hits relevant to acute PE diagnosis ("acute pulmonary embolism" and "acute pulmonary embolism with right ventricular dysfunction"). For this same period, 46 patients had acute PE confirmed by another imaging test due to contraindications for contrast enhanced CT (renal insufficiency, allergy to iodine media,...). In 24 other patients, diagnosis was confirmed after the first 24 hours of hospital course as they were already in other hospital departments. CT angiography and clinical charts were restrospectively analyzed.

Clinical Endpoints

The primary endpoint was defined as all-cause mortality at 30 days, 3 months, 6 months and one year after diagnosis of acute PE. Mortality data were collected from the hospital computer database or by phone calls to the patients and/or their GP.

We first led the statistical analysis on all 228 patients included. We then identified a subset of 20 patients presenting chronic pulmonary disease (CPD+ ; n=20), defined as patients presenting chronic obstructive pulmonary disease (CPD) or chronic respiratory insufficiency (all causes) or treated by β2 mimetics or corticoids. The other 208 CPD-free patients formed a second group (CPD- ; n=208). We then repeated the statistical analysis on these groups and compared their one-year mortality rates.

Computed tomography angiography

Scanning protocol

All CT angiographies were performed on a 64-detector row CT scanner (750 HD, GENERAL ELECTRIC®, Milwaukee, WI). Injection protocol consist in 75 mL at a flow rate of 4 mL/sec using a contrast media of 370 mg iodine/mL or more, followed by serum flush of 45 mL at a flow rate of 3 mL/sec in an antebrachial vein.

We systematically used bolus detection software allowing an optimal enhancement of pulmonary arteries [23] and rrealized a cranio-caudal acquisition with 0.625 mm slice thickness and 0.625 mm interval.

Cardiac measurements

Measurements were performed retrospectively on the same image processing workstations as used for diagnosis (ADW 4.4, GENERAL ELECTRIC®) by two expert observers (NB, LC, 10 years experience in cardio-thoracic imaging) blinded to clinical and outcome data.

Right-to-left ventricular diameter ratio (RV/LV) was measured on axial views (RV/LVax) and on four-chamber reconstructed views (RV/LV4c) using RV and LV minor axis, measured at their widest point, from the inner surface of the free wall to the surface of the interventricular septum, as described in Quiroz *et al*. Finding the widest diameters can hinge on working with different levels for right and left ventricles. Here we used the cutoff value of RV/LV>0.9, defined by existing literature [8] as a strong predictor of in-hospital death in patients admitted for acute PE.

Main PA diameter was assessed on axial views by measuring the greatest diameter perpendicular to the main axis of the vessel. A cutoff value of 30 mm was defined, according to Kuriyama *et al* [15].

Aorta diameter (Ao) was measured on the same axial section, making it possible to assess PA/Ao diameter ratio with a cutoff value of 1, as described in the literature [17].

Finally, we established specific RV/LVax, PA and PA/Ao cutoff values for our population.

Statistical analysis

Patient demographics, biometrics and comorbid conditions were compared between each group (and according to the respective size of the group) using a Student's t-test for quantitative variables and a chi-square test (or Fisher's exact test if needed) for qualitative variables.

These same tests were used to compare 30-day, 3-month, 6-month and one-year mortalities in patients with RV/LV ax>0.9 versus RV/LV ax<0.9, in patients with PA>30 mm versus <30 mm, and in patients with PA/Ao>1 versus <1. Survival functions of CPD+ and CPD- patients were assessed by Kaplan-Meier's method and compared by a Mantel-Cox test. RV/LVax and RV/LV4c values were compared by a correlation test. Finally, our own cutoff values for cardiac measurements were defined by ROC curves based on the prediction of significantly higher 30-day, 3-month, 6-month and one-year mortalities. When area under curve (AUC) was significantly different from the 0.5 value (which defines a low power of testing), we

selected the cutoff value that offered the best compromise between sensitivity (Se) and specificity (Sp).

All of these tests set a p-value of 0.05 as significance threshold.

Statistical analysis was based on outcome data given by all our hospital physicians or by the patients' GPs. As the study was observational study and not interventional, there was no requirement to secure institutional review board approval.

RESULTS

Population

Mean age of the 228 patients was 66.9 ± 21.2 years. The patient population included 110 women (48.2%). The vast majority of patients (n=210 ; 92.1%) presented one or more cardiovascular risk factors (age over 50 for men, over 60 for women, smoking, dyslipidemia, diabetes mellitus, hypertension, family history of cardiovascular diseases). Sixtyone (26.8%) had prior venous thromboembolic disease and 41 (18%) had at least one prior cardiovascular disease. The characteristics of the full patient population and the patient subgroups are reported in table 1.

Mortality rates

– According to RV/LV ratio :

For a RV/LVax ratio >0.9 (n= 164 ; 72%), mortality rate was 7.9% at 30 days (13/164 patients) rising to 17.7% at one year of follow-up (29/164 patients), compared to 1.6% (1/64) and 6.2% (4/64), respectively, in patients without RV/LVax disruption (28% ; n=64) (Tables 1 & 2). In patients with RV/LVax>0.9, mortality was significantly higher at 3 months, 6 months and one year of follow-up (p=0.037, p=0.046, p=0.027, respectively) (Table 2). The strong correlation between RV/LV ratio values in axial views and four-chamber views (ρ=0.95) prompted us to base all other analyses on RV/LVax.

– According to PA diameter

Analysis of PA diameter (with a cutoff at 30 mm) showed significantly higher mortality at 6 months for PA diameter >30 mm (17.3% *vs* 8.2%; p=0.038) and one year of follow-up (21% *vs* 10.9%; p=0.038) (Table 2).

There was no significant association between PA/Ao disruption (PA/Ao>1) and mortality (Table 2). However, one-year mortality tended to be higher in patients with PA/Ao>1 (23.3% *vs* 12.4%, p=0.069).

– In CPD-/CPD+ groups

In the CPD- group, patients presenting RV/LVax >0.9, mortality was significantly higher from one month until the end of follow-up (at 30 days : 7.5% *vs* 0%, p=0.036; at 3 months: 11% *vs* 1.6%, p=0.024; at 6 months: 12.3% *vs* 3.2%, p=0.042; at one year: 15.7% *vs* 4.8%, p=0.029). The same analysis on the CPD+ group did not find any significant association between mortality and CT findings. However, survival analysis comparing CPD+ against CPD- found significantly higher mortality in CPD+ patients (Figure 1).

– New cut-off calculation

In terms of cutoff values, for RV/LVax ratio, there was only one cutoff that correlated significantly to mortality. Indeed, a RV/LVax ratio cutoff of 1.05 was a significant predictor of 30-day mortality in the CPD- group (AUC=0.67, Se=63.6%, Sp=64%, p=0.047) (Figure 2). For PA diameter, across all 228 patients included, cutoff values of 29.4 mm and 29.3 mm were significant predictors of 6-month mortality (AUC=0.63, Se=61%, Sp=62%, p=0.036) and 12-month mortality (AUC=0.63, Se=61%, Sp=62%, p=0.017), respectively (Figure 3). No PA/Ao cutoff value was associated with significantly higher all-population, CPD+ or CPDmortality.

DISCUSSION

This study found that a RV/LV ratio>0.9 defined on axial views was associated with significantly higher mortality at 3 months, 6 months and one year of follow-up. RV/LVax was not a significant predictor of 30-day mortality, as reported by Quiroz *et al* [8], but they had established that a cutoff value of 0.9 showed high specificity (92.3%) but low sensitivity (37.5%) (AUC = 0.67). Schoepf *et al* [14] reported significantly higher 30-day mortality for the same RV/LV cutoff value (15.6% *vs* 7.7%), even in multivariate analysis, and therefore regardless of presence or absence of prior chronic pulmonary disease. These reported 30-day mortality rates were higher than the 30-day mortality rate found here (17.7% *vs* 6.2%) and even reached our one-year mortality rate. A recent study [24] comparing RV dysfunction in patients with acute PE by CT and echocardiography with RV strain analysis found similarly significant prognosis between the two techniques for 30-day mortality rate, but the cut-off used for RV/LV ratio was >1 However, our results tend to fit those reported by Araoz *et al* [25] on 1193 patients which showed no significant association between RV/LV ratio disruption and 30-day mortality. These results could be explained by inter-observer variability and the fact that previous studies had not used

double-blinded measurements [10], [14].

Considering our conclusions, the population studied here looks similar to the population studied by Araoz *et al* [25]. Indeed, both studies showed a higher mortality in patients with CPD but no significant correlation between RV/LVax>0.9 and 30-day mortality regardless of associated chronic PE. Our study warrants credit as the first work to demonstrate that a disrupted RV/LVax ratio is a pejorative prognostic factor for 3-month, 6-month and one-year mortality in patients presenting acute PE regardless of CPD. Van der Meer *et al* [10] reached the same conclusion for 3-month mortality with a cutoff value defined as RV/LVax>1 but only after excluding patients with massive PE. Moroni *et al* [26] found a predictive value of RV/LV on 3-month mortality but only when associated with low embolic burden (<40%). To our knowledge, only one prior study [13] has assessed the prognostic value of several CT findings (including RV/LV) on 3-month mortality but it found that the only significant predictor of long-term mortality was initial embolic burden. Unlike Quiroz *et al* [8], who concluded that 4-chamber reconstructions offered better performances in terms of prognostic assessment, we did not find any added value of using 4-chamber reconstructed views.

In our cohort, PA diameter >30 mm correlated with a significantly higher 6-month and one-year mortality (17.3% *vs* 8.2, p=0.038 and 21% *vs* 10.9%, p=0.038, respectively). These results are interesting, as most prior studies have only investigated the association between this CT parameter and PHT [15], [18], [19] and all have found cutoff values for PA diameter that were close to 30 mm (see Table 3). Only Ghaye *et al* [11] evaluated the prognostic value of PA diameter on in-hospital death, but they failed to find a correlation. Our results suggest that early death, predicted by a disrupted RV/LVax, could be explained by hemodynamic failure as an immediate consequence of PE whereas later death, predicted by an increased PA diameter and RV/LVax ratio, could be linked to the mortality inherent to PHT. The pre-existence of a CPD could bias these considerations, as PA diameter was significantly different between CPD+ and CPD- patients (Table 1). There is a need for prospective studies on greater cohorts to compare initial CT findings to a follow-up CT at 3 or 6 months.

This study found that PA/Ao diameter ratio had no significant prognostic value, consistently with Van der Meer *et al* [10]. However, note that patients with PA/Ao>1 showed near-significantly higher mortality (p=0.069), at one year after acute PE,

which could be another consequence of PHT, as was the case with PA diameter.

Here we defined cutoff values for the three CT parameters based on our mortality data. The only RV/LVax cutoff value suggesting significantly higher mortality was RV/LVax>1.05 for 30-day mortality in patients without CPD. Indeed, RV/LVax may need a cutoff value > 0.9, as suggested by most recent research on CT findings [27], [28]. PA>29.4 mm is a significant predictor of 6-month mortality and PA>29.3 mm is a significant predictor of one-year mortality, independently of a prior CPD.

These values are very close to values used elsewhere to define PHT [15], [18], [19].

LIMITATIONS

We included retrospectively the patients and did not correlate CT results to arterial pulmonary obstruction index nor to echocardiography.

However, a recent study comparing RV/LV ratio on MDCT and echocardiography in a cohort of patients with PE found a modest correlation between the two techniques [29].

The computed tomographies were not electrocardiogram-gated as our institution uses the standard acquisition. Consequently, we did not correlate mortality rate to distensibility of the pulmonary artery trunk, which is a marker of PHT.

We studied all-cause mortality and not only mortality related to heart failure or respiratory insufficiency.

CONCLUSION

Contrast-enhanced chest CT is still the first-line imaging test for acute PE diagnosis. CT enables short-term (1 month, 3 months) and midterm (6 months, one year) prognosis assessment if RV/LV ratio exceeds 0.9 on axial views, suggesting the importance of close follow-up in these patients. PA diameter measurement could reveal a PHT at the time of diagnosis and suggest higher mid-term mortality. PA/Ao ratio appears to have no prognostic significance in acute PE.

REFERENCES

[1] S. Z. Goldhaber, L. Visani, and M. De Rosa, “Acute pulmonary embolism: clinical outcomes in the International Cooperative Pulmonary Embolism Registry (ICOPER),” *Lancet*, vol. 353, no. 9162, pp. 1386–1389, Apr. 1999.

[2] W. Kasper, S. Konstantinides, A. Geibel, M. Olschewski, F. Heinrich, K. D. Grosser, K.Rauber, S. Iversen, M. Redecker, and J. Kienast, “Management strategies and determinants of outcome in acute major pulmonary embolism: results of a multicenter registry,” *J. Am. Coll. Cardiol.*, vol. 30, no. 5, pp. 1165–1171, Nov. 1997.

[3] F. A. Anderson Jr, H. B. Wheeler, R. J. Goldberg, D. W. Hosmer, N. A. Patwardhan, B.Jovanovic, A. Forcier, and J. E. Dalen, “A population-based perspective of the hospital incidence and case-fatality rates of deep vein thrombosis and pulmonary embolism. The Worcester DVT Study,” *Arch. Intern. Med.*, vol. 151, no. 5, pp. 933–938, May 1991.

[4] K. E. Wood, “Major pulmonary embolism : review of a pathophysiologic approach to the golden hour of hemodynamically significant pulmonary embolism,” *Chest*, vol. 121, no.3, pp. 877–905, Mar. 2002.

[5] F. Jardin, O. Dubourg, and J. P. Bourdarias, “Echocardiographic pattern of acute cor pulmonale,” *Chest*, vol. 111, no. 1, pp. 209–217, Jan. 1997.

[6] K. M. McIntyre and A. A. Sasahara, “The hemodynamic response to pulmonary embolism in patients without prior cardiopulmonary disease,” *Am. J. Cardiol.*, vol. 28, no. 3,pp. 288–294, Sep. 1971.

[7] A. Torbicki, A. Perrier, S. Konstantinides, G. Agnelli, N. Galiè, P. Pruszczyk, F. Bengel,A. J. B. Brady, D. Ferreira, U. Janssens, W. Klepetko, E. Mayer, M. Remy-Jardin, J.-P. Bassand,A. Vahanian, J. Camm, R. De Caterina, V. Dean, K. Dickstein, G. Filippatos, C. Funck-Brentano,I. Hellemans, S. D. Kristensen, K. McGregor, U. Sechtem, S. Silber, M. Tendera, P. Widimsky, J. L. Zamorano, J.-L. Zamorano, F. Andreotti, M. Ascherman, G. Athanassopoulos, J. De Sutter, D. Fitzmaurice, T. Forster, M. Heras, G. Jondeau, K. Kjeldsen, J. Knuuti, I. Lang, M.Lenzen, J. Lopez-Sendon, P. Nihoyannopoulos, L. Perez Isla, U. Schwehr, L. Torraca, and J.-L. Vachiery, “Guidelines on the Diagnosis and Management of Acute Pulmonary Embolism The Task Force for the Diagnosis and Management of Acute Pulmonary Embolism of the European Society of Cardiology (ESC),” *Eur Heart J*, vol. 29, no. 18, pp. 2276–2315, Sep. 2008.

[8] R. Quiroz, N. Kucher, U. J. Schoepf, F. Kipfmueller, S. D. Solomon, P. Costello, and S. Z.Goldhaber, “Right ventricular enlargement on chest computed tomography: prognostic role in acute pulmonary embolism,” *Circulation*, vol. 109, no. 20, pp. 2401–2404, May 2004.

[9] D. Collomb, P. J. Paramelle, O. Calaque, J. L. Bosson, G. Vanzetto, D. Barnoud, C.Pison, M. Coulomb, and G. Ferretti, “Severity assessment of acute pulmonary embolism: evaluation using helical CT,” *Eur Radiol*, vol. 13, no. 7, pp. 1508–1514, Jul. 2003.

[10] R. W. van der Meer, P. M. T. Pattynama, M. J. L. van Strijen, A. A. van den Berg-Huijsmans, I. J. C. Hartmann, H. Putter, A. de Roos, and M. V. Huisman, “Right ventricular dysfunction and pulmonary obstruction index at helical CT : prediction of clinical outcome during 3-month follow-up in patients with acute pulmonary embolism,” *Radiology*, vol. 235, no. 3, pp. 798–803, Jun. 2005.

[11] B. Ghaye, A. Ghuysen, V. Willems, B. Lambermont, P. Gerard, V. D’Orio, P. A.Gevenois, and R. F. Dondelinger, “Severe pulmonary embolism : pulmonary artery clot load scores and cardiovascular parameters as predictors of mortality,” *Radiology*, vol. 239, no. 3,pp. 884–891, Jun. 2006.

[12] D. K. Kang, C. Thilo, U. J. Schoepf, J. M. Barraza Jr, J. W. Nance Jr, G. Bastarrika, J. A.
Abro, J. G. Ravenel, P. Costello, and S. Z. Goldhaber, “CT signs of right ventricular dysfunction: prognostic role in acute pulmonary embolism,” *JACC Cardiovasc Imaging*, vol. 4, no. 8, pp. 841–849, Aug. 2011.

[13] M. F. Morris, B. A. Gardner, M. B. Gotway, K. M. Thomsen, W. S. Harmsen, and P. A. Araoz, “CT Findings and Long-Term Mortality After Pulmonary Embolism,” *AJR*, vol. 198, no.6, pp. 1346–1352, Jun. 2012.

[14] U. J. Schoepf, N. Kucher, F. Kipfmueller, R. Quiroz, P. Costello, and S. Z. Goldhaber, “Right ventricular enlargement on chest computed tomography: a predictor of early death in acute pulmonary embolism,” *Circulation*, vol. 110, no. 20, pp. 3276–3280, Nov. 2004.

[15] K. Kuriyama, G. Gamsu, R. G. Stern, C. E. Cann, R. J. Herfkens, and B. H. Brundage, “CT-determined pulmonary artery diameters in predicting pulmonary hypertension,” *Invest Radiol*, vol. 19, no. 1, pp. 16–22, Feb. 1984.

[16] A. Devaraj, A. U. Wells, M. G. Meister, T. J. Corte, S. J. Wort, and D. M. Hansell, “Detection of pulmonary hypertension with multidetector CT and echocardiography alone and in combination,”

Radiology, vol. 254, no. 2, pp. 609–616, Feb. 2010.
[17] C. S. Ng, A. U. Wells, and S. P. Padley, “A CT sign of chronic pulmonary arterial hypertension: the ratio of main pulmonary artery to aortic diameter,” *J Thorac Imaging*, vol. 14, no. 4, pp. 270–278, Oct. 1999.
[18] P. D. Edwards, R. K. Bull, and R. Coulden, “CT measurement of main pulmonary artery diameter,” *Br J Radiol*, vol. 71, no. 850, pp. 1018–1020, Oct. 1998.
[19] R. T. Tan, R. Kuzo, L. R. Goodman, R. Siegel, G. B. Haasler, and K. W. Presberg, “Utility of CT scan evaluation for predicting pulmonary hypertension in patients with parenchymal lung disease. Medical College of Wisconsin Lung Transplant Group,” *Chest*, vol. 113, no. 5, pp. 1250–1256, May 1998.
[20] A. Ribeiro, P. Lindmarker, A. Juhlin-Dannfelt, H. Johnsson, and L. Jorfeldt, “Echocardiography Doppler in pulmonary embolism: right ventricular dysfunction as a predictor of mortality rate,” *Am. Heart J.*, vol. 134, no. 3, pp. 479–487, Sep. 1997.
[21] W. Kasper, S. Konstantinides, A. Geibel, N. Tiede, T. Krause, and H. Just, “Prognostic significance of right ventricular afterload stress detected by echocardiography in patients with clinically suspected pulmonary embolism,” *Heart*, vol. 77, no. 4, pp. 346–349, Apr. 1997.
[22] S. Grifoni, I. Olivotto, P. Cecchini, F. Pieralli, A. Camaiti, G. Santoro, A. Conti, G. Agnelli, and G. Berni, “Short-term clinical outcome of patients with acute pulmonary embolism, normal blood pressure, and echocardiographic right ventricular dysfunction,” *Circulation*, vol. 101, no. 24, pp. 2817–2822, Jun. 2000.
[23] J. Kirchner, R. Kickuth, U. Laufer, M. Noack, and D. Liermann, “Optimized enhancement in helical CT: experiences with a real-time bolus tracking system in 628 patients,” *Clin Radiol*, vol. 55, no. 5, pp. 368–373, May 2000.
[24] E. George, K. K. Kumamaru, N. Ghosh, C. Gonzalez Quesada, N. Wake, A. Bedayat, R. M. Dunne, S. S. Saboo, A. Khandelwal, A. R. Hunsaker, F. J. Rybicki, and M. Gerhard-Herman, “Computed tomography and echocardiography in patients with acute pulmonary embolism: part 2: prognostic value,” *J Thorac Imaging*, vol. 29, no. 1, pp. W7–W12, Jan. 2014.
[25] P. A. Araoz, M. B. Gotway, J. R. Harrington, W. S. Harmsen, and J. N. Mandrekar, “Pulmonary embolism : prognostic CT findings,” *Radiology*, vol. 242, no. 3, pp. 889–897, Mar. 2007.
[26] A.-L. Moroni, J.-L. Bosson, N. Hohn, F. Carpentier, G. Pernod, and G. R. Ferretti, “Nonsevere pulmonary embolism: prognostic CT findings,” *Eur J Radiol*, vol. 79, no. 3, pp. 452–458, Sep. 2011.
[27] A. Furlan, A. Aghayev, C.-C. H. Chang, A. Patil, K. N. Jeon, B. Park, D. T. Fetzer, M. Saul, M. S. Roberts, and K. T. Bae, “Short-term mortality in acute pulmonary embolism: clot burden and signs of right heart dysfunction at CT pulmonary angiography,” *Radiology*, vol. 265, no. 1, pp. 283–293, Oct. 2012.
[28] M. F. Bazeed, A. Saad, A. Sultan, M. A. Ghanem, and D. M. Khalil, “Prediction of pulmonary embolism outcome and severity by computed tomography,” *Acta Radiol*, vol. 51, no. 3, pp. 271–276, Apr. 2010.
[29] N. Wake, K. K. Kumamaru, E. George, A. Bedayat, N. Ghosh, C. Gonzalez Quesada, F. J. Rybicki, and M. Gerhard-Herman, “Computed tomography and echocardiography in patients with acute pulmonary embolism: part 1: correlation of findings of right ventricular enlargement,” *J Thorac Imaging*, vol. 29, no. 1, pp. W1–6, Jan. 2014.

Table 1: Patient characteristics and CT findings for total population, patients with chronic pulmonary disease (CPD+) and patients without chronic pulmonary disease (CPD-).

	Total Population		CPD+		CPD -		p-value
Patients, n (% total)	228	-	20	(8.8%)	208	(91.2%)	
Demographics							
Men, n (%)	118	(51.8%)	14	(70.0%)	104	(50.0%)	0.087
Mean age (±SD)	66.9	(±21.2)	75.9	(±21.2)	66.0	(±21.2)	<0.001*
Comorbid conditions							
Cardiovascular risk factors, n (%)	210	(92.1%)	20	(100.0%)	190	(91.3%)	0.379
Prior cardiovascular disease, n (%)	41	(18.0%)	5	(25.0%)	36	(17.3%)	0.370
Prior PE and/or deep venous thrombosis, n (%)	61	(26.8%)	5	(25.0%)	56	(26.9%)	0.853
CT findings							
RV/LVax > 0.9, n (%)	164	(71.9%)	18	(90.0%)	146	(70.2%)	0.060
PA > 30mm, n (%)	81	(35.5%)	13	(65.0%)	68	(32.7%)	0.004*
PA/Ao > 1.0, n (%)	43	(18.9%)	5	(25.0%)	38	(18.3%)	0.548

CT = Computed Tomography; PE = Pulmonary Embolism; RV/LVax = Ratio between right and left ventricle diameters on axial views; PA = Pulmonary artery diameter; PA/Ao = Ratio between Pulmonary artery and aorta diameters on axial views; CPD = Chronic Pulmonary Disease

Table 2: Mortality rates at the different stages of follow-up (total population) as a function of the 3 CT findings.

CT Findings	***Mortality rates after 1 month***		***Mortality rates after 3 months***		***Mortality rates after 6 months***		***Mortality rates after 12 months***	
RV/LV axial *(>0.9 versus others)*	7.9% vs 1.6%	*p=0.12*	12.2% vs 3.1%	*p=0.037**	14% vs 4.7%	*p=0.046**	17.7% vs 6.2%	*p=0.027**
PA diameter *(>30mm versus others)*	6.2% vs 6.1%	*p > 0.5*	13.6% vs 7.5%	*p=0.136*	17.3% vs 8.2%	*p=0.038**	21% vs 10.9%	*p=0.038**
PA/Ao *(>1 versus others)*	9.3% vs 5.4%	*p=0.308*	14% vs 8.6%	*p=0.266*	16.3% vs 10.3%	*p=0.288*	23.3% vs 12.4%	*p=0.069*

CT = Computed Tomography; RV/LV axial = Right-to-left ventricular diameter ratio on axial views; PA = Pulmonary artery; PA/Ao: Ratio between pulmonary artery and aorta diameters

N(E6SC Comparison of survival functions : patients presenting chronic pulmonary disease (CPD+) versus others (CPD-).

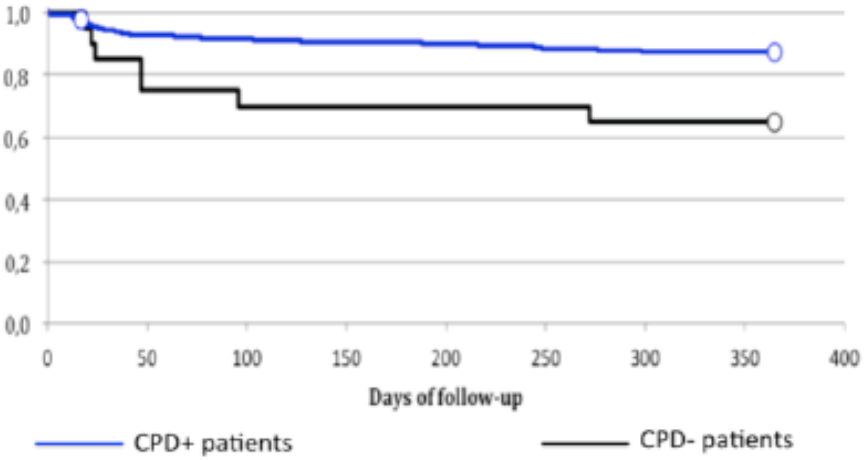

Survival analysis by Kaplan-Meier method; ***Mantel-Cox (p<0.001)***

Figure 2 – Cutoff value calculation for RV/LVax (ratio of right-to-left ventricle diameter on axial views), considering one-month mortality in patients without chronic pulmonary disease.

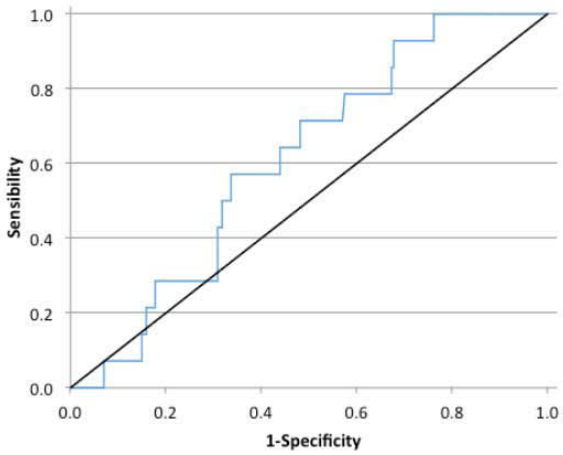

RV/Lvax value	Sensibility	Specificity
1.047	0.615	0.571
1.049	0.538	0.571

AUC	SD	Inferior limit	Superior limit	p-value
0.612	0.064	0.486	0.739	0.176

Tu

Figure 3- Cutoff value calculation for pulmonary artery (PA) diameter, considering one-year mortality in the total patient population.

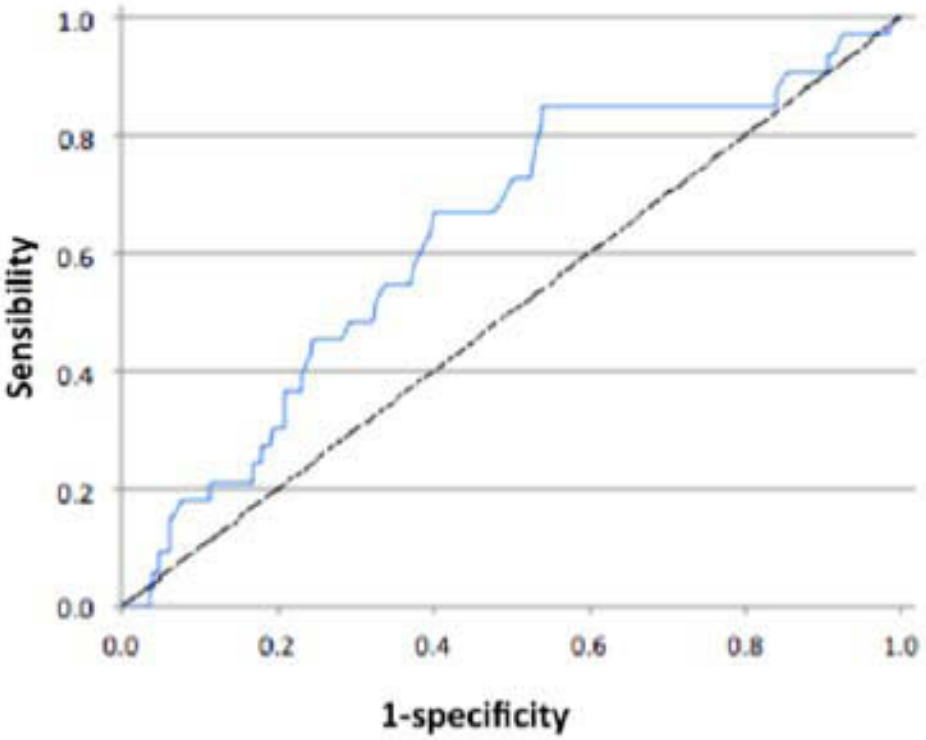

Value	Sensibility	Specificity
29.100	0.636	0.605
29.300	0.606	0.615
29.400	0.576	0.626

AUC	SD	Inferior limit	Superior limit	p-value
0.630	0.052	0.528	0.732	0.017*

Table 3: Cutoff values for pulmonary artery (PA) diameter suggesting the presence of pulmonary hypertension in three prior cohorts.

Study	Year	Number of patients included	Criteria	Sensibility	Specificity
Kuriyama et al.	1984	58	PA > 30 mm*	69%	100%
Edwards et al.	1998	112	PA > 33.2mm	58%	95%
Tan et al.	1998	45	PA > 29mm	Total population: 87% CPD+: 84%	Total population: 89% CPD+: 75%

*(=28.6mm + 2SD); CPD= Chronic Pulmonary Disease

Conclusion

L'angioscanner permet non seulement le diagnostic initial d'embolie pulmonaire mais également d'approcher le retentissement hémodynamique de cet épisode aigu. Le suivi à long terme de ces patients nous a permis de montrer que le signe scanographique de défaillance cardiaque droite initiale (rapport VD/VG), même après résolution de l'épisode d'embolie pulmonaire aigue, est associé à un taux de mortalité à 1 an plus élevé. Cette notion était connue pour des délais à court et moyen terme, cette association persiste même à 1 an de l'épisode aigu.

L'analyse scanographique initiale des patients présentant une embolie pulmonaire aigue doit toujours intégrer une évaluation (même approximative sur des scanners sans gating) du retentissement cardiaque et hémodynamique de l'obstruction artérielle pulmonaire.

Le score de Qanadli est peu utilisé en pratique courante, car difficile et long à calculer. La mesure simple et rapide du rapport VD/VG apparaît aujourd'hui à tous les auteurs comme une alternative sensible et spécifique à l'évaluation de la tolérance de l'embolie pulmonaire.

Étude de la corrélation par imagerie spectrale entre le volume de défaut de perfusion pulmonaire/ volume pulmonaire total et le rapport VD/VG, le score de Qanadli et le score de Genève dans l'embolie pulmonaire aigue.

C.Taille, O. Risch, P. Morin, B. Perreira, L. Boyer, L. Cassagnes

Article soumis American Journal of Roentgenology

Étude prospective en imagerie spectrale chez les patients adressés pour suspicion d'embolie pulmonaire, afin d'évaluer la corrélation entre le pourcentage de volume pulmonaire hypoperfusé et le rapport VD/VG.

On sait que la technique d'imagerie spectrale, ou de double énergie (appelation variant selon les constructeurs), sensibilise la détection des embolies pulmonaires, notamment les embolies périphériques. L'utilisation de cette technique permet de visualiser le parenchyme pulmonaire hypoperfusé en aval du thrombus.

Dans cette étude prospective monocentrique nous avons cherché à évaluer la corrélation entre le pourcentage du volume de defect perfusionnel et le rapport VD/VG, le score de Qanadli et le score de Genève.

Il existe de nombreuses méthodes permettant d'évaluer la gravité de l'embolie pulmonaire en angioTDM thoracique, parmi lesquelles l'index de Qanadli (17) et la mesure du rapport VD/VG (18) semblent offrir la meilleure corrélation avec l'état clinique du patient.

L'imagerie TDM en double énergie permet d'établir une cartographie de perfusion, avec mesure du volume sanguin, du parenchyme pulmonaire en objectivant les zones de defect perfusionnel, sans nuire à la qualité diagnostique de l'angioTDM thoracique standard.

Il a été prouvé que cette technique augmente la sensibilité de l'examen pour les defects périphériques, avec une sensibilité globale de 94% et une spécificité de 93.6% (19).

L'objet de cette étude était d'évaluer prospectivement par angioTDM thoracique de perfusion en double énergie la corrélation entre le volume de parenchyme pulmonaire hypoperfusé et le retentissement sur les cavités cardiaques dans l'embolie pulmonaire aigue.

Abstract

Objectif :

Évaluer prospectivement la corrélation entre le volume parenchymateux pulmonaire avec défaut de perfusion/ volume pulmonaire total (PDvol/TLvol) et les cavités cardiaques droites (rapport VD/VG), le score de Qanadli et le score de Genève dans l'embolie pulmonaire aigue par imagerie spectrale.

Matériel et méthodes :

Étude prospective monocentrique entre aout 2015 et mars 2016, incluant les patients présentant une embolie pulmonaire aigue diagnostiquée par angioscanner thoracique avec imagerie spectrale. Les données ont été analysées par 2 radiologues.

Résultats :

34 patients ont été inclus. La corrélation entre PDvol/TLvol et le rapport VD/VG était excellent pour le lecteur 1 ($r = 0,82$; $p < 0,001$) et bon pour le lecteur 2 ($r = 0,66$; $p<0,001$). La valeur seuil de PDvol/TLvol avec inversion du VD/VG était de 14,48 % (Se=71%, Sp = 100%) pour le lecteur 1 et de 8,85% (Se=50%, Sp= 100%) pour le lecteur 2. La corrélation inter-observateur etait bonne ($r= 0,91$; $p<0,001$) mais avec un faible agrément ($\kappa= 0.40$), les mesures du lecteur 1 étant systématiquement supérieures à celles du lecteur 2. Aucune corrélation n'était retrouvée entre le score de Genève et PDvol/TLvol ou VD/VG.

Conclusion :

Notre étude montre une bonne corrélation entre PDvol/TLvol et le rapport VD/VG avec une bonne corrélation inter-observateurs mais un faible agrément. Aucune corrélation n'était retrouvée entre le score de Genève et PDvol/TLvol ou VD/VG.

Correlation study between perfusion defect volume / total pulmonary parenchyma volume ratio correlated to RVD/LVD ratio, Geneva score and Qanadli score using spectral imaging CT in acute PE

Abstract

Purpose:
To evaluate prospectively the correlation between perfusion defect volume / total pulmonary parenchyma volume ratio (PD vol/TL vol) and the right heart chambers (RVD/LVD), Geneva score and Qanadli score in acute pulmonary embolism (PE) by spectral imaging in thoracic CT.

Materials and Methods:
Monocentric prospective analysis was conducted at our institution between 08/2015 and 03/2016. Patients with PE diagnosed by chest CT with spectral imaging protocol were included. Data were analyzed by two radiologists.

Results:
34 patients were enrolled. The correlation between PD vol/TL vol and RVD/LVD ratio was excellent for reader 1 ($r = 0.82$; $p < 0.001$) and good for reader 2 ($r = 0.66$; $p < 0.001$). The threshold values for readers 1 and 2 of the relative volume were 14.48% (Se = 71%, Sp= 100%) and 8.85% (Se = 50%, Sp = 100%). Inter-observer correlation was good ($r = 0.91$; $p< 0.001$), but we noted a poor agreement ($\kappa = 0.40$); measures for reader 1 were always greater than those for reader 2. Any correlation was found between Geneva score and PD vol/TL vol, neither RVD/LVD ratio.

Conclusion:
This study shows a good correlation between PD vol/TL vol and RVD / LVD ratio in two readers with a good inter-observer correlation but poor agreement. Any correlation was found between Geneva score and PD vol/TL vol, neither RVD/LVD ratio.

Key words: Pulmonary Embolism, Spectral Imaging, Right heart failure, lung parenchyma perfusion, Chest CT.

I. Introduction

Chest pain is a frequent reason for consultation in hospital emergency wards, resulting in ranging diagnosis comprising potentially serious health disorders, and regularly requiring medical imaging (1). Pulmonary embolism (PE) is a frequent finding in this clinical situation with an estimated overall mortality of 1–10% in hemodynamically stable patients (2,3).

Quantifying the impact of PE is important in the acute phase for optimal management of patient care, since we know that there is a correlation between the effects of PE on the right heart chambers and short-, medium- and long-term mortality (4).

Chest CT has become a gold standard (1,5), offering very high sensitivity and specificity (Se = 83%, Sp = 96%) and high negative value (6).

This widely available imaging procedure also offers better diagnostic discrimination (7) than ventilation/perfusion scintigraphy.

A number of indices can be used to evaluate the haemodynamic severity of PE by chest CT: among these is the CT obstruction index of Qanadli (8), and the the right-to-left ventricle diameter ratio measurement (RVD/LVD) (9,10), which correlate with the patient's clinical state and prognosis.

Pulmonary perfusion was classically evaluated by scintigraphic methods, involving the intravenous injection of enough radiotracer based on technetium 99m to be trapped in the lung capillaries. This study is generally extended by a ventilation examination. Ventilation/perfusion pulmonary (V/P) scintigraphy thus diagnoses acute PE when a v/p mismatch is visualized.

Spectral CT imaging, by material decomposition based on dual-energy acquisition, can provide iodine map and thereby evaluate the blood volume in the pulmonary parenchyma, detecting low-perfused areas, without impairing the diagnostic quality of the standard chest CT scan, and improving the detection of segmental and non-segmental PE (11), with an overall sensitivity of 94% and a specificity of 93.6% (12).

The main aim of this study was to evaluate prospectively by angiographic spectral imaging chest CT the correlation between perfusion defect volume relatively to the total lung volume without the use of any scoring system and RVD/LVD ratio, Qanadli score, and Geneva score in acute pulmonary embolism.

Our secondary aim was to study the inter-observer reproducibility of the measurements and to conduct a dosimetry study.

II. Materials and methods

A. Population

Patients suspected of pulmonary embolism prospectively underwent spectral imaging pulmonary CT angiography at our center from August 2015 to March 2016.

The Ethics Committee was contacted before inclusions and considered that informed written consent of patients was unnecessary since care was unchanged, there was no loss of chance, and radiation according to literature was under diagnosis reference levels (475 mGy.cm)(13,14).

The patients were referred by emergency unit, ordinary hospital wards, or by the PEAS.

<u>The inclusion criteria were:</u>

- Geneva score (revised) medium to high (15); The Geneva score (revised) (15) was calculated allowing to classify patients according to clinical probability (low, medium, high).
- D-dimers (ELISA) > 500 µg/l.

  ELISA D-dimer measurement was reported retrospectively and the positivity threshold of our laboratory was 500 µg/ml.

  Patients with a low clinical probability score and a significant elevation of D-dimers were included.

The exclusion criteria were: (a) Patients under 18yo;(b) Known heart disorder (dilated cardiomyopathy, myocardial infarct, known pulmonary arterial hypertension, etc.): RVD/LVD is meaningless in those patients;(c) Proven allergy toward iodinated contrast media; (d) Evolving lung tumor; (e) Concomitant lung infection; (f) Non-interpretable examination results: the image quality was rated using a subjectively 3 points scale quality score: good, moderate or poor according to artifacts and opacification; (g) patient with more of 8 % percent of emphysema.

B. CT imaging protocol

1. Spectral imaging acquisition

Spectral imaging was performed on General Electric Discovery 64-channel scanner (750 HD, GENERAL ELECTRIC®, Milwaukee, WI) with one tube allowing to make an acquisition in the same helical series with fast switching (0.25 ms) between the two energies 80 kV and 140 kV, with a field of view (FOV) of 50 cm in order to obtain two attenuation spectra.

Following the standard injection protocols for the chest CT, a power injector was used to administer 80 to 90 ml of iopromidine (Ultravist 370; Bayer Schering Pharma™, Berlin, Germany) pulsed with 50 ml of saline, with an injection rate of 3–4 ml/s (16).

The acquisition provides an iodine-water image (lung perfusion) and a water-iodine image (equivalent of a non injected acquisition).

These acquisitions also provide post-treatment monochromatic images at an energy level chosen between 40 keV and 140 keV, which optimizes contrast for image reading.

An automatic 70keV reconstruction was generated for PE diagnosis (DIAGNOSTIC serie).

In order to reduce streak artefacts (figure 1) cause by dense contrast material in the superior vena cava, imaging was performed in a caudo-cranial direction (16).

Two protocols were used according to the patient's Body Mass Index (BMI): (a)BMI < 25: 80 kV and 140 kV, 375 mA, helical pitch 1.375, gantry rotation 0.7 s, collimation: 40, FOV 50 cm, slice thickness 2 mm, (b) BMI > 25: 80 kV and 140 kV, 630 mA, helical pitch 1.375, gantry rotation 0.5 s, collimation 40, FOV 50 cm, slice thickness 2 mm.

A bolus test technique was used, using ROI in the pulmonary trunk, acquisition delay was increased from 2 to 4 s to provide sufficient contrast in the pulmonary arterial vasculature (16).

The patient was asked to keep a breath hold for a few seconds during the examination.

2. Reconstruction of images and post-treatment

Three series of images from the acquired data by adaptive statistical iterative reconstruction (ASIR):

- An axial CT serie with a standard filter: quality check (140 kVp, thickness 2.5 mm, increment 2 mm);
- A spectral imaging serie (RESEARCH): iodine distribution maps were generated by a specific post-processing workstation (ADW 4.6, General Electric™, Milwaulkee). This series provided a monochromatic series for which the energy level was adjustable between 40 keV and 140 keV at 101 different energy levels, including the displayed default energy of 70 keV, considered as the energy level that offers the best signal-to-noise ratio. The iodine-water series was used to analyze the iodine mapping image and

determine the low-perfused parenchymal areas. The water-iodine series gave images equivalent to acquisition without contrast agent injection, useful for assessing calcification.

- A diagnostic serie (DIAGNOSTIC), with an energy set at 80 keV for examination of pulmonary arteries with a standard filter.

To limit respiration artefacts, the patient was intelligibly informed about holding their breath before acquisition triggering.

B. CT Data analysis

PE was diagnosed if there was:

- A full endoluminal defect in a pulmonary artery with no enhancement of the downstream arterial segment, and possible widening of the arterial bore compared with adjacent arteries;
- A partial central endoluminal defect with longitudinal peripheral opacification of the vessel;
- A peripheral defect making an acute angle with the vessel wall.

The patients with proven acute PE were included.

Images were analyzed by two radiologists, with respectively 4 years and 15 years experience.

Gsi Volume Viewer® software provides MPR evaluation of iodine-water map and allow volume analysis.

The opacification quality of the pulmonary arteries was assessed with a ROI positioned at the center of the pulmonary arterial trunk, with satisfactory opacification if the value for the ROI exceeded 250 HU.

Respiratory artifacts were also subjectively reported. Examinations giving perfectly interpretable, moderately interpretable, and non-interpretable results were separated.

1. Perfusion defect volume

The supplier's default settings were used for the spectral imaging analysis. For the extraction of iodine: −1000 HU for air at 140 kV and 80 kV, 60 HU for soft tissues at 140 kV, 54 HU at 80 kV.

The perfusion defects were classically triangular, pleural based, systematic, downstream of a thrombus, in a pulmonary artery or in one of its dividing branches (17).

This analysis may be difficult in cases of proximal PE where these hyperdense areas may be patchy, variably delimited, and less specific (18). In those poorly delimited areas, the volume was measured only if located downstream of an obstructive thrombus.

The volume was calculated by successive manual contouring of several adjacent sections until the volume was fully delimited (Figures 2-3).

The perfusion defect volume was used to calculate the ratio relative to the total pulmonary parenchyma.

2. Lung volume

The total pulmonary volume was calculated automatically using add-on software "thoracic VCAR" ® in allowing reliable, reproducible determination of the parenchymal volume of the right and left lungs, and the proportion of emphysema for pixels < −950 UH. This volume of emphysema was taken into account in the total lung volume.

The perfusion defect volume / total pulmonary parenchyma volume ratio was thus obtained.

3. Qanadli angiographic obstruction score

In parallel, the Qanadli angiographic obstruction index (8) was calculated for each patient, to assess, as one of our secondary objectives, the correlation between low-perfused parenchyma / total parenchyma ratio and Qanadli angiographic obstruction index.

For this score, the pulmonary parenchyma is divided on each side into 10 segments. Each of these segments is graded, with a score from 0 to 3:

- 0 = no thrombus;
- 1 = partial occlusive thrombus;
- 2 = thrombus fully occluding the vascular lumen.

The obstruction index was calculated by:

$OI = \Sigma (n \times d) /40 \times 100$ (%),

n is the value of the proximal obstruction site, equal to the number of segmental arteries downstream of the obstruction, and *d* is the degree of obstruction.

The number, side, low-perfused areas and obstruction index were recorded.

4. RVD/LVD ratio

The presence of a blood clot in the lumen of a pulmonary artery results in an increased afterload in the right heart chambers, and in extreme cases can cause heart failure. The RVD/LVD ratio can reveal right ventricular dysfunction in PE, and is a medium-to long-term prognostic factor (4,10).

The literature threshold value is RVD/LVD < 0.9 (19).

This measurement was made according to literature on axial sections centered on the cardiac cavities (20), by the two readers on the same day the perfusion images were analyzed (Figure 4).

C. Statistical analysis

Statistical analysis was performed using Stata 13 software (StataCorp LP, College Station, TX, US). The tests were two-sided, with a type I error set at a = 0.05. Subject's characteristics were presented as mean (± standard-deviation) or median [interquartile range] for continuous data (assumption of normality assessed using the Shapiro–Wilk test) and as the number of patients and associated percentages for categorical parameters. The statistical analysis concerning inter-observer reproducibility was carried out (i) by calculating Lin's concordance correlation coefficient (for quantitative outcomes) and (ii) representing by the method of Bland and Altman. The study of relationships between quantitative parameters was performed using correlation coefficients (Pearson or Spearman, according to the statistical distribution), particularly to study (i) the relation between relative volume of low-perfused parenchyma and dilation of right heart chambers and (ii) the relation between low-perfused / total ratio and Qanadli score. Finally, to define a threshold value for the low-perfused pulmonary parenchyma /total parenchyma ratio, predictive of an increase in the RVD/LVD ratio, a receiver operating characteristic (ROC curve) analysis was proposed. The area under the curve was estimated and presented with the 95% confidence interval. Then, the optimal threshold value was determined according to clinical relevance and several indices presented usually in literature (Youden index, Liu index, efficiency).

III. Results

A. Patients included

During the period of inclusion, 242 chest CT for suspected acute PE were recorded using the study protocol.

43 patients presented acute pulmonary embolism; out of these patients, 9 patients were excluded (2 for advanced emphysema (Figure 5), 2 for known heart disorders, 1 for voluminous lung tumor with pericarditis and 4 for technical problems).

Finally, 34 patients (19 males, 15 females) were included: 6 sub segmental PEs (17.7%), 14 segmental PEs (41.1%), 6 lobar PEs (17.7%) and 8 proximal PEs (23.5%). The data collected are summarized in Table 1.

B. Image quality

The whole of the pulmonary parenchyma was included in the FOV for all the examinations. The overall quality of the examination was subjectively judged to be good in 64%, moderate in 21% and poor in 15% of cases. The occurrence of respiratory artifacts was as follow: 41% no artifacts, 47% moderately affected, and 12% markedly affected. In this serie, opacification of pulmonary arteries was judged adequate in 33 patients (97%), and insufficient in 1 patient (3%).

The mean percentage of parenchymal emphysema calculated automatically by the thoracic VCAR software was 0.76% (SD = 1.57%; min 0, max 7%)

C. Correlation between perfusion defect volume/ total lung volume and RVD/LVD ratios

Statistical analysis showed a close correlation between perfusion defect volume/ total lung volume and dilation of right heart chambers ($r = 0.82$, $p < 0.001$ for reader 1, and $r = 0.66$, $p < 0.001$ for reader 2) (Figures 6 and 7). With a cutoff value of 0.9, reader 1 found 12 patients (35%) with no dilation of right heart chambers; reader 2 found 10 such patients (29%). For each reader in this series a relative perfusion defect threshold value was calculated before dilation of the right ventricle was visualized. For this purpose, two ROC curves were plotted for the diagnostic characteristics of the two analyses, determining for each reader the low-perfusion ratio from which a right heart chamber dilation was observed. This threshold value was 14.48% of perfusion defect volume/ total lung volume for reader 1 (Se = 71%, Sp = 100%, AUC = 0.86) and 8.85% for reader 2 (Se = 50%, Sp = 100%, AUC = 0.87) (Figures 8 and 9).

D. Inter-observer reproducibility

We found a close correlation between the two observers, with a correlation coefficient of 0.91 ($p < 0.001$), but concordance was poor ($\kappa = 0.40$), the measurements made by reader 1 being systematically higher than those of reader 2. This variability was particularly noteworthy for large low-perfused volumes (>10%); concordance seemed to be better with small volumes.

The mean difference between the two readers was 12.9%.

E. Correlation between perfusion defect volume/ total lung volume ratio and Qanadli score

The correlation between the low-perfused / total lung volume ratio and the Qanadli angiographic obstruction score was excellent for reader 1 and good for reader 2, at r=0.84 ($p < 0.001$) and r=0.76 ($p < 0.001$) (Figure 10).

F. RVD/LVD ratio

An excellent inter-observer reproducibility was found for the measurement of the RVD/LVD ratio. The concordance was 0.871 ($p < 0.001$), and the correlation was 0.882 ($p < 0.001$).

G. Geneva score (revised)

No significant correlation was found between the Geneva score (revised) and the perfusion defect volume / total parenchyma ratio, with a correlation coefficient of 0.078 ($p = 0.66$) for reader 1 and 0.099 ($p = 0.58$) for reader 2.

Likewise, no correlation was found between the Geneva score (revised) and the RVD/LVD ratio, with a correlation coefficient of 0.0723 ($p = 0.68$) for reader 1 and 0.12 ($p = 0.51$) for reader 2.

H. D-dimers

The average blood level of D-dimers measured was 3985 µg/ml (SD = 3282; min 490, max 11800). Data were missing for 4 patients, only one patient presented a level of D-dimers below our detection threshold.

I. Dosimetry study

The mean dose-length product (DLP) was 517.33 mGy.cm (SD = 155; min 407, max 733) for all the patients. The mean CTDI was 12.69 +/− 2.02 mGy (min 9.25, max 15.64).
The mean effective dose received was 7.24 mSv (SD = 2.17).

IV. Discussion

The applicability and utility of the DECT lung perfusion imaging in the diagnosis of acute PE are largely demonstrated in the literature (20–23).
Our study found a close correlation between the perfusion defect volume / total volume ratio (PD vol/TL vol) and the RVD/LVD ratio for two readers, although concordance between the readers was poor.
This result is correlated with other results already published (16,22,24,25). The fact that we didn't used automatic graduation of perfusion can explain the poor correlation between 2 readers, but correlation was good concerning PD vol/TL vol and the RVD/LVD ratio for the 2 readers. Respiratory and beam-hardening artifacts were also probably responsible for the inter-observer variability found in our study. Threshold of PD vol/TL vol with RVD/LVD ratio> 0,9 were respectively 14,48 % and 8,85 % for the 2 readers, in patients without known cardiac pathologies.
In the literature, a variability in perfusion defect volume measurements is also reported: 12–57% (mean 25%) in Apfaltrer & al. (25), and 0.2–22.9% (median 3.1%) in Bauer & al. (18), despite being recorded using the same material (Siemens ™), highlighting a wide margin in the interpretation of results in series that overall were closely similar.
The inter-observer reproducibility was excellent in both the above studies. These differences question the reliability of the measurement, and may reflect different operating methods, particularly for windowing. Using 99mTc scintigraphy and cardio echography, Kjaergaard & al. found a deterioration in right heart function when more than 25% low-perfusion occurred (26). This difference may be related to population in our study, in particular age (mean age 64 years).

According to already published studies, we found an excellent correlation between PD vol/TL vol and Qanadli score (16,22,25,27).

Geneva score is widely used in emergency units to assess clinical probability of acute pulmonary embolism (low, medium, high). In our study, any correlation was found between Geneva score and PD vol/TL vol, neither RVD/LVD ratio in case of pulmonary embolism. Meyer et al. (28) have reported that combination of troponin and cardiac CT parameters improves the diagnostic accuracy for detecting RVD and predicting adverse clinical outcomes. Geneva score combining clinical data does not correlate to the severity of PE in our study.

Many studies have found a close correlation between angiographic obstruction scores based on pulmonary segmentation (22,24).

The present study, based on quantitative analysis, confirms the results of this earlier work. In addition to the iodine spectral imagery, researchers have developed a new method of CT scan analysis of lung ventilation/perfusion using spectral decomposition of xenon (25) or krypton (26) for mapping comparable to that obtained by pulmonary ventilation scintigraphy.

This technique requires two distinct acquisitions, with a resulting increased exposure of the patient to radiation (mean = 2.6 +/− 0.8 mSv in the series of Zhang & al (29). This interesting technique has so far been used only for obstructive disorders of the airways, such as asthma. Pulmonary scintigraphy can also be used in acute PE to obtain ventilation/perfusion images, though with a long acquisition time and poorer spatial resolution. The V/P SPECT technique can be used to study the low-perfused pulmonary parenchyma more reliably and reproducibly than conventional V/P scintigraphy, and correlate it with low-ventilated tissues, with a detection capacity similar to that of a chest CT angiography (30).

Spectral imaging provides a better spatial resolution than by plane imaging with V/P scintigraphy or V/P SPECT (31). However, one advantage offered by the techniques of nuclear medicine is their low radiation dose compared with spectral imaging. The mean received dose in an adult during V/P scintigraphy is about 1.1 mSv against 2–6 mSv for a chest CT. In our study this value reached 7.24 mSv (SD = 2.17). This is explained by the fact that mAs modulation is not available in spectral imaging.

The routine applicability of the measurement of PD vol/TL vol ratio was limited in our study by the poor concordance between the readers. We found that the assessment of the low-perfused parenchymal volume was hindered by the many artifacts associated with spectral imaging (32,33).

In addition, we note several factors influencing the distribution of iodine in the pulmonary parenchyma, in particular vascular effects, as shown by Kim & al., who studied causes of low perfusion in iodine spectral imaging other than PE (34). This study showed that the quality of lung perfusion depends not only on

volume, flow rate and contrast agent injection site, but also on factors that are more difficult to anticipate by adapting the acquisition protocol, such as the state of right heart, superior vena cava and pulmonary arteries or pulmonary veins, left heart and aorta, but also microcirculation. Moreover, the participation of systemic vascularization, given that the bronchial arteries can supply 25% of blood oxygen.

In our protocol, the acquisition parameters were adjusted according to patient BMI, but not the amount of contrast agent, which could cause a difference in blood iodine concentration. Another possible cause of high inter-observer variability was the absence of preset windowing for iodine imaging, a major limit of this study, but it was difficult to standardize windowing for all the patients (18), which largely depended on the quality of the examination.

It would have been interesting to set a threshold value of blood volume, based on an ROI measurement in a given area, to define low-perfusion of the pulmonary parenchyma. Some studies have shown the utility of a relative ROI in spectral imaging to improve sensitivity in the detection of PE, which can be especially useful in cases of distal PE. Ikeda & al. demonstrated that the measured pulmonary blood volume (PBV) fell significantly in the downstream lung tissues when an artery branch was fully obstructed, compared with adjacent pulmonary parenchyma (35).

By contrast, no significant difference was found in iodine concentration compared with controls when arterial obstruction was incomplete. Miura and al. (23) and Sakamoto and al. (36) demonstrated that lowered PBV throughout the parenchyma was correlated with right heart dysfunction measured by echocardiography. All these studies were based on a differential analysis relative to healthy parenchyma, and absolute values were not given. Anterior paracardiac areas and apices were probably incorrectly analyzed, appearing regularly lowperfused, imposing a difficult windowing adjustment and generating errors. These artifacts are described in the literature and are explained by the X-ray beam-hardening effect at the level of the superior vena cava and by heart movement artifacts (37).

Most of the studies on this topic have used Siemens™ instruments, which use different acquisition technology, with two tubes and two separate detectors positioned at 90° making two distinct acquisitions at 80 kV and 140 kV.

However, a major limit of this technique is a restricted FOV for the 80 kV series (26 cm), with cropping of peripheral pulmonary parenchyma in some cases. Our results show that besides the poor inter-observer concordance, the measurements of low-perfused pulmonary parenchyma differed by one order of magnitude: the mean recorded perfusion defect parenchyma volume was 19.33% (min 0, max 66.49%, SD = 20.27) for reader 1 against 6.67% (min 0, max 26.58%, SD = 7.32) for reader 2.

The dosimetry study in the present work found values higher than those classically reported in the literature for diagnosis of PE by spectral imaging, with measured DLP averaging 517 +/− 155 mGy.cm. In the literature, the mean dose ranges between 280 mGy.cm in Pontana & al. (38) and 474 mGy.cm in Geyer & al. (39). This divergence can be ascribed to the use of different instruments and techniques for image acquisition. The single tube, single receptor technology used in our study operates with a fixed current, as it is technically difficult to vary it rapidly in step with voltage. Also, this variable is increased to lower noise at 80 kV. This significant increase in the dose administered to the patient is described in the literature by Ho & al. (40) who showed a three-fold increase in radiation in a study centered on the abdomen and pelvis.

Technological solutions are thus needed to allow rapid current variation and so reduce radiation exposure. Lastly, precise volume analysis is time-consuming for the radiologist, and difficult to use routinely, as the analysis takes about 20 minutes per patient for a radiologist familiar with the software. This argues for the development of specific software to segment the low-perfused regions automatically, which would improve patient care.

A major limit of our study is thus a lack of standardized windowing defined to measure defect perfusion volume. Standardization might improved inter-observer concordance. Intra-observer variability was not studied, but might have partially explained the marked intraobserver variability observed in our study. We also note that 21% of the patients with PE were excluded from the study: most of these did not meet our inclusion criteria.

A follow-up of the population could also have been carried out, and might have provided further evidence supporting the predictive power of PD vol/TL vol ratio for short- and medium-term complications of PE.

V. Conclusion

The aim of this study was to evaluate the correlation between PD vol/TL vol ratio and RVD/LVD ratio by iodine spectral imaging in pulmonary embolism. Our study found a close correlation between the relative volume of defect perfusion volume measured by spectral imaging and dilation of the right heart chambers independently of the reader, despite inter observer poor correlation in PD volume evaluation, confirming results of published studies. Threshold of PD vol/TL vol with RVD/LVD ratio> 0,9 were respectively 14,48 % and 8,85 % for the 2 readers, in patients without known cardiac pathologies. Patient's hemodynamic state and the blood concentration of the contrast agent influence the density of low-perfused areas relative to those normally perfused. A study of the correlation between right ventricular flow rate and intraparenchymal iodine concentration might provide further information to help make better use of lung perfusion imaging. Any correlation was found between Geneva score, widely used clinical probability score, and PD vol/TL vol, neither RVD/LVD ratio in case of pulmonary embolism.

VI. References

1. Remy-Jardin M, Pistolesi M, Goodman LR, Gefter WB, Gottschalk A, Mayo JR, et al. Management of suspected acute pulmonary embolism in the era of CT angiography: a statement from the Fleischner Society. Radiology. 2007 Nov;245(2):315–29.

2. Goldhaber SZ, Visani L, De Rosa M. Acute pulmonary embolism: clinical outcomes in the International Cooperative Pulmonary Embolism Registry (ICOPER). Lancet Lond Engl. 1999 Apr 24;353(9162):1386–9.

3. Pollack CV, Schreiber D, Goldhaber SZ, Slattery D, Fanikos J, O'Neil BJ, et al. Clinical characteristics, management, and outcomes of patients diagnosed with acute pulmonary embolism in the emergency department: initial report of EMPEROR (Multicenter Emergency Medicine Pulmonary Embolism in the Real World Registry). J Am Coll Cardiol. 2011 Feb 8;57(6):700–6.

4. Sanchez O, Trinquart L, Colombet I, Durieux P, Huisman MV, Chatellier G, et al. Prognostic value of right ventricular dysfunction in patients with haemodynamically stable pulmonary embolism: a systematic review. Eur Heart J. 2008 Jun;29(12):1569–77.

5. Agnelli G, Becattini C. Acute pulmonary embolism. N Engl J Med. 2010 Jul 15;363(3):266–74.

6. Stein PD, Fowler SE, Goodman LR, Gottschalk A, Hales CA, Hull RD, et al. Multidetector computed tomography for acute pulmonary embolism. N Engl J Med. 2006 Jun 1;354(22):2317–27.

7. Green DB, Raptis CA, Alvaro Huete Garin I, Bhalla S. Negative Computed Tomography for Acute Pulmonary Embolism: Important Differential Diagnosis Considerations for Acute Dyspnea. Radiol Clin North Am. 2015 Jul;53(4):789–99, ix.

8. Qanadli SD, El Hajjam M, Vieillard-Baron A, Joseph T, Mesurolle B, Oliva VL, et al. New CT index to quantify arterial obstruction in pulmonary embolism: comparison with angiographic index and echocardiography. AJR Am J Roentgenol. 2001 Jun;176(6):1415–20.

9. Meinel FG, Nance JW, Schoepf UJ, Hoffmann VS, Thierfelder KM, Costello P, et al. Predictive Value of Computed Tomography in Acute Pulmonary Embolism: Systematic Review and Meta-analysis. Am J Med. 2015 Jul;128(7):747–59.e2.

10. Schoepf UJ, Kucher N, Kipfmueller F, Quiroz R, Costello P, Goldhaber SZ. Right ventricular enlargement on chest computed tomography: a predictor of early death in acute pulmonary embolism. Circulation. 2004 Nov 16;110(20):3276–80.

11. Kang M-J, Park CM, Lee C-H, Goo JM, Lee HJ. Dual-energy CT: clinical applications in various pulmonary diseases. Radiogr Rev Publ Radiol Soc N Am Inc. 2010 May;30(3):685–98.

12. Kuriakose J, Patel S. Acute pulmonary embolism. Radiol Clin North Am. 2010 Jan;48(1):31–50.

13. de Broucker T, Pontana F, Santangelo T, Faivre J-B, Tacelli N, Delannoy-Deken V, et al. Single- and dual-source chest CT protocols: Levels of radiation dose in routine clinical practice. Diagn Interv Imaging. 2012 Nov;93(11):852–8.

14. Institut de radioprotection et de sureté nucléaire (IRSN). Analyse des données relatives à la mise à jour des niveaux de référence diagnostiques en radiologie et en médecine nucléaire. Bilan 2007–2008. Rapport DRPH n° 2010-15. internet; 2010.

15. Gruettner J, Walter T, Lang S, Meyer M, Apfaltrer P, Henzler T, et al. Importance of Wells score and Geneva score for the evaluation of patients suspected of pulmonary embolism. Vivo Athens Greece. 2015 Apr;29(2):269–72.

16. Thieme SF, Ashoori N, Bamberg F, Sommer WH, Johnson TRC, Leuchte H, et al. Severity assessment of pulmonary embolism using dual energy CT - correlation of a pulmonary perfusion defect score with clinical and morphological parameters of blood oxygenation and right ventricular failure. Eur Radiol. 2012 Feb;22(2):269–78.

17. Cai X-R, Feng Y-Z, Qiu L, Xian Z-H, Yang W-C, Mo X-K, et al. Iodine Distribution Map in Dual-Energy Computed Tomography Pulmonary Artery Imaging with Rapid kVp Switching for the Diagnostic Analysis and Quantitative Evaluation of Acute Pulmonary Embolism. Acad Radiol. 2015 Jun;22(6):743–51.

18. Bauer RW, Kerl JM, Weber E, Weisser P, Korkusuz H, Lehnert T, et al. Lung perfusion analysis with dual energy CT in patients with suspected pulmonary embolism--influence of window settings on the diagnosis of underlying pathologies of perfusion defects. Eur J Radiol. 2011 Dec;80(3):e476–82.

19. Kang DK, Thilo C, Schoepf UJ, Barraza JM, Nance JW, Bastarrika G, et al. CT signs of right ventricular dysfunction: prognostic role in acute pulmonary embolism. JACC Cardiovasc Imaging. 2011 Aug;4(8):841–9.

20. Meyer M, Haubenreisser H, Sudarski S, Doesch C, Ong MM, Borggrefe M, et al. Where do we stand? Functional imaging in acute and chronic pulmonary embolism with state-of-the-art CT. Eur J Radiol. 2015 Dec;84(12):2432–7.

21. Lu GM, Zhao Y, Zhang LJ, Schoepf UJ. Dual-energy CT of the lung. AJR Am J Roentgenol. 2012 Nov;199(5 Suppl):S40–53.

22. Chae EJ, Seo JB, Jang YM, Krauss B, Lee CW, Lee HJ, et al. Dual-energy CT for assessment of the severity of acute pulmonary embolism: pulmonary perfusion defect score compared with CT angiographic obstruction score and right ventricular/left ventricular diameter ratio. AJR Am J Roentgenol. 2010 Mar;194(3):604–10.

23. Miura S, Ohno Y, Kimura H, Kichikawa K. Quantitative lung perfused blood volume imaging on dual-energy CT: capability for quantitative assessment of disease severity in patients with acute pulmonary thromboembolism. Acta Radiol Stockh Swed 1987. 2015 Mar;56(3):284–93.

24. Bauer RW, Frellesen C, Renker M, Schell B, Lehnert T, Ackermann H, et al. Dual energy CT pulmonary blood volume assessment in acute pulmonary embolism – correlation with D-dimer level, right heart strain and clinical outcome. Eur Radiol. 2011 Apr 30;21(9):1914–21.

25. Apfaltrer P, Bachmann V, Meyer M, Henzler T, Barraza JM, Gruettner J, et al. Prognostic value of perfusion defect volume at dual energy CTA in patients with pulmonary embolism: correlation with CTA obstruction scores, CT parameters of right ventricular dysfunction and adverse clinical outcome. Eur J Radiol. 2012 Nov;81(11):3592–7.

26. Kjaergaard J, Schaadt BK, Lund JO, Hassager C. Quantification of right ventricular function in acute pulmonary embolism: relation to extent of pulmonary perfusion defects. Eur J Echocardiogr J Work Group Echocardiogr Eur Soc Cardiol. 2008 Sep;9(5):641–5.

27. Meinel FG, Graef A, Bamberg F, Thieme SF, Schwarz F, Sommer WH, et al. Effectiveness of automated quantification of pulmonary perfused blood volume using dual-energy CTPA for the severity assessment of acute pulmonary embolism. Invest Radiol. 2013 Aug;48(8):563–9.

28. Meyer M, Fink C, Roeger S, Apfaltrer P, Haghi D, Kaminski WE, et al. Benefit of combining quantitative cardiac CT parameters with troponin I for predicting right ventricular dysfunction and adverse clinical events in patients with acute pulmonary embolism. Eur J Radiol. 2012 Nov;81(11):3294–9.

29. Zhang LJ, Yang GF, Zhao YE, Zhou CS, Lu GM. Detection of pulmonary embolism using dual-energy computed tomography and correlation with cardiovascular measurements: a preliminary study. Acta Radiol Stockh Swed 1987. 2009 Oct;50(8):892–901.

30. Phillips JJ, Straiton J, Staff RT. Planar and SPECT ventilation/perfusion imaging and computed tomography for the diagnosis of pulmonary embolism: A systematic review and meta-analysis of the literature, and cost and dose comparison. Eur J Radiol. 2015 Jul;84(7):1392–400.

31. Thieme SF, Graute V, Nikolaou K, Maxien D, Reiser MF, Hacker M, et al. Dual Energy CT lung perfusion imaging--correlation with SPECT/CT. Eur J Radiol. 2012 Feb;81(2):360–5.

32. Fraioli F, Ciarlo G, Anzidei M. Dual-energy CT: too many artifacts? AJR Am J Roentgenol. 2011 Oct;197(4):W783.

33. Thieme SF, Johnson TRC, Lee C, McWilliams J, Becker CR, Reiser MF, et al. Dual-energy CT for the assessment of contrast material distribution in the pulmonary parenchyma. AJR Am J Roentgenol. 2009 Jul;193(1):144–9.

34. Kim BH, Seo JB, Chae EJ, Lee HJ, Hwang HJ, Lim C. Analysis of perfusion defects by causes other than acute pulmonary thromboembolism on contrast-enhanced dual-energy CT in consecutive 537 patients. Eur J Radiol. 2012 Apr;81(4):e647–52.

35. Ikeda Y, Yoshimura N, Hori Y, Horii Y, Ishikawa H, Yamazaki M, et al. Analysis of decrease in lung perfusion blood volume with occlusive and non-occlusive pulmonary embolisms. Eur J Radiol. 2014 Dec;83(12):2260–7.

36. Sakamoto A, Sakamoto I, Nagayama H, Koike H, Sueyoshi E, Uetani M. Quantification of lung perfusion blood volume with dual-energy CT: assessment of the severity of acute pulmonary thromboembolism. AJR Am J Roentgenol. 2014 Aug;203(2):287–91.

37. Kang M-J, Park CM, Lee C-H, Goo JM, Lee HJ. Focal iodine defects on color-coded iodine perfusion maps of dual-energy pulmonary CT angiography images: a potential diagnostic pitfall. AJR Am J Roentgenol. 2010 Nov;195(5):W325–30.

38. Pontana F, Faivre J-B, Remy-Jardin M, Flohr T, Schmidt B, Tacelli N, et al. Lung perfusion with dual-energy multidetector-row CT (MDCT): feasibility for the evaluation of acute pulmonary embolism in 117 consecutive patients. Acad Radiol. 2008 Dec;15(12):1494–504.

39. Geyer LL, Scherr M, Körner M, Wirth S, Deak P, Reiser MF, et al. Imaging of acute pulmonary embolism using a dual energy CT system with rapid kVp switching: initial results. Eur J Radiol. 2012 Dec;81(12):3711–8.

40. Ho LM, Yoshizumi TT, Hurwitz LM, Nelson RC, Marin D, Toncheva G, et al. Dual energy versus single energy MDCT: measurement of radiation dose using adult abdominal imaging protocols. Acad Radiol. 2009 Nov;16(11):1400–7.

Figure 1. Example of a beam-hardening artifact caused by massive arrival of contrast agent in the superior vena cava in a patient with low perfusion of right apex due to upper right lobar pulmonary embolism, hindering interpretation in this area.

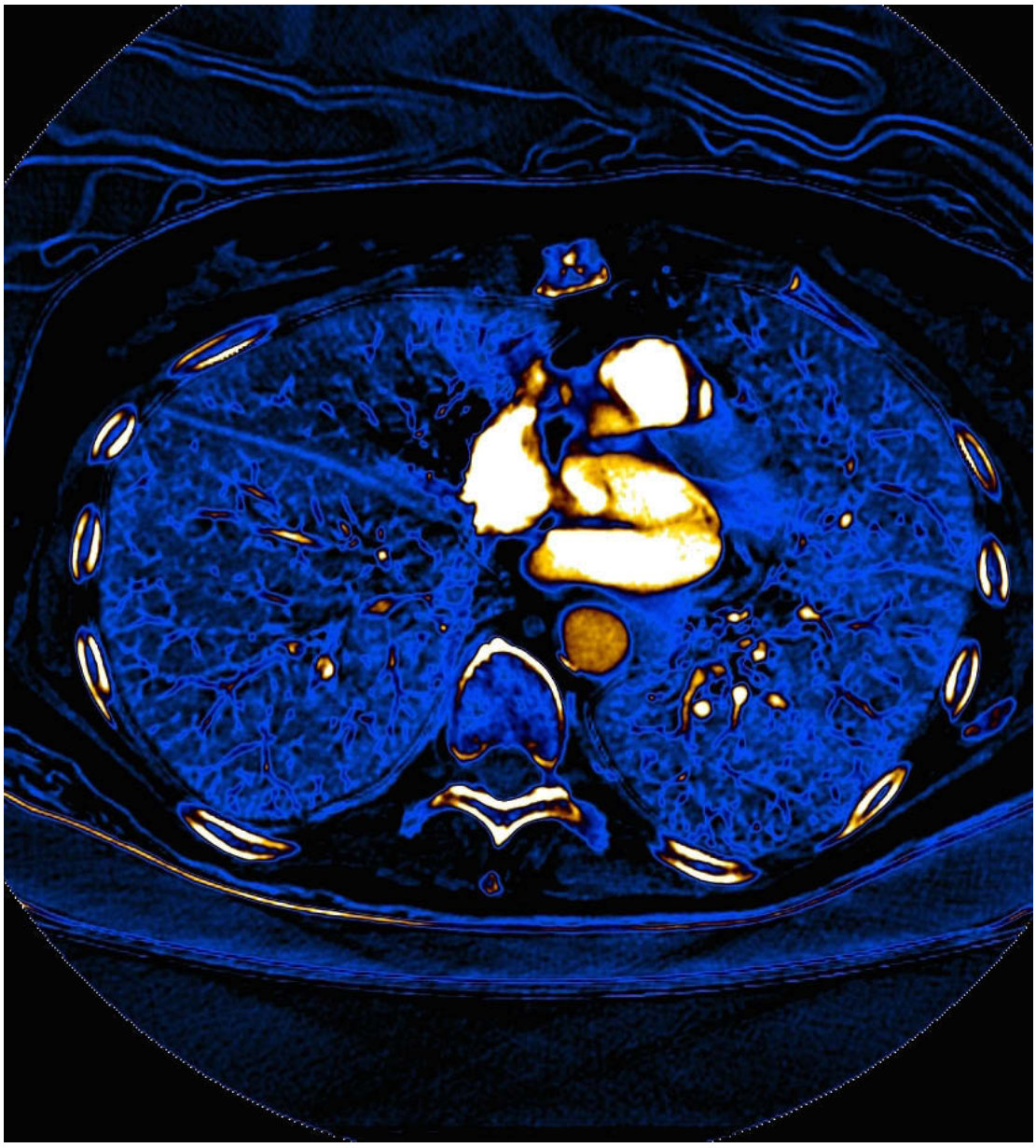

Figure 2. Example of a contoured low-perfused area of parenchyma in a patient aged 19 years with a distal pulmonary embolism.

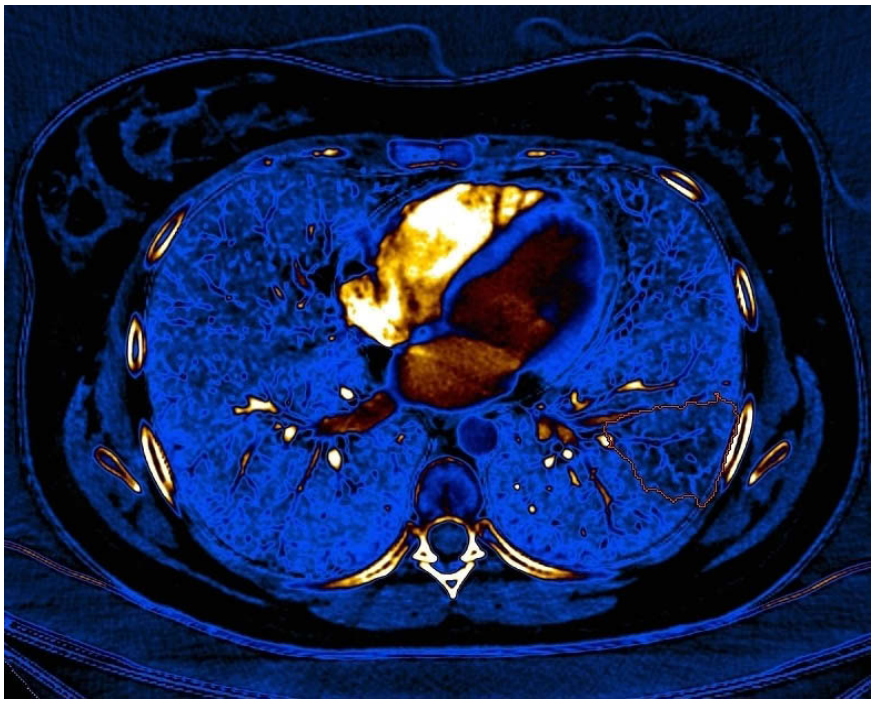

Figure 3. MPR reconstructions in coronal plan in the same patient showing the contoured defect interpolated from axial sections.

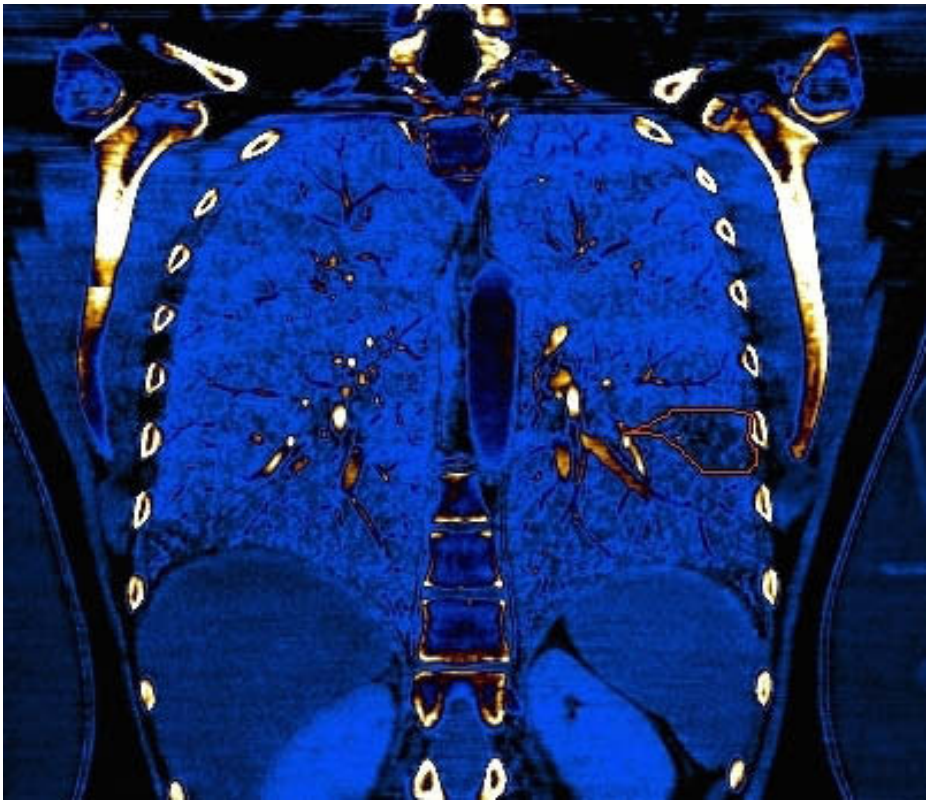

S O

Figure 4. Example of ventricle diameter ratio measurement on CT sections in the axial plane showing marked dilation of the right ventricle (RVD/LVD = 1.8) in a proximal acute pulmonary embolism.

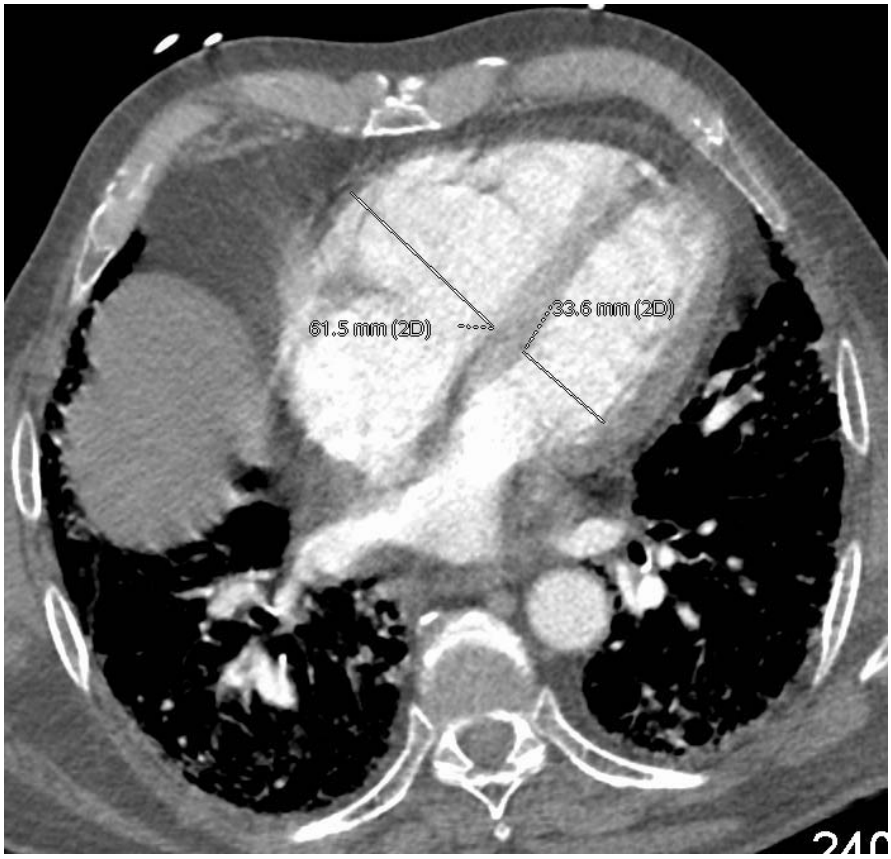

Figure 5. Example of pulmonary perfusion in a patient with advanced emphysema (22%). All the parenchyma shows perfusion defect.

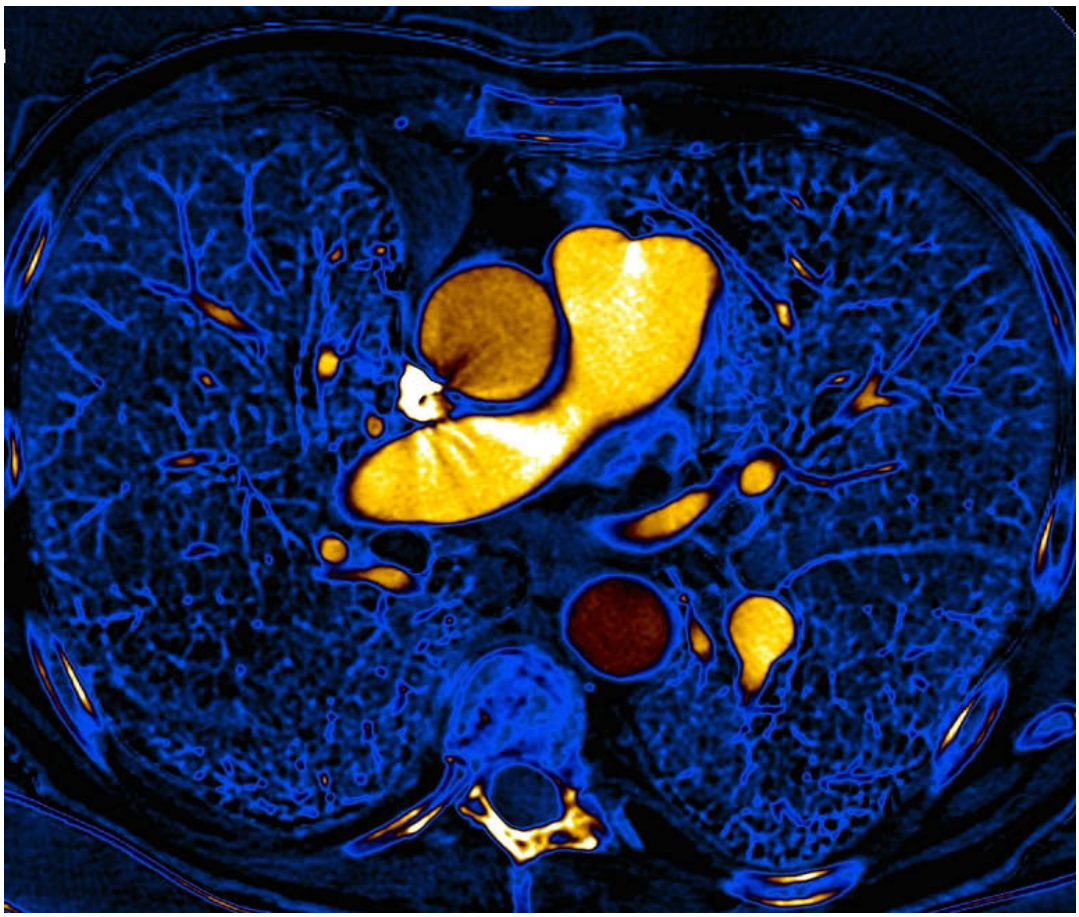

sT

Figure 6. correlation between perfusion defect volume / total parenchyma volume and RVD/LVD ratios for reader 1

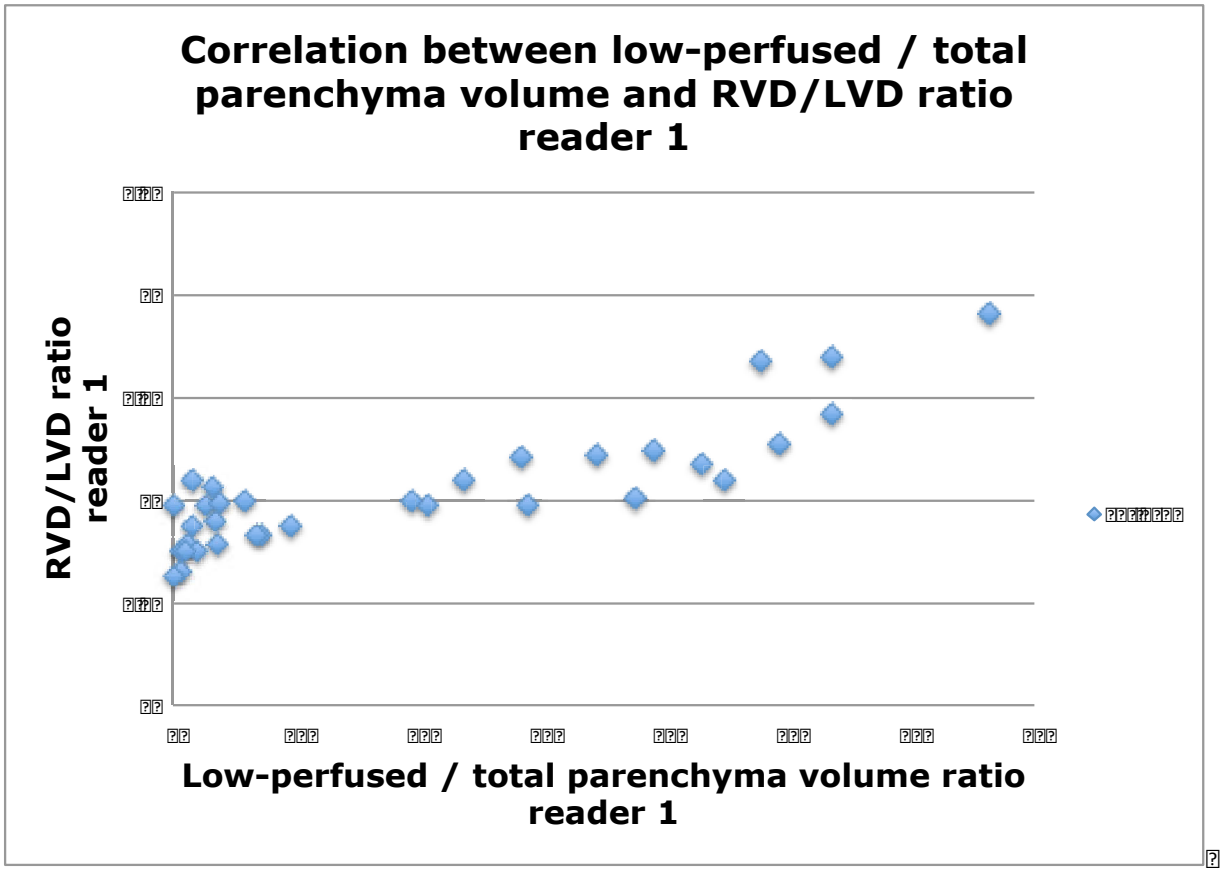

Figure 7. correlation between perfusion defect volume / total parenchyma volume and RVD/LVD ratios for reader 2

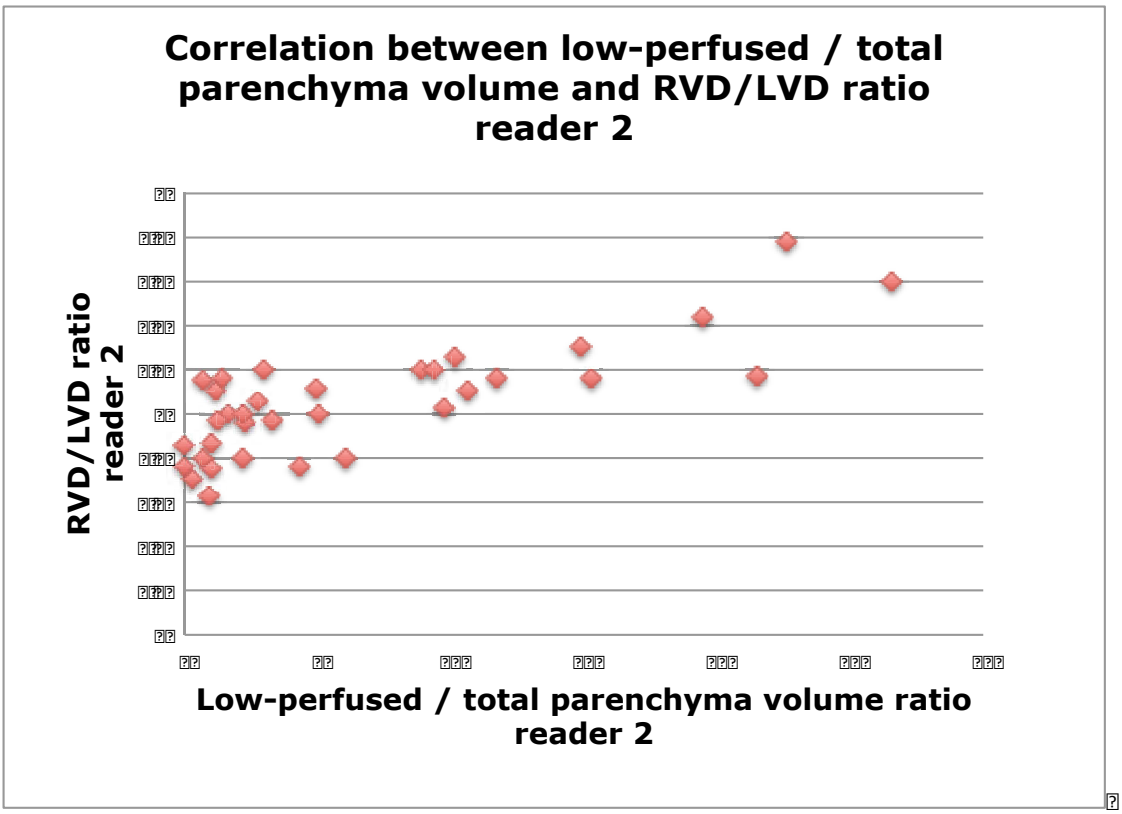

sè

Figure 8. ROC curve plotted from data recorded by reader 1 for a defect perfusion volume/ total lung volume ratio threshold value of 14.48% before elevation of RVD/LVD > 0.9

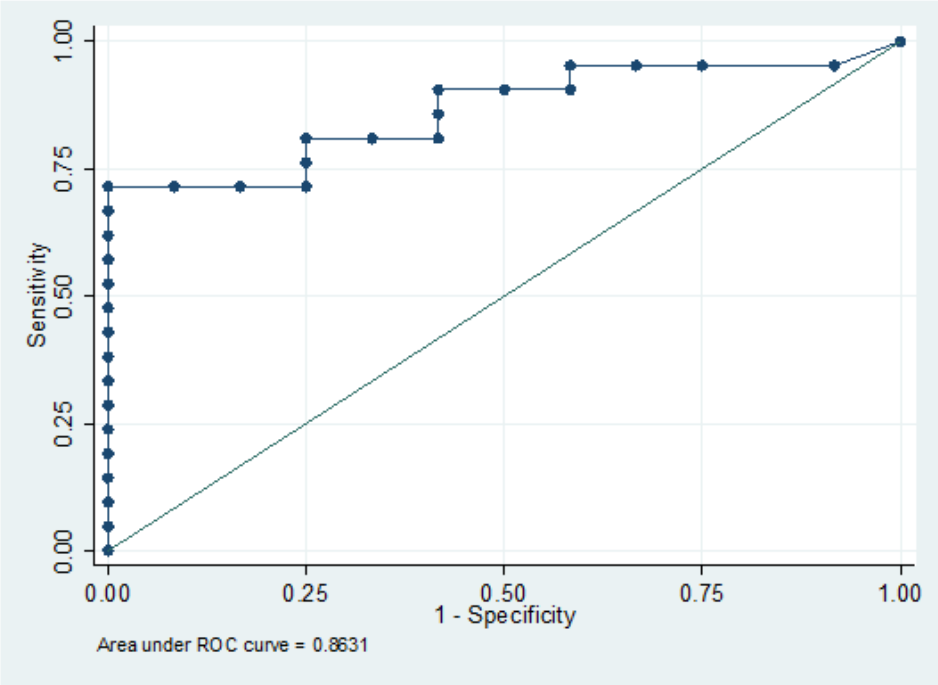

Figure 9. ROC curve plotted from data recorded by reader 2 for a [illegible] threshold value of 8.85% before elevation of RVD/LVD > 0.9

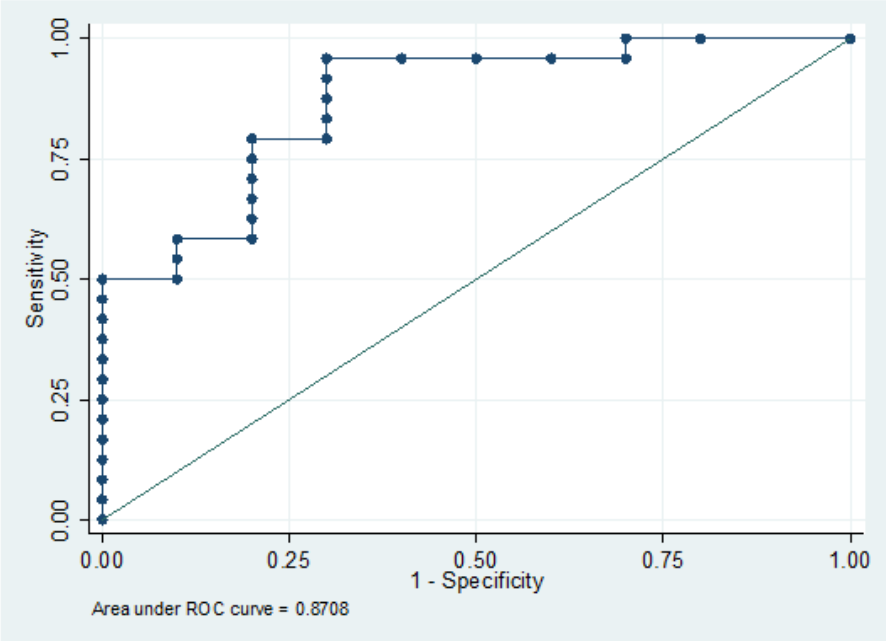

Figure 10. Bland & Altman graph showing inter-observer differences in the measurements of perfusion defect volume / total lung volume ratio.

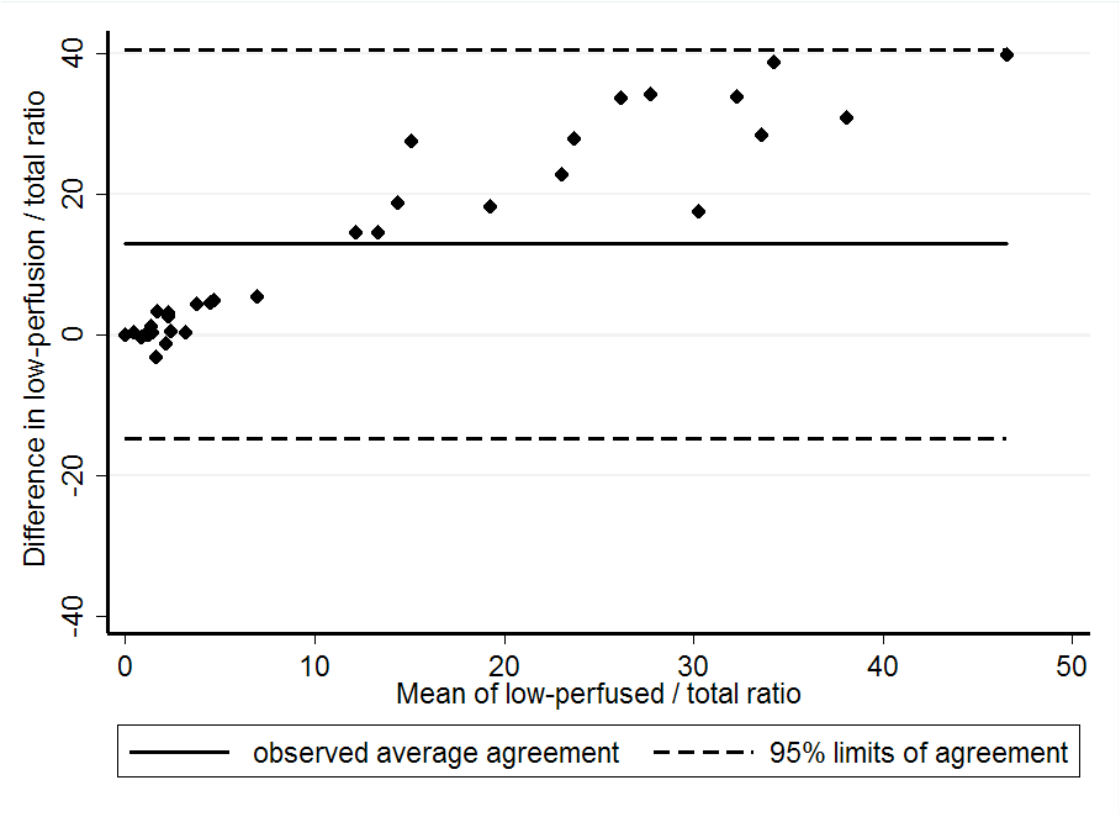

s L

	Mean	SD	(min/max)
Age (years)	64.3	18.75	20/93
Geneva score (revised) (/15)	6.84	3.29	1/17
D-dimers Elisa (µg/ml)	3985	3282	490/11800
Respiratory artifacts	0.7	0.67	0/2
Volume of contrast agent (ml)	85.44	13.04	60/110
ROI of pulmonary arterial trunk	341.38	82.53	180/514
Emphysema (%)	0.76	1.57	0/7
Qanadli score(/40)	13.08	11.07	1/34
RVD/LVD ratio, reader 1	1.04	0.29	0.63/1.91
RVD/LVD ratio, reader 2	1.05	0.25	0.63/1.78
Low-perfused / total vol., reader 1	19.33	20.2	0/66.49
Low-perfused / total vol., reader 2	6.67	7.32	0/26.58

Conclusion

Notre étude souffre d'un petit nombre de patients, mais permet cependant de retrouver une corrélation significative entre les paramètres etudiés (rapport volume de defect de perfusion / volume pulmonaire total et rapport VD/VG).

Nos résultats soulignent les difficultés, voire l'impossibilité, de mettre en place un niveau de lecture standardisé des examens, entrainant une importante variabilité inter-observateur. La concentration en iode au sein du parenchyme pulmonaire dépend de beaucoup de paramètres : fonction cardiaque, volume sanguin total, déclenchement optimal de l'acquisition… Nous avons choisi, dans un soucis d'économie de dose d'irradiation, de ne réaliser qu'une seule acquisition au temps artériel pulmonaire de l'injection de produit de contraste iodé. Une acquisition plus tardive, à un temps « parenchymateux », comme pour l'exploration hépatique par exemple, permettrait sans doute d'augmenter le contraste entre les zones hypoperfusées et normalement perfusées, rendant la standardisation de la lecture possible.

En revanche aucune corrélation n'était retrouvée entre le score de Genève, score clinique de probabilité largement utilisé, et les paramètres étudiés.

Nous souhaitons poursuivre cette première étude afin de confirmer ces résultats : à pourcentages volume de defect de perfusion égaux, retrouve-t-on cette corrélation en cas d'embolie pulmonaire proximale ou uniquement distale ? Il semblerait logique de penser qu'une obstruction proximale ai plus de retentissement sur la post charge ventriculaire droite, mais des embolies multiples distales engendrent-elles la même augmentation de pression pulmonaire ? Il est nécessaire pour cela disposer d'une plus grande série de patients.

Le Coeur gauche et la pathologie néoplasique pulmonaire

Left atrial resection for T4 lung cancer without cardiopulmonary bypass: technical aspects and outcomes.

Galvaing G, Tardy MM, Cassagnes L, Da Costa V, Chadeyras JB, Naamee A, Bailly P, Filaire E, Pereira B, Filaire M.

Ann Thorac Surg. 2014 May; 97(5):1708-13.

Dans la pathologie néoplasique pulmonaire, les patients classés T4 (tumeur envahissant directement une des structures suivantes: médiastin, coeur, gros vaisseaux, trachée, nerf laryngé récurrent, œsophage, corps vertébral, carène.) sont classiquement récusés pour une prise en charge chirurgicale.

Notamment l'envahissement du massif cardiaque par contiguité, par le biais d'une atteinte de veines pulmonaires et s'étendant au septum inter auriculaire, ne permettait pas jusqu'à récemment un chirurgie carcinologiquement complète.

La mise au point d'une technique chirurgicale de résection partielle de l'oreillette gauche avec dissection du septum inter-auriculaire permettrait d'opérer ces patients.

Nous avons réalisé dans notre centre une étude prospective chez 19 patients présentant un envahissement cardiaque avec suivi post opératoire pour juger de la possibilité de prise en charge chirurgicale carcinologiquement satisfaisante de ces patients.

Abstract

Introduction:

Une resection chirurgicale étendue peut améliorer la survie de patients affectés de cancer bronchique sélectionnés. La resection de l'oreillette gauche est rarement réalisée et les techniques chirurgicales rarement rapportées, c'est pourquoi les résultats oncologiques et les taux de survie restent incertains.Notre étude décrit les techniques chirurgicales, les résultats post-opératoires et les résultats oncologiques de patients ayant bénéficié d'un traitement combiné.

Methode:

Entre Octobre 2004 et Mars 2012 dans notre hôpital, 19 patients ont bénéficié d'une resection pulmonaire étendue incluant l'oreillette gauche sans pontage cardiopulmonaire. Nous avons passé en revue les traitements, les procedures chirurgicales, la morbidité et la mortalité post-opératoires, ainsi que la survie à long terme.

Resultats:

Seize patients (68.4%) ont bénéficié d'un traitement néo-adjuvant incluant chimiothérapie ou radiothérapie.

18 pneumonectomies (94.7%) ont été réalisées, parmis lesquelles 12 (63.1%) du côté droit.

La dissection du septum inter-auriculaire était complète chez 4 patients (33.3%). Une resection complete a été réalisée chez 17 patients (89.4%) et 2 autres patients (10.5%) étaient considérés R1. Tous les patients étaient classes T4. La morbidité post-opératoire était de 52,6%. Le taux de mortalité à 30 jours s'élevait à 10,5 % et à 90 jours à 15,7 %.

Quinze patients (93,7 %) ont bénéficié d'un traitement adjuvant. Le suivi moyen était de 32,5 mois. La probabilité de survie à 5 ans était de 43,7 %. Trois patients patients (15,7 %) étaient en vie à plus de 6 ans post chirurgie.

Conclusion:

Une chirurgie pulmonaire étendue avec resection partielle de l'oreillette gauche est réalisable avec une morbidité acceptable. La dissection du septum inter-auriculaire, en augmentant la longueur du repli auriculaire, permet une resection complete. La survie à long terme peut être obtenue chez des patients sélectionnés et bénéficiant de traitements adjuvants.

Left Atrial Resection for T4 Lung Cancer Without Cardiopulmonary Bypass: Technical Aspects and Outcomes

Geraud Galvaing, MD, Marie M. Tardy, Lucie Cassagnes, MD, Valinkini Da Costa, MD, Jean Baptiste Chadeyras, MD, Adel Naamee, MD, Patrick Bailly, MD, PhD, Edith Filaire, PhD, Bruno Pereira, PhD, and Marc Filaire, MD

Centre Jean Perrin, Service de chirurgie thoracique, Université Clermont 1, Clermont-Ferrand; Clermont Université, Univ Clermont 1, Faculté de Médecine, Laboratoire d'anatomie; CHU Clermont-Ferrand, service de radiologie, Hôpital G. Montpied; CHU Clermont-Ferrand, The biostatistic division, Clermont-Ferrand University Hospital; Institut Nationale de Recherche Agronomique, Unité Mixte de Recherche 1019, Centre de Recherche en Nutrition Humaine Auvergne, Clermont-Ferrand; Centre National de Recherche Scientifique, Institut des Sciences de l'Image pour les Techniques interventionnelles, Unité Mixte de Recherche 6284; Université Orléans, Laboratoire Complexité Innovation et Activités Motrices et Sportives, Equipe d'Accueil 452, Université Paris-Sud; and Unité de Formation et de Recherche Sciences et Techniques des Activités Physiques et Sportives, 2 allée du Château, Orléans, France

Background. **Extended resection for lung cancer may improve survival of selected patients. Left-atrial resection is infrequently performed and surgical techniques are rarely reported; thus, oncologic results and survival rates remain uncertain. Our study describes surgical techniques, postoperative outcomes, and oncologic results of patients who received a combined multimodality treatment.**

Methods. **Between October 2004 and March 2012 in our institution, 19 patients underwent extended lung resection involving the left atrium without cardiopulmonary bypass. We reviewed perioperative treatments, surgical procedures, and postoperative morbidity, mortality, and long-term survival rates.**

Results. **Sixteen patients (68.4%) underwent neoadjuvant treatment including chemotherapy or radiotherapy. Eighteen pneumonectomies (94.7%) were performed, of which 12 (63.1%) were right sided. Dissection of the interatrial septum was complete in 4 patients (33.3%). Complete resection was achieved in 17 patients (89.4%) and 2 other patients (10.5%) were considered R1. The T-status was pT4 in all patients. Overall postoperative morbidity was 52.6%. The 30-day mortality rate was 10.5% and the 90-day mortality rate was 15.7%. Fifteen patients (93.7%) underwent adjuvant treatment. The mean follow-up time was 32.5 months. The 5-year probability of survival was 43.7%. Three patients (15.7%) were alive at greater than 6 years postsurgery.**

Conclusions. **Extended lung surgery with partial resection of the left atrium is a feasible procedure with acceptable morbidity. An interatrial septum dissection, by increasing the length of the atrial cuff, allows complete resection. Long-term survival can be achieved in highly selected patients who have undergone multimodal therapy.**

(Ann Thorac Surg 2014;97:1708–14)

Results from resections of non-small-cell lung cancer (NSCLC) depend on its stage. In patients with stage IIIa NSCLC, 5-year survival rates vary from 19.1% to 57% [1]. Most patients who have T4 NSCLC are considered not suitable for surgery. However, lung tumors with left-atrial involvement may be surgically removed in selected patients with limited nodal invasion [2]. Few specific studies on T4 NSCLCs invading the left atrium have been published, though reported 5-year survival rates range from 0% to 36% [3, 4].

The aim of our study was to report our experience with left-atrial resection for T4 lung cancer without cardiopulmonary bypass (CPB), and to describe the results from complete dissection of the interatrial septum (IAS), postoperative complications, and survival rates.

Patients and Methods

A retrospective review of our database, Epithor [5], was carried out between October 2004 and March 2012. A total of 1,081 patients underwent pulmonary resection for NSCLC. Among these, we focused on 19 patients (1.75%) who had an extended resection for lung cancer that was invading the left atrium (pT4). All pathology reports were reviewed to ensure that cardiac-muscle fibers with tumor cells, or sterilized tissues in cases of neoadjuvant therapy, were investigated in intrapericardial specimens. Patients with an intrapericardial resection without intrapericardial invasion by a tumor of

Accepted for publication Dec 30, 2013.

Address correspondence to Dr Galvaing, Thoracic Surgery Department, Jean Perrin Cancer Center, 58 rue Montalembert, 63000 Clermont-Ferrand, France; e-mail: geraud.galvaing@cjp.fr.

Published by Elsevier Inc

0003-4975/$36.00
http://dx.doi.org/10.1016/j.athoracsur.2013.12.086

the pulmonary veins or left atrium were excluded from this study. The study was approved by our Institutional Review Board, which waived individual consent.

Preoperative Evaluation

Chest and cerebral computed tomography (CT) scans, positive emission tomography (PET), pulmonary function tests, perfusion lung scintigraphy, and cardiac evaluation with transthoracic echocardiography were systematically performed. If left atrial infiltration was suspected, cardiac magnetic resonance imaging with cardiac gating was conducted for right-sided tumors in order to assess the invasion of the IAS. Radiologic criteria were used if there was suspicion of atrial involvement and if there was a large contact between the tumor and the left atrium, obstruction of a pulmonary vein, or loss of definition of the left atrial wall in a CT scan.

Patients with mediastinal lymph nodes greater than 1 cm on a CT scan, or PET positive in 2, 4, and 7 lymph-node stations, or both, underwent mediastinoscopy. Induction chemotherapy, associated or not with induction radiotherapy, was administered in cases of N2 disease or to reduce tumor size, thus reducing the risk of an incomplete resection. Patients who underwent neoadjuvant treatment were all reevaluated before surgery. No surgery was performed in patients with a distant metastasis, N3 disease, bulky N2, progression after neoadjuvant therapy, or a malignant pleural or pericardial effusion. Among our patients eligible for surgery, none had suspected invasion of both atria, the presence of an intraatrial thrombi, or a polypoid tumor inside the atrium. For these reasons, no procedure needed to be performed using CPB.

Technique

Under general anesthesia and selective bronchial intubation, a muscle-sparing lateral thoracotomy or a posterolateral thoracotomy was performed. To ensure resectability, the pericardium was opened and involvements of the pulmonary and left atrium were assessed. Dissection of the intrapericardial portion of the pulmonary artery, posterior mediastinum, and bronchus were initiated. Subaortic lymph nodes on the left side and subcarinal lymph nodes on both sides were generally resected to enable resectability of the bronchus. Once resectability was established, resection began by the pulmonary artery following the pulmonary veins.

We know that right-sided tumors can invade the left atrium faster than left-sided tumors, as pulmonary veins are shorter. This unfavorable anatomic condition is counterbalanced by good exposure of the right aspect of the left atrium, the ending of the right pulmonary veins, and the junction of the 2 atria. Moreover, this junction is superficially marked by the interatrial groove and can be dissected to increase the length of the atrial cuff. Originally, this approach was performed by Söndergaard and Wälti [6] to close the patent foramen ovale. As previously reported by our team [7], the Söndergaard technique can be extended to include the interatrial muscle, allowing an extra length of atrial wall.

Here, we describe our practice of surgical dissection of the IAS. The dissection begins in the sulcus, just behind the connection to the superior vena cava with the right atrium, and is continued caudally where the sulcus is hardly noticeable. Initially, the fatty tissue is easily divided with the tips of scissors. Within this fatty tissue, anteriorly and superiorly, dissection can be done up to a certain point in a very narrow space under the muscular roof of the atria. Thin vessels running between the 2 sides of the dissected sulcus can be observed and should be sectioned after electrocauterization or ligation. The atrial roof attaching the superior and anterior aspects of both atria is composed of interatrial muscle fibers. This musculature leads to the posterior aspect of the aortic roots and increases the length of dissection in the upper part of the interatrial groove by twofold (facing the upper pulmonary vein). It is important to note that the thickness of the right and left side of the dissected IAS is unequal. The limits of depth of the dissection are represented by the limbus of the fossa ovalis and by the Koch triangle at the lower extremity. In addition, the resectable left atrial cuff can be a mean distance of 40 mm at the level of the upper pulmonary vein after sectioning the interatrial muscle.

Based on this anatomic description, we have defined 3 levels of left atrial resection. Depending of the depth of the IAS dissection, as detailed in Table 1, this classification allowed accurate description of the surgical procedure.

Resection of the left atrium was preceded by preliminary clamping using a Satinsky clamp to observe hemodynamic reduction in atrial volume. Then, resection was performed either "on clamp" or with an automatic stapler (AutoSuture; United States Surgical, Tyco Healthcare, Norwalk, CT or Endo-GIA universal stapler, Covidien, Mansfield, MA). Green cartridges (2-mm staples) were used for atrial stapling. Two running 4-0 polypropylene sutures were placed on the remainder of the left atrium.

Frozen sections of the left atrial cuff and bronchial stump were obtained to ensure complete resection. Complete lymph-node dissection was finally performed as recommended [8]. Left-sided tumors were treated using the same operative steps except for dissection of the IAS, which is not feasible by a thoracotomy.

No intraoperative anticoagulation was routinely administered. Postoperative thromboprophylaxis (with the use of low molecular weight heparin) was administered on the first postoperative day and lasted 21 days. Exceptions to this protocol were superior vena

Table 1. Classification of Left Atrial Resection According to Dissection of the Interatrial Septum (IAS)[a]

Level	Definition
Level 1	No dissection of the IAS
Level 2	Dissection of the IAS without sectioning the interatrial muscle
Level 3	Complete dissection of the IAS with sectioning of the interatrial muscle

[a] According to Filaire and colleagues [7].

cava graft and cardiac arrhythmia requiring curative anticoagulation.

All cases were preoperatively discussed at a thoracic oncology meeting within our hospital. This committee was composed of oncologists, pneumologists, radiologists and surgeons.

Follow-Up

Postoperatively, all patients were admitted into the intensive care unit and received cardiac monitoring. Analgesia was given through thoracic epidural analgesia or intravenous patient-controlled analgesia. Morbidity and postoperative mortality were analyzed according to the classification proposed by Seely and colleagues [9]. Ninety-day mortality was also evaluated. Patients were assessed at 1 month after surgery and every 6 months afterward. Information for this study was obtained by contacting patients directly or their referring physicians.

Statistical Analyses

Qualitative data were expressed as numbers and associated frequencies. Quantitative data were expressed as means (and standard deviations) or medians (and ranges), as appropriate. Estimates of survival were performed using the Kaplan-Meier method and comparisons between groups were made using the log-rank test or the Cox bootstrap model. A p value less than 0.05 was considered statistically significant. All analyses were performed using STATA V10 software (StataCorp, College Station, TX).

Results

Sixteen of the 19 patients (median age of 62 years; range, 38 to 73) were men (84.2%) and 3 were women. All were smokers and 88% had stopped smoking at least 6 weeks before surgery. None suffered from cardiac arrhythmia or had a history of a prior thoracic or cardiac procedure even if they would not have been contraindicated. Five patients (26.4%) underwent mediastinoscopy for mediastinal staging to rule out pN3. Clinical nodal status was cN0 in 10 patients (52.6%), cN1 in 4 patients (21.0%), and cN2 in 5 patients (26.4%).

Neoadjuvant cisplatin-based chemotherapy was administered to 12 patients (63.1%). Neoadjuvant radiotherapy was administered to 2 patients (10.5%), and 1 of these patients received neoadjuvant radiochemotherapy. Response to neoadjuvant treatment was evaluated by CT-scan prior to surgery. Candidates for surgery did not progress under neoadjuvant treatment. The remaining 6 patients (31.5%) underwent extended surgery without any neoadjuvant treatment.

Right-sided left atrial involvement was suspected on reevaluation CT scan in 5 patients prior to surgery. A cardiac magnetic resonance image confirmed tumor extension inside the left atrium wall without extension to the IAS, therefore extended surgery without CPB could be performed. Transthoracic echocardiography was not used to assess interatrial groove involvement, but did rule out intraatrial thrombi.

Eighteen pneumonectomies (94.7%) and 1 right inferior lobectomy were performed. Twelve pneumonectomies were right sided (63.1%). Complementary extended resections involved the superior vena cava in 2 cases (10.5%), aortic adventitia in 2 cases (10.5%), and the carina in 1 case (5.2%). One patient (5.2%) experienced cardiac arrhythmia during the procedure. This was treated by fluid remplissage and resolved spontaneously; it did not modify the operative strategy.

Over the same period, 18 explorative thoracotomies were performed. We never experienced explorative thoracotomy due to unresectable atrial involvement.

Pathology examinations confirmed 19 squamous cell carcinomas (100%). Seventeen patients (89.4%) underwent a complete resection (R0) and 2 patients (10.5%) underwent a microscopically incomplete resection (R1). Two patients underwent a complementary resection of the left atrium (from a level 2 to a level 3 dissection), as frozen sections showed residual tumor cells. The patients' operative characteristics and outcomes are reported in Table 2.

The mean length of stay within the intensive care unit was 5.94 ($\pm$ 10.15) days, and the mean length of stay in the hospital was 12.64 ($\pm$ 12.06) days. The overall postoperative morbidity rate was 52.6% (n = 10). Complications and their grades are reported in Table 3. The postoperative mortality rate was 10.5% (n = 2) and the 90-day mortality rate was 15.7% (n = 3). Patient 2 died within 2 months postsurgery from a complicated bronchopleural fistula, patient 15 died at 3 months postsurgery from single-lung pneumonia, and patient 19 died of necrotizing enteritis at 5 days after surgery.

Among the 15 survivors (93.7%) at 90 days postsurgery who had undergone adjuvant therapy, 8 (50%) underwent chemotherapy alone, 6 (37.5%) underwent radiotherapy alone, and 2 (12.5%) underwent radiochemotherapy. Patient 10 refused to undergo chemotherapy, the 14 other survivors had a complete neoadjuvant or adjuvant treatment.

The mean follow-up time was 32.5 months (range, 5 days to 91 months). At completion of the study, 10 patients (52.6%) were still alive and 1 (5.2%) (patient 17) had evidence of disease recurrence (single brain metastasis treated by radiosurgery). The 5-year survival rate was 43.7%, and the median survival time was 28.9 months (Fig 1). The recurrence rate was 21.0% (Fig 2). Two patients (10.4%) suffered from distant metastases (brain) and 2 patients (10.4%) had a local recurrence. Three patients (15.7%) were alive for greater than 6 years postsurgery and were considered cured.

Survival was not affected by the type of surgical procedure (pneumonectomy versus lobectomy), the side of resection, the pathology of the N status, or the completeness of the resection. However, the absence of any statistical differences needs to be interpreted with caution due to the limited number of patients.

Comment

The main results of our study are the following: (1) surgery combined with chemotherapy or radiotherapy for NSCLC that had invaded the left atrium gave acceptable

Table 2. Patients' Operative Characteristics and Outcomes

Patient Number	Age (Years)	Gender	Neoadjuvant Therapy	Procedure	Interatrial Septum Dissection	pTNM	Completeness of Resection	Adjuvant Therapy	Outcome
1	52	M	ChemoT + radioT	Right pneumonectomy	2	T4N0M0	R0	ChemoT	7y 5m alive
2	60	M	0	Right pneumonectomy	1	T4N1M0	R0	0	2m died
3	52	M	RadioT	Right pneumonectomy	2	T4N2M0	R0	ChemoT	6y 6m alive
4	59	M	ChemoT	Right pneumonectomy	2	T4N1M1	R0	ChemoT	6y 2m alive
5	66	M	0	Left pneumonectomy	-	T4N2M0	R0	ChemoT	4y 6m died
6	66	M	0	Left pneumonectomy	-	T4N1M0	R0	ChemoT + radioT	4y 6m alive
7	64	M	ChemoT	Left pneumonectomy	-	T4N1M0	R0	RadioT	4m died
8	52	M	ChemoT	Right pneumonectomy	3	T4N1M0	R0	RadioT	3y died
9	57	F	ChemoT	Right pneumonectomy	3	T4N1M1	R0	RadioT	4y 2m alive
10	63	M	ChemoT	Right pneumonectomy	2	T4N1M0	R0	0	3y 6m alive
11	67	M	ChemoT	Left pneumonectomy	-	T4N2M0	R0	RadioT	3y 2m alive
12	38	F	0	Right pneumonectomy	3	T4N2M0	R0	ChemoT	3y died
13	67	M	0	Right inferior lobectomy	2	T4N1M0	R0	ChemoT	3y alive
14	63	M	ChemoT	Left pneumonectomy	-	T4N2M0	R0	ChemoT + radioT	2y 6m alive
15	60	M	ChemoT	Left pneumonectomy	-	T4N2M0	R1	RadioT	3m died
16	53	M	ChemoT	Right pneumonectomy	2	T4N1M0	R1	RadioT	1y 6m died
17	62	M	0	Left pneumonectomy	-	T4N1M0	R0	ChemoT	1y 8m alive
18	67	M	ChemoT	Right pneumonectomy	1	T4N2M0	R0	RadioT	4m died
19	73	F	ChemoT	Right pneumonectomy	3	T4N1M0	R0	0	5 days died

ChemoT = chemotherapy; F = female; M = male; m = month; RadioT = radiotherapy; y = year.

Table 3. Postoperative Morbidity Rates

Grade	Event	n (%)
II	Pneumopathy	2 (10.5)
	Pulmonary edema	1 (5.2)
	Cardiac arrhythmia	1 (5.2)
IIIa	Acute renal failure	1 (5.2)
IIIb	Pleural clotting	2 (10.5)
	Chylopericardium	1 (5.2)
V	Bronchopleural fistula	1 (5.2)
	Necrotizing enteritis	1 (5.2)

results; and (2) complete dissection of the IAS improved resectability of these T4 tumors without the need for CPB. No major hemodynamic impairment had been experienced in such procedures.

Locally advanced NSCLCs are rarely suitable for surgery. However, it is currently admitted that T4N0 and T4N1 should be considered for surgery whenever complete resection can be achieved [1]. Non-small cell lung cancers of any size that invade the intrapericardial portion of the pulmonary veins or the left atrium are classified as T4, although an intrapericardial section of the pulmonary veins cannot be considered a T4 tumor.

In our study, we took care to include only patients where cardiac muscle fibers with tumors cells had been identified after pathology examination of specimens. We did not find any specimens with necrotic tissue, thus indicating a good response to neoadjuvant treatments.

We achieved a 5-year survival rate of 43.7%. This result is higher than that reported in the literature, which ranges from 0% to 36% [2–4, 10–14]. This difference may be due to several factors (see Table 4).

A large majority (all postoperative survivors but 1) of patients (68.4%) underwent complete neoadjuvant therapy, and 84.2% also underwent complete adjuvant therapy including at least 50 grays of radiation therapy and chemotherapy. The role of neoadjuvant therapy is still debatable but we believe it can increase the likelihood of

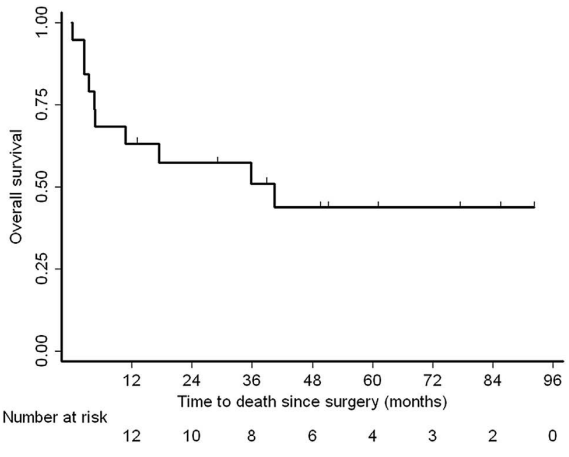

Fig 1. Overall survival curve (Kaplan-Meier method).

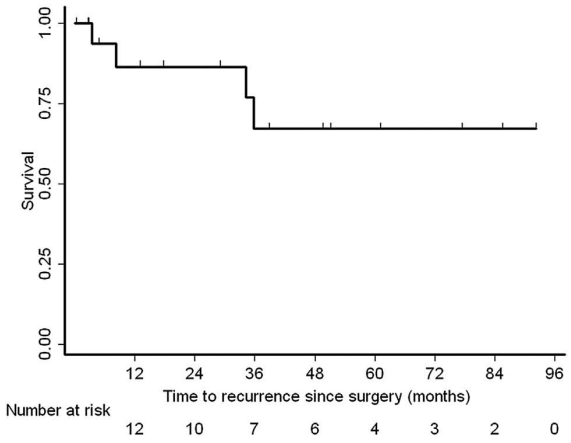

Fig 2. Overall recurrence rate (Kaplan-Meier method).

a complete resection. This positive effect has already been reported by Borri and colleagues [15]. It may enable accurate selection of patients for surgery and exclude those who have rapid tumor progression. Recently, Spaggiari and colleagues [10] reported a 5-year survival rate of 25% for 35 patients who were T4 and who had undergone left atrial resection without CPB. The largest study to date [12] included 44 patients who underwent left atrial resection without CPB; only 7 (16%) of these patients survived for greater than 3 years. Also, 3 patients from this study had a pT3 disease. Perioperative multimodal therapies were not specified in this surgical report.

In our study, only 7 patients (36.8%) were found to be pN2 after definitive pathology explorations. Five patients underwent mediastinoscopy in order to rule out a pN3 status. All died during the follow-up, even though some had prolonged survival. The number of pN2 patients in our study was lower than in other reports (Table 4). Although pathologic N2 status is considered a predictor for a poor prognosis [9], in our study pN2 status did not appear to be a pejorative risk factor, probably because of the smaller number of patients. Persistent N2 after induction therapy probably do not benefit from surgery, confirming the need for accurate restaging.

We propose 3 levels of left atrial resection in order to specify the operative technique used. The interatrial septum can be dissected down to the ascending aorta root. The extra length of the left atrial cuff permits a complete resection. The left atrial surgical margin can be analyzed by frozen section; in cases of microscopically invaded section, the interatrial groove can be widely dissected to achieve a complete resection with no need for CPB. This type of procedure was performed in 2 patients in our study, and permitted complete disease resection.

Only 2 patients in our study were R1; 1 patient underwent a left pneumonectomy where no dissection of the IAS was possible, and 1 patient (who underwent a level-2 IAS dissection) could not have a frozen section examined due to technical impairment. Seventeen of our patients (89.4%) were R0. This rate of complete resection may explain the longer survival rates. Published surgical

Table 4. Published Reports on Survival After a Pulmonary Resection Extended to the Left Atrium for Lung Cancer

Authors	Year	Patients (n)	Complete Resection (%)	pN2–pN3 (%)	30-Day Mortality (%)	5-Year Survival (%)
Fukuse et al [3]	1997	42	35	22	2,4	17 (3-year)
Ratto et al [13]	2004	19	58	57	0	14
Bobbio et al [14]	2004	23	83	17	9	10
Spaggiari et al [2]	2005	15	100	53	0	39 (3-year)
Wang et al [4]	2010	25	92	32	NR	36
Spaggiari et al [10]	2013	35	86	45	0	25

NR = not reported.

series report a complete resection rate that ranges from 35% to 100% [2, 3]. In these reports, the surgical techniques used are rarely mentioned; although clamping of the left atrium was sometimes performed its relationship to the IAS was not defined. All patients were found to suffer squamous cell carcinoma. The histologic subtype is more frequent in central bronchi than adenocarcinoma, and tends to spread locally. It's also correlated with a history of smoking.

We did not experience any cases of major cardiac arrhythmia despite dissecting the IAS. The overall morbidity rate (52.6%) was high in our series as we recorded every complication. However, most incidents were rapidly resolved without impairment to the patients. Based on experimental studies on dogs [16], up to a third of the left atrium can be resected [11]. To our knowledge, no study in humans has provided precise information on this limit. Our study shows that a large resection, by complete resection of the IAS, can be done without hemodynamic disturbance. A larger defect, however, should be corrected using a patch graft under CPB. Moreover, it is now widely accepted that CPB does not increase the occurrence of metastases or tumor recurrence [17]. In our experience, we never had to conduct left atrial resection under CPB. It should be a useful technique especially for left-sided tumors as no IAS can be dissected on that side.

Extended resection surgery is only suitable for highly selected patients; ie, those with a minor medical history and who have good physical health and nutritional status. Our study involved a homogeneous population of 19 patients who were all treated according to current medical practice. None had disease in an extrathoracic site and all could be treated in a curative intent. Our surgical technique is now well established and we work closely with pathologists.

In conclusion, extended lung surgery with partial resection of the left atrium is a feasible procedure with acceptable morbidity rates. In highly selected patients, who eventually underwent neoadjuvant treatment, it enabled complete resection of the disease. This resulted in improved long-term survival, which should be the surgeon's goal. We propose a classification of IAS dissection to clearly identify the type of surgery that can be performed; a level-3 dissection increases the length of the left atrium that can be resected without CPB. Thus, we believe this classification could allow accurate comparison with other similar surgical studies.

References

1. Chambers A, Routledge T, Billè A, Scarci M. Does surgery have a role in T4N0 and T4N1 lung cancer? Interact Cardiovasc Thorac Surg 2010;11:473–9.
2. Spaggiari L, D'Autio M, Veronesi G, et al. Extended pneumonectomy with partial resection of the left atrium, without cardiopulmonary bypass, for lung cancer. Ann Thorac Surg 2005;79:234–40.
3. Fukuse T, Wada H, Hitomi S. Extended operation for non-small cell lung cancer invading great vessels and left atrium. Eur J Cardiothorac Surg 1997;11:664–9.
4. Wang XX, Liu TL, Yin XR. Surgical treatment of IIIb-T4 lung cancer invading left atrium and great vessels. Chin Med J (Engl) 2010;123:265–8.
5. Bernard A, Rivera C, Pages PB, Falcoz PE, Vicaut E, Dahan M. Risk-model of in-hospital mortality after pulmonary resection for cancer: a national database of the French Society of Thoracic and Cardiovascular Surgery (Epithor). J Thorac Cardiovasc Surg 2011;141:449–58.
6. Söndergaard T, Wälti R. Circumclusion of atrial septal defects. [Article in German] Thoraxchir Vask Chir 1967;15:569–75.
7. Filaire M, Nohra O, Sakka L, et al. Anatomical bases of the surgical dissection of the interatrial septum : a morphological and histological study. Surg Radiol Anat 2008;30:369–73.
8. Goldstraw P. International Association for the Study of Lung Cancer handbook in thoracic oncology. Orange Park (FL): Editorial Rx Press; 2009.
9. Seely AJ, Ivanovic J, Threader J, et al. Systematic classification of morbidity and mortality after thoracic surgery. Ann Thorac Surg 2010;90:936–42.
10. Spaggiari L, Tessitore A, Casiraghi M, et al. Survival after extended resection for mediastinal advanced lung cancer: lessons learned on 167 consecutive cases. Ann Thorac Surg 2013;95:1717–25.
11. Shirakusa T, Kimura M. Partial atrial resection in advanced lung carcinoma with and without cardiopulmonary bypass. Thorax 1991;46:484–7.
12. Tsuchiya R, Asamura H, Kondo H, Goya T, Naruke T. Extended resection of the left atrium, great vessels, or both for lung cancer. Ann Thorac Surg 1994;57:960–5.
13. Ratto GB, Costa R, Vassallo G, Alloisio A, Maineri P, Bruzzi P. Twelve-year experience with left atrial resection in the treatment of non-small cell lung cancer. Ann Thorac Surg 2004;78:234–7.
14. Bobbio A, Carbognani P, Grapeggia M, et al. Surgical outcome of combined pulmonary and atrial resection for lung cancer. Thorac Cardiovasc Surg 2004;52:180–2.
15. Borri A, Leo F, Veronesi G, et al. Extended pneumonectomy for non-small cell lung cancer: morbidity, mortality, and long-term results. J Thorac Cardiovasc Surg 2007;134:1266–72.
16. Yamamoto N. Experimental study for combined left atrium resection for lung cancer. [Article in Japanese] Nihon Kyobu Geka Gakkai Zasshi 1986;34:958–65.
17. Muralidaran A, Detterbeck FC, Boffa DJ, Wang Z, Kim AW. Long-term survival after lung resection for non-small cell lung cancer with circulatory bypass: a systematic review. J Thorac Cardiovasc Surg 2011;142:1137–42.

Conclusion

Le développement de nouvelles techniques chirurgicales permet de prendre en charge des patients qui auraient auparavant été récusés avec un résultat carcinologique satisfaisant et une morbidité réduite, améliorant ainsi la survie. L'imagerie occupe donc une place déterminante en amont de la prise en charge chirurgicale : en réalisant scanner mais également IRM chez ces patients, le radiologue doit affirmer ou infirmer la présence d'un envahissement du septum inter auriculaire, le plus souvent par contiguité, d'un envahissement de la veine pulmonaire, et d'évaluer l'extension de cet envahissement.

Une série postérieure à notre travail, publiée en 2016 par Langer et al.(20) portant sur 375 patients, insiste sur l'interêt de la circulation extra-corporelle dans la prise en charge des patients T4. Les auteurs ne retrouvaient pas de différence significative à long terme entre les différents groupes de patients, mais disposaient d'un groupe ayant bénéficié de la CEC de petite taille (20 patients). En revanche le taux de R0 etait plus important chez les patients bénéficiant de la CEC sans complication per-opératoire surajoutée, laissant penser que ceux-ci ont un meilleur pronostic.

Analyse de critères tomodensitométriques d'envahissement cardiaque dans la pathologie néoplasique pulmonaire, comparaison à l'anatomopathologie.

R. Steinberg, G. Galvaing, A. Gallon, B.Perreira, L.Boyer, M.Filaire, L.Cassagnes.

Article en cours de soumission « The Annals of Thoracic Surgery ».

Secondairement à la validation de cette technique chirurgicale de dissection du septum inter-auriculaire, il nous paraissait légitime d'évaluer la pertinence des signes scanographiques pré-opératoires chez ces nouveaux candidats à la chirurgie.
Nous avons analysé une série de patients porteurs d'un cancer broncho-pulmonaire classés cT4, et donc normalement récusés pour toute chirurgie curative. Nous nous sommes attachés sur les scanners pré-opératoires à évaluer les signes scanographiques d'envahissement médiastinal ou cardiaque, notamment au niveau de l'oreillette gauche, une nouvelle technique chirurgicale permettant une dissection de celle ci avec de bon résultats post-opératoires. Le but de notre étude était donc de dégager des signes scannographiques prédictifs de cet envahissement, nos observations étant corrélés aux résultats anatomopathologiques de la pièce opératoire.
Le bilan d'imagerie pré-opératoire étant fondamental dans la technique chirurgicale utilisée chez ces patients, nous avons cherché les critères scanographiques les plus prédictifs d'une atteinte des structures médiastinales et donc d'un envahissement.
Certains critères notamment, comme un épanchement péricardique pathologique, nous paraissaient initialement constituer un indicateur défavorable ; il s'est avéré que ce signe, lorsqu'il était présent et relevé comme d'allure pathologique, n'était pas corrélé à une atteinte médiastinale de manière significative.

Abstract

Objectifs
L'objectif de notre étude était de déterminer une association statistique entre des critères scanographiques d'envahissement médiastinal et les résultats anatomopathologiques dans une population de patients cT4 opérés.

Matériels et méthodes
Lecture en double aveugle rétrospective de 38 scanners thoraciques pré-opératoires, évaluation de 20 critères d'envahissement médiastinal côtés 0 ou 1 en fonction de la présence de signes d'invasion ou non. Le gold standard pour affirmer l'envahissement était le compte rendu anatomopathologique de la pièce opératoire.

Résultats
Les résultats anatomopathologiques ont retrouvé une invasion des structures médiastinales chez 23 patients (60%). La concordance inter-observateur était supérieur à 75 % sauf pour 5 structures : veines pulmonaires (71,88%), oreillette gauche (72,73%), artère pulmonaire (63,64%), bronche souche (44,12%), bourgeon endoluminal (48,48%). La concordance entre l'analyse scanner d'envahissement et le compte rendu anatomopathologique étaient les suivants: concordance modérée (50%) pour le sous-groupe péricarde, faible concordance (25%) pour plévre et paroi thoracique, concordance négligeable (12.5%) pour les voies aériennes, bonne concordance (80%) pour les vaisseaux artériels (aorte et artère pulmonaire) et excellente concordance (90%) pour les structures veineuses (VCS, veines pulmonaires et oreillettes gauche).

Conclusion
Notre étude démontre clairement les limites du scanner dans le staging des concers broncho pulmonaires invasifs. L'évaluation par IRM apparait cruciale pour éviter la sur-stadification et permettre une chirurgie curative.

CORRELATION OF COMPUTED TOMOGRAPHY AND PATHOLOGY FINDINGS IN PATIENTS OPERATED FOR CT4 STAGE LUNG CANCER POPULATION

R. Steinberg, G. Galvaing, A. Gallon, B. Perreira, L. Boyer, M. Filaire, L. Cassagnes

ABSTRACT

Objective: The aim of the present study was to determine a statistical association between computed tomography (CT) criteria and surgical pathology results of mediastinal invasion in a population of stage cT4 lung cancer patients.

Methods: Two blinded readers retrospectively reviewed 38 pre-operative thoracic CT and evaluated mediastinal invasion; 20 criteria were rated as 0 or 1 according to whether invasion signs were absent or present. The gold standard for invasion assessment was the surgical pathology report.

Results: Pathology reports revealed mediastinal structure invasion in 23 patients (60%). Interobserver agreement exceeded 75% except for 5 structures: pulmonary veins (71.88%), left atrium (72.73%), pulmonary artery (63.64%), main bronchus (44.12 %), intraluminal bud (48.48 %). Agreement assessments between CT analysis and invasion localisation in pathology findings for each defined subgroup were as follows: moderate agreement (50%) for pericardium subgroup, low agreement (25 %) for pleura and chest wall, negligible agreement (12.5%) for airways, good agreement (80%) for arterial vessels (aorta and pulmonary artery) and excellent agreement (90%) for venous structures (SVC, pulmonary veins and left atrium).

Conclusion: Our study clearly demonstrates the limits of CT in the pre-therapeutic assessment of invasive broncho-pulmonary cancer. MRI evaluation appears crucial to avoid overstaging and enable curative surgery.

INTRODUCTION

A multidisciplinary approach is generally discussed for patient with locally advanced non small lung cancer (NSCLC). These tumours are classified as stage III according to the prognostic TNM classification which is of a paramount importance for decision (1). Among stage III disease, tumours invading the heart, the great vessels, the trachea, the carina, the esophagus, the recurrent laryngeal nerve, the spine, or with nodule in an other ipsilateral lobe are classified as T4. If the T4 tumour is not associated with mediastinal adenopathies (N0-1), the disease is classified as stage IIIA, and if associated with, the tumour is classified as IIIB. Because of a 9% 5-year-survival, patients with stage IIIB disease are not currently suitable for surgery. With a 24% 5-year-survival, patients with stage IIIA disease and good functional status are eligible for a multidisciplinary approach including surgery. In this cases, the quality of the resection should be anticipated and it is the crucial point of the debate. In fact, with a 5-year-survival rate of 43% (2) (3) only patients with free margin resection (R0) can benefit from surgery and it depends particularly of the surgical team experience, the accuracy of the exams and often the imaging. In fact, the difficulty to diagnose a T4 tumour is variable. For example, it is more evident when the laryngeal recurrent nerve attempt is

affirmed by the vocal cord paralysis, the spine invasion is precised with MRI, and tracheal/esophageal invasion with endoscopy eventually helped by ultrasound imaging. Sometimes, it is rather more difficult when there is a contact with the great vessels, pericardium and by the way the heart. In practice, preoperative staging is usually based on an association of thoracic CT scans and PET-CT scans. But for T4 tumour, CT scan has a key role as the first line imaging (4).

Few studies have evaluated the accuracy of CT scan for mediastinal invasion in NSCLC.

In 1989, Glazer and associates retrospectively correlated CT scans classified indetermined for mediastinal invasion and operative resecability of 80 patients. They concluded that CT scan was not helpful in differentiating tumors with and without mediastinal invasion (5). Nevertheless, 97% of the patients with one or more of the 3 following criterias were resectable: contact of 3 cm or less with mediastinum, less than 90 degrees of contact with aorta, and mediastinal fat between mass and mediastinal structures. R0 resection were not documented. In fact, concerning the aorta, only 4 patients out of 8 with a tumour contacting more than 90° of the aortic were non resectable. Nearly 30 years after this publication, these criteria are still valuable to predict aortic invasion (6).

In 2007, in order to evaluate T-staging, Pauls and associates prospectively compared the reliability of integrated (18)F-FDG PET/CT to CT scan alone in 80 patients operated for NSCLC but including only six patients with T4-tumour. Integrated (18) F-FDG PET/CT no provided advantages in T4-tumour diagnosis (4).

Several studies have demonstrated the benefit of surgical resection with (7) (8) (9) (10) (11) (12) (13) favourable survival rates and low morbidity and mortality.

Accordingly, Yildizeli et al. reported on a series of 271 patients with surgical management of T4 lung cancer (2) and found 3 factors impacting survival: nodal status, complete (R0) resection and invasion of the subclavian artery. The authors reported a 5-year survival rate of 43 % in T4 lung cancer upon achieving complete (R0) resection. Surgical management has moreover been associated with increased survival in stage IV patients (14), and pre-therapeutic staging must be able to determine patients who may benefit from complete resection even in stage IV lung cancer. Thus, the first goal of pre-therapeutic staging is to identify patients eligible for curative surgery.

CT criteria of invasion and resecability in cT4 rely on small series with a limited number of patients with diagnostic accuracy around 50% (e.g. aortic invasion in Glazer serie. In Surgical studies, evaluation rely on pathologic results.

The aim of the present study was to determine a statistical agreement between cT4 and p T4 disease using respectively computed tomography criteria and surgical, pathological results of mediastinal invasion in patients preoperatively screened with cT4 NSCLC.

MATERIAL AND METHODS

Population

Our thoracic surgery department (Jean Perrin Cancer Center) database was retrospectively reviewed from January 2004 to December 2014 in order to select patients presenting cT4 lung cancer treated surgically, with or without neo-adjuvant treatment.

All included patients underwent thoracic Computed Tomography (CT) scans for preoperative evaluation of tumoral pulmonary mass with suspected mediastinal extension, and subsequently classified as cT4 according to TNM classification.

Only those patients with thoracic CT scans after iodine contrast media injection, whether arterial, portal phase or both, were included. Exclusion criteria were: (a) CT scans without contrast media injection, (b) non-neoplasic thoracic lesions on pathology reports. All cases were preoperatively discussed at a thoracic oncology meeting within our hospital, by a committee comprised of oncologists, pneumologists, radiologists and surgeons.

Pathological Analysis

All pathologic reports were reviewed. Mediastinal invasion was assessed according to pathological examination of the resected tissues, and defined as the gold standard for assessment of pT4.

Analysis of CT parameters

CT criteria for mediastinal invasion were used according to the revised 7th TNM classification (1), to bibliographic references (5) (6) as well as the 8th TNM classification proposals (15)(4).

CT criteria included the following: (a) tumour contact of more than 3 cm with the mediastinum with or without fat plane obliteration, (b) tumour contact with more than one fourth (90 degrees) of the circumference of the aorta or other mediastinal structures (superior vena cava, esophagus), (c) obliteration of the fat planes normally seen adjacent to the aorta or other mediastinal structures, (d) compression of mediastinal structures by a mass, (e) mediastinal pleural or pericardial thickening of more than 5 or 2 mm (6).

Altogether, 20 selected criteria were analysed for tumour characterisation (T).

The CT criteria of invasion were applied to the following structures:

- Pericardium: pericardial effusion (circumferential or not, of more than 5 mm in thickness), pericardial thickening (thickening of more than 2 mm, with or without infiltration of epicardial fat), pericardial nodules (pericardial tissular mass wathever the size).

- Heart: endocardial bud (tissue mass of more than 1 cm in heart cavities).
- Superior vena cava: tumour contact with more than one fourth (90 degrees) of the circumference, superior vena cava syndrome.
- Thoracic aorta: tumour contact with more than one fourth (90 degrees) of the circumference.
- Pleura: pleural nodule (nodular thickening of more than 1 cm in diameter), pleural effusion of more than 5 mm in thickness, (16)
- Pulmonary veins radish tail aspect, thrombus, lack of opacification
- Left atrium: inter-atrial septum thickening, fat plane obliteration
- Pulmonary artery: tumour contact with more than one fourth (90 degrees) of the circumference, superior vena cava syndrome
- carina, trachea, main bronchus: tumour contact with more than one fourth (90 degrees) of the circumference, superior vena cava syndrome
- oesophagus: tumour contact with more than one fourth (90 degrees) of the circumference.

Subgroups were defined according to the localisation of the neoplasic invasion:

-pericardium: effusion, thickening, nodules, endocardial bud

-pleura and chest wall: pleural effusion, pleural nodule,

-airways: main bronchus, carina

-arterial vessels: aorta, pulmonary artery

-venous structures: pulmonary veins, left atrium, superior vena cava, superior vena cava syndrome.

Thoracic CT scans were obtained on several imaging systems, with image analysis performed using the PACS system (Mc Kesson Radiology)

All aforementioned invasion criteria were first determined by 2 CT readers, with respectively 4 and 15 years experience in reading CT scans, and blinded to the pathological findings, followed by a consensus reading between the 2 readers in case of conflicting analysis.

Each criterion was rated as 0 if absent and 1 if present.

Statistical analysis

All analyses were performed using Stata software (version 13, StataCorp, College Station, TX). All tests were performed for a two-sided type I error of 5%. Categorical data are expressed as number and percentage, while quantitative data are expressed as mean ± standard deviation (SD) or as median and interquartile range [IQR] according to statistical distribution (assumption of normality assessed using the Shapiro-Wilk test). Concordance was studied using the kappa coefficient (k) and accuracy. Kappa values were studied in

relation to usual recommendations to define interobserver agreement level: <0.2 (negligible), 0.2-0.4 (low/weak consistency), 0.4 to 0.6 (moderate agreement), 0.6-0.8 (substantial/good agreement) and > 0.8 (excellent agreement) [*Altman 1991 (17)*, *Terwee et al. (18)*]. Lastly, diagnostic values (sensitivity, specificity, negative and positive predictive values) were calculated and presented with their respective 95% confidence interval.

RESULTS

Study population

During the inclusion period, fifty-five patients considered as T4 upon preoperative evaluation had surgery for lung cancer resection.

Seventeen patients were ultimately excluded from the study: 2 for non-tumoral lesions on pathological findings, 4 for whom only TEP scans without contrast media injection were available, 1 for whom only a CT scan without contrast media injection could be collected, and 10 patients for whom preoperative CT scans could not be recovered for analysis.

The final study population hence included 38 patients with the following characteristics: 30 male (79%) and 8 female patients, with a median age (±SD) of 60 years (±11).

Surgical results

A complete R0 resection with healthy margins was obtained in 31 patients (82%), a partial R1 resection in 1 patient (2%) and indeterminate margins in 6 patients (16%).

Procedures consisted of 26 pneumonectomies (69%), 5 bilobectomies (14%), 3 lobectomies (8%), and 4 biopsies (9 %).

Pathology results

Pathological distribution of the lesions was as follows: 23 squamous cell carcinomas (60%), 6 adenocarcinomas, 2 undifferentiated carcinomas, 2 neuroendocrinal carcinomas, 1 thymic carcinoma, 1 invasive bronchopulmonary carcinoma, 1 malpighian carcinoma, 1 sarcoma and 1 thymoma.

Pathological analysis found mediastinal structure invasion in 23 patients (60%), no invasion in 13 patients (34%) and was inconclusive in 2 patients (6%).

CT scan interpretation

Interobserver agreement for each criterion is summarised in table 1.

There was excellent interobserver agreement (>80%) for 12 studied criteria, good agreement (0.6 to 0.8) for 5 criteria and moderate agreement for 1 (main bronchus). Interobserver agreement where not available for 2 criteria, not present in our population. The worth agreement was obtain for main bronchus (44.12%) and intraluminal bud (48.48%).

Kappa values were close to 0 or at times negative.

Statistical agreement between cT4 and pT4

Only 6 criteria displayed moderate agreement between CT scan evaluation and pathological findings: pulmonary veins (54.29%), pulmonary artery (52.78%), main bronchus (50%), intraluminal bud (59.38%), pericardial thickening (50%), pleural effusion (50%).

Agreement assessments between CT analysis and invasion localisation in pathology findings for each defined subgroup were as follows: moderate agreement (50%) for pericardium subgroup, low agreement (25 %) for pleura and chest wall, negligible agreement (12.5%) for airways, good agreement (80%) for arterial vessels (aorta and pulmonary artery) and excellent agreement (90%) for venous structures (SVC, pulmonary veins and left atrium).

No kappa value was available due to the small population size.

Interobserver agreement, reproducibility factors, sensibility, specificity, NPV and PPV for each subgroup are summarised in table 2.

The negative predictive value where under or equal to 40 % for each group reflecting the fact that CT alone is not appropriate to define invasion. We found a good specificity and positive predictive value for pericardium evaluation, chest wall and pleura, airways.

DISCUSSION

Determination of cTNM is crucial in determining treatment strategy in patients with broncho-pulmonary cancer, the ultimate goal being to determine the feasilbilty of complete surgical resection R0.

For most of the criteria we found excellent or good interobserver agreement. In the present study, we found very excellent interobserver agreement, with over 90% concordance for 10 criteria, consolidating the reproducibility and relevance of CT-based standards pertaining to the definition of mediastinal invasion. Apart from Arterial vessel and venous structures criteria, the agreement between CT findings and pathology findings never exceed 50 % (moderate agreement).

In the present study, negative predictive values for each subgroup pertaining to localisation of invasion were under 50%. Such findings are similar with those reported in the literature. Accordingly, Quint noted that CT was inaccurate in excluding and in diagnosing mediastinal fat invasion, unless in the presence of gross findings (19). With regard to pleural or pericardial effusion, both CT and MR imaging findings have been deemed inconclusive for the determination of benign vs. malignant pleural and pericardial disease (20).

Concerning aorta invasion, recent publications evaluate dynamic CT for preoperative assessment of invasion: the authors evaluated differential movements between the tumour and the adjacent structures, suggesting the absence of overt malignant invasion (21). As reported by Uramoto and associates, MRI gives advantages to eliminates aortic invasion when it is suspected with CT scan. These authors report five cases of complete resection

without aortic invasion (22). In an other case of suspected aortic invasion on preoperative CT, a cine MRI was achieved demonstrating a clear area of isolation between aorta and lung mass allowing complete resection (23). Authors used cineMRI or respiratory dynamic MRI to assess great vessels invasion (24).

However, only a good interobserver agreement was found regarding the left atrium (72.73%) and pulmonary veins (71.88%), hence highlighting a pitfall of CT scanning in this instance: as a result, a cine cardiac MRI with cardiac gating examination should be the rule in any suspicion of cardiac structure invasion. Indeed, obliteration of the fat planes reflecting mediastinal invasion is hard to assess with any degree of certainty on CT scans: cine MRI with high contrast resolution provides excellent assistance in diagnosis, enabling to assess bonding between tumour mass and mediastinal structures. Uramoto and al. reported five cases of thoracic aorta invasion suspicion on pre-operative evaluation using both CT scan and MRI: the resecability of all lesions was achieved without invasion in all cases (22). These authors also reported a case of suspected aortic invasion on preoperative CT, upon which a cine MRI was performed demonstrating a clear area of isolation between the aorta and lung tissue allowing complete resection (23). Clear aortic invasion may hence be overestimated with CT, and thus MRI should be performed when in doubt. In our centre, cardiac MRI is performed in order to confirm tumour extension in case of pulmonary vein invasion, allowing to assess extensions inside the left atrium and interatrial wall (25). Seo et al. also reported the usefulness of cine MRI in evaluating cardiovascular invasion, in which the presence of sliding motion exhibited a 94.4% accuracy in predicting non-invasion (26).

We found moderate agreement to assess pericardium invasion. Again cardiac cineMRI have the capacity to evaluate efficiently local invasion. Trough the excellent contrast resolution, MRI allows to assess fat plane integrity, tissular thickening or pericardial nodule after gadolinium injection. Thanks to cineMRI, we have the capacity to see potential cleavage plane in identifying sliding plane reflecting absence of invasion. Myocardial characterization can also be evaluated with cardiac MRI, as well for ventricular myocardium as inter atrial septum (25).

The interobserver agreement determined herein for main bronchus criteria (44.12%) supports the recommendation in which a bronchoscopy should be performed in case of suspected invasion (27). The difficulty in CT evaluation is to differenciate wether the tumour is only compressing the airway or wether it is actually infiltrating the bronchialor tracheal wall. Herth et al.evaluate endobronchial ultrasound (EBUS) in 131 patients with thoracic tumors located close to the large airways, and compared CT and EBUS in assessment of airways invasion, histology was the gold standard (28). The authors report for EBUS an accuracy of 94%, sensitivity of 89% and specificity of 100 %; chest CT had an accuracy of 51 %, sensitivity of 75 %, and specificity of 28 %, with no false positive results for EBUS. A review for the managment of NSCLC, report the crucial role of EBUS in T staging to allow curative surgery (29).

Several studies report the usefulness of video-assisted thoracoscopy (VATS) for staging T3 and T4 (30) and in T4 tumours described by CT scan a multimodality evaluation should be performed (29) (31).

Likewise, oesophageal endoscopy is required to assess tumour invasion, supporting our result of 76.47% regarding oesophageal criteria. Nevertheless, The reliability of oesophageal ultrasound and fine needle aspiration (EUS-FNA) for staging the direct tumour invasion into the mediastinum (T staging) was evaluated in one study. The authors reported a false-negative rate of about 30%, indicating that this technique should not be recommended for assessing mediastinal invasion for primary tumours (31).

We found low agreement for chest wall and pleura invasion between CT findings and pathologic results. Pleuroscopy with pathologic analysis should be performed in any doubt of invasion. MRI can also be helpfull to determine pleural and chest wall invasion. Nomori and al. report a serie of 145 patients explored with Diffusion-weighted magnetic resonance imaging in NSCLC compared to histology: they found that signal intensity is useful for predicting tumor aggressiveness, helping treatment decision (32).

Surgical biopsy or CT guided biopsy with histologic analysis can also assess pleural invasion. Some authors reported the usefulness of dynamic four dimensional computed tomography for resecability evaluation: differential movements between the tumour and the adjacent structures suggest the absence of overt malignant invasion, the findings were confirmed by intraoperative assessments (20).

While the association of PET-CT and CT is the rule in preoperative staging (33), the place of MRI (with the exception of superior sulcus tumours) remains to be defined.

Our data are similar with previously published studies, underlying the pitfalls of CT imaging in lung cancer staging. Although the association of PET-CT and CT remains the classical initial evaluation for staging, it would appear additionally appropriate to perform a MRI with better contrast resolution and dynamic evaluation when there is suspicion of mediastinal invasion.

LIMITATIONS

Certain limitations should be acknowledged in the current study:

This is a retrospective study and pathology reports were only available for cT4 stage patients who underwent surgery. cT3 stage lesions on pre-operative imaging and subsequently redefined as pT4 were not taken into account.

In addition, only T stage was evaluated whereas M status was not since only thoracic CTs were analysed.

Our study displayed low statistical power due to the limited number of included patients, in particular for kappa evaluation, and compounded by the fact that a limited number of stage cT4 patients underwent surgery. Most published studies suffer from the same limitation, with 36 patients for the study of Hanagiri (34), and 19 patients for the study of Doddoli (35).

Only 60% of our study population had a mediastinal invasion on pathological examination such that the incidence of pT4 was low.

The lack of objective definition regarding certain criteria may also be a cause of significant bias: for invasion of the phrenic nerve for example, both CT readers considered this criterion

as positive when the tumoral mass was present at the anatomical site of the nerve. Moreover, given that superior vena cava syndrome has a clinical definition, the readers considered this criterion as positive when extrinsic compression associated with collateral circulation was present.

CONCLUSION

As surgical developments allow to cure certain T4 BPC, with left atrium reconstruction for example, providing R0 resection Our study shows clearly the limits of CT in pre-therapeutic evaluation of invasive broncho-pulmonary cancer. Taking into account those limits of CT, MRI evaluation seems to be crucial today to avoid overstaging and allow curative surgery for selected localization as left atrium, aorta, pulmonary veins or pericardium. Endoscopy and bronchoscopy are still mandatory to assess main bronchus or esophagal invasion.

Table 1- interobserver agreement for each CT criterion (NA: Not Available)

	CT criteria	Agreement (%)	Kappa
pericardium	Pericardial effusion	94.12	0.4687
	Pericardial thickening	79.41	-0.1121
	Pericardial nodule	91.18	0.0000
	Endocardial bud	94.12	0.0000
Venous structures	Left atrium clot	91.18	0.3704
	SVC invasion	85.29	0.2202
	Left atrium invasion	72.73	0.1391
	Pulmonary vein invasion	71.88	0.3455
Pleura and chest wall	Pleural nodule	88.24	-0.0462
	Pleural effusion	91.18	0.8118
airways	Carinal invasion	97.06	0.6531
	Main bronchus invasion	44.12	0.1003
	Tracheal invasion	100.00	1.0000
Arterial vessels	Aorta invasion	97.06	0.0000
	Pulmonary artery invasion	63.64	0.3125
	Oesophagus invasion	76.47	0.3366
	Vertebrae invasion	NA	NA
	Brachial plexus invasion	NA	NA
	SVC Syndrome	97.06	0.6531
	Endoluminal bud	100.00	1.0000

Table 2: Interobserver agreement and reproducibility factors for each studied subgroup

Subgroup	Agree (%)	kappa	Sen (IC 95%)	Spe (IC 95%)	PPV(IC 95%)	NPV(IC 95%)
Pericardium	50.00	0.0975	34.8 (16.4-57.3)	76.9 (46.2-95)	72.7 (39-94)	40 (21.1-61.3)
Chest wall and pleura	52.78	0.0838	47.8 (26.8-69.4)	61.5 (31.6-86.1)	68.6 (41.3-89)	40 (19.1-63.9)
Airways	50.00	0.0442	43.5 (23.2-65.5)	61.5 (31.6-86.1)	66.7 (38.4-88.2)	38.1 (18.1-61.6)
Arterial vessels	52.78	0.0255	56.5 (34.5-76.8)	46.2 (19.2-74.9)	65 (40.8-84.6)	37.5 (15.2-64.6)
Venous structures	55.56	0.0035	69.6 (47.1-86.8)	30.8 (9.09-61.4)	64 (42.5-82)	36.4 (10.9-69.2)

Sen: sensibility; Spe: specificity;

PPV: positive predictive value; NPV: negative predictive value.

BIBLIOGRAPHY

1. Goldstraw P, Crowley J, Chansky K, Giroux DJ, Groome PA, Rami-Porta R, et al. The IASLC Lung Cancer Staging Project: proposals for the revision of the TNM stage groupings in the forthcoming (seventh) edition of the TNM Classification of malignant tumours. J Thorac Oncol Off Publ Int Assoc Study Lung Cancer. août 2007;2(8):706-14.

2. Yıldızeli B, Dartevelle PG, Fadel E, Mussot S, Chapelier A. Results of Primary Surgery With T4 Non–Small Cell Lung Cancer During a 25-Year Period in a Single Center: The Benefit is Worth the Risk. Ann Thorac Surg. 1 oct 2008;86(4):1065-75.

3. Galvaing G, Tardy MM, Cassagnes L, Da Costa V, Chadeyras JB, Naamee A, et al. Left atrial resection for T4 lung cancer without cardiopulmonary bypass: technical aspects and outcomes. Ann Thorac Surg. mai 2014;97(5):1708-13.

4. Pauls S, Buck AK, Hohl K, Halter G, Hetzel M, Blumstein NM, et al. Improved non-invasive T-Staging in non-small cell lung cancer by integrated 18F-FDG PET/CT. Nukl Nucl Med. 2007;46(1):9-14-2.

5. Glazer HS, Kaiser LR, Anderson DJ, Molina PL, Emami B, Roper CL, et al. Indeterminate mediastinal invasion in bronchogenic carcinoma: CT evaluation. Radiology. oct 1989;173(1):37-42.

6. Webb WR, Higgins CB. Thoracic Imaging: Pulmonary and Cardiovascular Radiology. Lippincott Williams & Wilkins; 2010. 940 p.

7. DiPerna CA, Wood DE. Surgical management of T3 and T4 lung cancer. Clin Cancer Res Off J Am Assoc Cancer Res. 1 juill 2005;11(13 Pt 2):5038s-5044s.

8. Bernard A, Bouchot O, Hagry O, Favre JP. Risk analysis and long-term survival in patients undergoing resection of T4 lung cancer. Eur J Cardio-Thorac Surg Off J Eur Assoc Cardio-Thorac Surg. août 2001;20(2):344-9.

9. de Perrot M, Fadel E, Mercier O, Mussot S, Chapelier A, Dartevelle P. Long-term results after carinal resection for carcinoma: does the benefit warrant the risk? J Thorac Cardiovasc Surg. janv 2006;131(1):81-9.

10. Dartevelle P, Macchiarini P. Techniques of pneumonectomy. Sleeve pneumonectomy. Chest Surg Clin N Am. mai 1999;9(2):407-417, xi.

11. Dartevelle P, Macchiarini P. Surgical management of superior sulcus tumors. The Oncologist. 1999;4(5):398-407.

12. de Perrot M, Fadel E, Mussot S, de Palma A, Chapelier A, Dartevelle P. Resection of locally advanced (T4) non-small cell lung cancer with cardiopulmonary bypass. Ann Thorac Surg. mai 2005;79(5):1691-1696; discussion 1697.

13. Endoh H, Yamamoto R, Satoh Y, Kuwano H, Nishizawa N. Risk analysis of pulmonary resection for elderly patients with lung cancer. Surg Today. mai 2013;43(5):514-20.

14. David EA, Canter RJ, Chen Y, Cooke DT, Cress RD. Surgical Management of Advanced Non-Small Cell Lung Cancer Is Decreasing But Is Associated With Improved Survival. Ann Thorac Surg. oct 2016;102(4):1101-9.

15. Rami-Porta R, Bolejack V, Crowley J, Ball D, Kim J, Lyons G, et al. The IASLC Lung Cancer Staging Project: Proposals for the Revisions of the T Descriptors in the Forthcoming Eighth Edition of the TNM Classification for Lung Cancer. J Thorac Oncol. 1 juill 2015;10(7):990-1003.

16. Cissé R, Latrabe V, Gene V, Rauturier J., Airaud G, Drouillard J, et al. Imagerie de la plèvre. Épanchements liquidiens et tumeurs pleurales. Feuill Radiol. 1998;38(6):426-440.

17. Altman DG. Practical Statistics for Medical Research. CRC Press; 1990. 628 p.

18. Terwee CB, Bot SDM, de Boer MR, van der Windt DAWM, Knol DL, Dekker J, et al. Quality criteria were proposed for measurement properties of health status questionnaires. J Clin Epidemiol. janv 2007;60(1):34-42.

19. Quint LE. Lung cancer: assessing resectability. Cancer Imaging Off Publ Int Cancer Imaging Soc. 1 oct 2003;4(1):15-8.

20. UyBico SJ, Wu CC, Suh RD, Le NH, Brown K, Krishnam MS. Lung cancer staging essentials: the new TNM staging system and potential imaging pitfalls. Radiogr Rev Publ Radiol Soc N Am Inc. sept 2010;30(5):1163-81.

21. Choong CKC, Pasricha SS, Li X, Briggs P, Ramdave S, Crossett M, et al. Dynamic four-dimensional computed tomography for preoperative assessment of lung cancer invasion into adjacent structures†. Eur J Cardio-Thorac Surg Off J Eur Assoc Cardio-Thorac Surg. févr 2015;47(2):239-243; discussion 243.

22. Uramoto H, Iijima Y, Nakajima Y, Kinoshita H. Accurate Diagnosis of Aortic Invasion in Patients with Lung Cancer. Anticancer Res. mai 2016;36(5):2391-5.

23. Uramoto H, Kinoshita H, Nakajima Y, Akiyama H. Easy Diagnosis of Aortic Invasion in Patients with Lung Cancer Using Cine Magnetic Resonance Imaging. Case Rep Oncol. août 2015;8(2):308-11.

24. Hong YJ, Hur J, Lee H-J, Kim YJ, Hong SR, Suh YJ, et al. Respiratory dynamic magnetic resonance imaging for determining aortic invasion of thoracic neoplasms. J Thorac Cardiovasc Surg. août 2014;148(2):644-50.

25. Galvaing G, Chadeyras JB, Merle P, Tardy MM, Naamee A, Bailly P, et al. Extended resection of non-small cell lung cancer invading the left atrium, is it worth the risk? Chin Clin Oncol [Internet]. 2015 [cité 11 août 2016];4(4). Disponible sur: http://cco.amegroups.com/article/view/6859/9402

26. Seo JS, Kim YJ, Choi BW, Choe KO. Usefulness of magnetic resonance imaging for evaluation of cardiovascular invasion: evaluation of sliding motion between thoracic mass and adjacent structures on cine MR images. J Magn Reson Imaging JMRI. août 2005;22(2):234-41.

27. Beigelman-Aubry C, Dunet V, Brun A-L. CT imaging in pre-therapeutic assessment of lung cancer. Diagn Interv Imaging. oct 2016;97(10):973-89.

28. Herth F, Ernst A, Schulz M, Becker H. Endobronchial ultrasound reliably differentiates between airway infiltration and compression by tumor. Chest. févr 2003;123(2):458-62.

29. Dooms C, Muylle I, Yserbyt J, Ninane V. Endobronchial ultrasound in the management of nonsmall cell lung cancer. Eur Respir Rev Off J Eur Respir Soc. 1 juin 2013;22(128):169-77.

30. Sebastián-Quetglás F, Molins L, Baldó X, Buitrago J, Vidal G, Spanish Video-assisted Thoracic Surgery Study Group. Clinical value of video-assisted thoracoscopy for preoperative staging of non-small cell lung cancer. A prospective study of 105 patients. Lung Cancer Amst Neth. déc 2003;42(3):297-301.

31. De Giacomo T, Rendina EA, Venuta F, Della Rocca G, Ricci C. Thoracoscopic staging of IIIB non-small cell lung cancer before neoadjuvant therapy. Ann Thorac Surg. nov 1997;64(5):1409-11.

32. Stamatis G. Staging of lung cancer: the role of noninvasive, minimally invasive and invasive techniques. Eur Respir J. août 2015;46(2):521-31.

33. Nomori H, Cong Y, Abe M, Sugimura H, Kato Y. Diffusion-weighted magnetic resonance imaging in preoperative assessment of non-small cell lung cancer. J Thorac Cardiovasc Surg. avr 2015;149(4):991-6.

34. Munden RF, Swisher SS, Stevens CW, Stewart DJ. Imaging of the patient with non-small cell lung cancer. Radiology. déc 2005;237(3):803-18.

35. Hanagiri T, Takenaka M, Oka S, Shigematsu Y, Nagata Y, Shimokawa H, et al. Results of a surgical resection for patients with stage IV non--small-cell lung cancer. Clin Lung Cancer. mai 2012;13(3):220-4.

36. Doddoli C, Rollet G, Thomas P, Ghez O, Serée Y, Giudicelli R, et al. Is lung cancer surgery justified in patients with direct mediastinal invasion? Eur J Cardiothorac Surg. 8 janv 2001;20(2):339-43.

Conclusion

Le bilan pré-opératoire des tumeurs broncho-pulmonaires repose aujourd'hui sur l'association TEP scanner et scanner. Nous avons montré les écueuils de la technique. Une publication de Uramoto montre l'intérêt de l'IRM dans l'affirmation de l'envahissement ou non de l'aorte thoracique, en utilisant notamment le ciné-IRM (21), qui a permis de mettre en evidence un plan de clivage entre la tumeur et l'aorte. La résolution en contraste de l'IRM et l'aspect dynamique de la ciné-IRM rendent le diagnostic plus facile. L'IRM est utilisée de manière systématique que dans le cas des tumeurs apicales à la recherche d'un envahissment du plexus brachial

On pourrait donc proposer la réalisation d'une IRM en cas de doute diagnostic d'envahissement médiastinal sur le scanner pré-opratoire. La place du TEP-scanner est également à définir, puisqu'il est d'un grand apport pour délimiter les zones d'hypermétabolisme mais souffre d'une mauvaise résolution en contraste.

Le développement des techniques chirurgicales permet aujourd'hui d'opérer un certains de patients classés cT4. Le bilan d'imagerie pré-opratoire doit en conséquence être exhaustif, et sans doute ne plus reposer uniquement sur le scanner mais également sur d'autres modalités d'imagerie au moindre doute d'envahissement de structures médiastinales, cardiaques ou de la paroi thoracique.

Conclusion Générale

La pathologie pulmonaire et la pathologie cardiaque interagissent et le bloc “Coeur-poumon” est à considerer comme une seule et même entité en imagerie: la lecture du coeur, des vaisseaux, des poumons et du médiastin doit être globale et intégrée, quelle que soit la modalité d’imagerie.

Nous avons pu ainsi illlustrer la contribution de la TDM dans l’évaluation de la prevalence de la pathologie coronarienne asymptomatrique au cours de la fibrose pulmonaire idiopathique, l’analyse du volume de l’oreillette gauche au cours des BPCO, la correlation entre volume pulmonaire hypoperfusé et le rapport VD/VG, et l’évaluation de l’envahissement cardiaque au cours des néoplasies pulmonaires.

Les avancées techniques en scannographie nous permettent désormais d’approcher outre la morphologie le versant fonctionnel, notamment par l’évaluation de la fonction cardiaque, de la perfusion pulmonaire, en attendant le développement en routine clinique de l’approche par TDM de la fonction de ventilation. Notre thèse avait pour ambition de contribuer modestement à la promotion d’une approche morphologique et fonctionnelle intégrée de l’imagerie du coeur, des vaisseaux thoraciques et du poumon, dont les bénéfices cliniques nous apparaissent quotidiens et dont l’enseignement nous apparait indissociable.

Réferences bibliographiques

1. Kalender WA, Quick HH. Recent advances in medical physics. Eur Radiol. 2011 Mar;21(3):501–4.
2. Menke J, Unterberg-Buchwald C, Staab W, Sohns JM, Seif Amir Hosseini A, Schwarz A. Head-to-head comparison of prospectively triggered vs retrospectively gated coronary computed tomography angiography: Meta-analysis of diagnostic accuracy, image quality, and radiation dose. Am Heart J. 2013 Feb;165(2):154–63.e3.
3. Sun M-L, Lu B, Wu R-Z, Johnson L, Han L, Liu G, et al. Diagnostic accuracy of dual-source CT coronary angiography with prospective ECG-triggering on different heart rate patients. Eur Radiol. 2011 Aug;21(8):1635–42.
4. Alkadhi H, Leschka S. Radiation dose of cardiac computed tomography - what has been achieved and what needs to be done. Eur Radiol. 2011 Mar;21(3):505–9.
5. Vorre MM, Abdulla J. Diagnostic accuracy and radiation dose of CT coronary angiography in atrial fibrillation: systematic review and meta-analysis. Radiology. 2013 May;267(2):376–86.
6. Haller S, Kaiser C, Buser P, Bongartz G, Bremerich J. Coronary Artery Imaging with Contrast-Enhanced MDCT: Extracardiac Findings. Am J Roentgenol. 2006 Jul 1;187(1):105–10.
7. Pinsky MR. Determinants of pulmonary arterial flow variation during respiration. J Appl Physiol. 1984 May;56(5):1237–45.
8. Ramu B, Thenappan T. Evolving Concepts of Pulmonary Hypertension Secondary to Left Heart Disease. Curr Heart Fail Rep. 2016 Feb 17;
9. Katikireddy CK, Singh M, Muhyieddeen K, Acharya T, Ambrose JA, Samim A. Left Atrial Area and Right Ventricle Dimensions in Non-gated Axial Chest CT can Differentiate Pulmonary Hypertension Due to Left Heart Disease from Other Causes. J Cardiovasc Comput Tomogr. 2016 Jan 30;
10. Eweda I, Hamada G. Concordance between Doppler and pulsed-wave Doppler tissue imaging in estimation of the degree of left ventricular dysfunction and correlating it to the degree of chronic obstructive pulmonary disease. J Saudi Heart Assoc. 2016 Jan;28(1):15–21.
11. Jörgensen K, Müller MF, Nel J, Upton RN, Houltz E, Ricksten S-E. Reduced intrathoracic blood volume and left and right ventricular dimensions in patients with severe emphysema: an MRI study. Chest. 2007 Apr;131(4):1050–7.
12. Cottin V, Crestani B, Valeyre D, Wallaert B, Cadranel J, Dalphin JC, et al. [French practical guidelines for the diagnosis and management of idiopathic pulmonary fibrosis. From the National Reference and the Competence centers for rare diseases and the Société de Pneumologie de Langue Française]. Rev Mal Respir. 2013 Dec;30(10):879–902.
13. Fell CD. Idiopathic pulmonary fibrosis: phenotypes and comorbidities. Clin Chest Med. 2012 Mar;33(1):51–7.
14. Ross R. Atherosclerosis--an inflammatory disease. N Engl J Med. 1999 Jan 14;340(2):115–26.
15. Mahabadi AA, Lehmann N, Möhlenkamp S, Pundt N, Dykun I, Roggenbuck U, et al. Noncoronary Measures Enhance the Predictive Value of Cardiac CT Above Traditional Risk Factors and CAC Score in the General Population. JACC Cardiovasc Imaging. 2016 Jul 14;

16. Aviram G, Soikher E, Bendet A, Shmueli H, Ziv-Baran T, Amitai Y, et al. Prediction of Mortality in Pulmonary Embolism Based on Left Atrial Volume Measured on CT Pulmonary Angiography. Chest. 2016 Mar;149(3):667–75.
17. Qanadli SD, El Hajjam M, Vieillard-Baron A, Joseph T, Mesurolle B, Oliva VL, et al. New CT index to quantify arterial obstruction in pulmonary embolism: comparison with angiographic index and echocardiography. AJR Am J Roentgenol. 2001 Jun;176(6):1415–20.
18. Schoepf UJ, Kucher N, Kipfmueller F, Quiroz R, Costello P, Goldhaber SZ. Right ventricular enlargement on chest computed tomography: a predictor of early death in acute pulmonary embolism. Circulation. 2004 Nov 16;110(20):3276–80.
19. Kuriakose J, Patel S. Acute pulmonary embolism. Radiol Clin North Am. 2010 Jan;48(1):31–50.
20. Langer NB, Mercier O, Fabre D, Lawton J, Mussot S, Dartevelle P, et al. Outcomes After Resection of T4 Non-Small Cell Lung Cancer Using Cardiopulmonary Bypass. Ann Thorac Surg [Internet]. 2016 May [cited 2016 Aug 14]; Available from: http://linkinghub.elsevier.com/retrieve/pii/S0003497516301539
21. Uramoto H, Iijima Y, Nakajima Y, Kinoshita H. Accurate Diagnosis of Aortic Invasion in Patients with Lung Cancer. Anticancer Res. 2016 May;36(5):2391–5.